UNIVERSIDADE FEDERAL DO PARANÁ

JANAINA MARQUES DE ALMEIDA

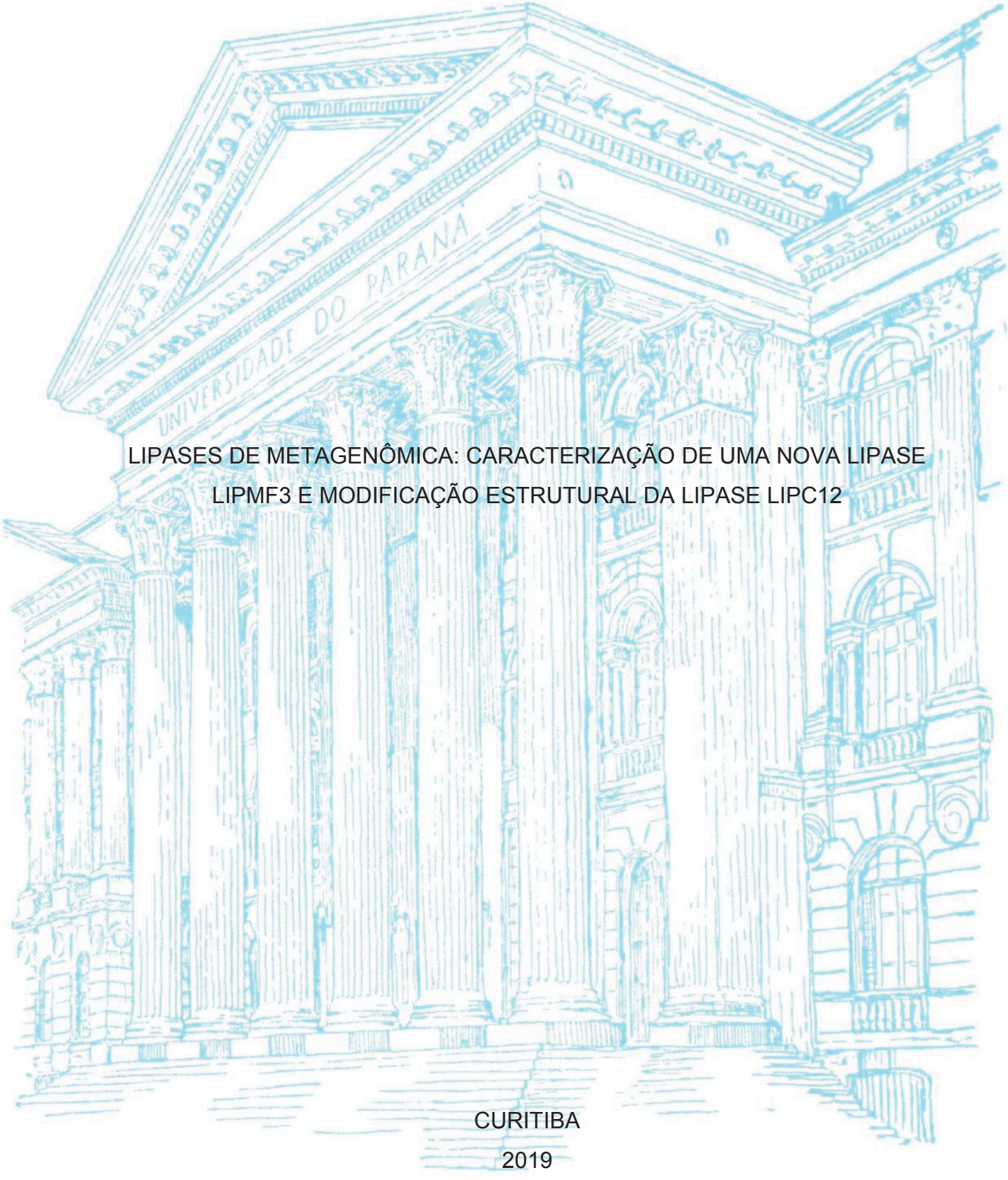

LIPASES DE METAGENÔMICA: CARACTERIZAÇÃO DE UMA NOVA LIPASE LIPMF3 E MODIFICAÇÃO ESTRUTURAL DA LIPASE LIPC12

CURITIBA

2019

JANAINA MARQUES DE ALMEIDA

LIPASES DE METAGENÔMICA: CARACTERIZAÇÃO DE UMA NOVA LIPASE LIPMF3 E MODIFICAÇÃO ESTRUTURAL DA LIPASE LIPC12

Tese apresentada ao curso de Pós-Graduação em Ciências-Bioquímica, Setor de Ciências Biológicas, Universidade Federal do Paraná, como requisito parcial à obtenção do título de Doutor em Ciências-Bioquímica.

Orientadora: Profª. Dra. Nadia Krieger
Coorientador: Prof. Dr. Marcelo Müller dos Santos
Coorientadora Dra. Vivian Rotuno Moure

CURITIBA

2019

Universidade Federal do Paraná. Sistema de Bibliotecas.
Biblioteca de Ciências Biológicas.
(Giana Mara Seniski Silva – CRB/9 1406)

Almeida, Janaina Marques de
Lipases de metagenômica: caracterização de uma nova lipase LIPMF3 e modificação estrutural da lipase LIPC12. / Janaina Marques de Almeida. – Curitiba, 2019.
158 p.: il. ; 30cm.

Orientador: Nadia Krieger
Coorientadores: Marcelo Müller dos Santos
Vivian Rotuno Moure

Tese (doutorado) - Universidade Federal do Paraná, Setor de Ciências Biológicas. Programa de Pós-Graduação em Bioquímica.

1. Lipase 2. Metagenômica 3. Biocatálise I. Título II. Krieger, Nadia III. Santos, Marcelo Müller dos IV. Moure, Vivian Rotuno V. Universidade Federal do Paraná. Setor de Ciências Biológicas. Programa de Pós-Graduação em Bioquímica.

CDD (20. ed.) 574.19253

MINISTÉRIO DA EDUCAÇÃO
SETOR CIÊNCIAS BIOLÓGICAS
UNIVERSIDADE FEDERAL DO PARANÁ
PRÓ-REITORIA DE PESQUISA E PÓS-GRADUAÇÃO
PROGRAMA DE PÓS-GRADUAÇÃO CIÊNCIAS
(BIOQUÍMICA)

TERMO DE APROVAÇÃO

Os membros da Banca Examinadora designada pelo Colegiado do Programa de Pós-Graduação em CIÊNCIAS (BIOQUÍMICA) da Universidade Federal do Paraná foram convocados para realizar a arguição da Tese de Doutorado de **JANAINA MARQUES DE ALMEIDA**, intitulada: **LIPASES DE METAGENÔMICA: CARACTERIZAÇÃO DE UMA NOVA LIPASE LIPMF3 E MODIFICAÇÃO ESTRUTURAL DA LIPASE LIPC12**, após terem inquirido a aluna e realizado a avaliação do trabalho, são de parecer pela sua APROVAÇÃO no rito de defesa.

A outorga do título de Doutor está sujeita à homologação pelo colegiado, ao atendimento de todas as indicações e correções solicitadas pela banca e ao pleno atendimento das demandas regimentais do Programa de Pós-Graduação.

Curitiba, 07 de Dezembro de 2018.

NADIA KRIEGER
Presidente da Banca Examinadora

THABATA MARIA ALVAREZ
Avaliador Externo (UP)

BEATRIZ GOMES GUIMARAES
Avaliador Interno ()

RODRIGO VOLCAN ALMEIDA
Avaliador Externo (UFRJ)

WANDERSON DUARTE DA ROCHA
Avaliador Interno (UFPR)

Dedico aos meus pais Valéria de Fátima Galvão e
Levi Marques de Almeida (*in memoriam*)

AGRADECIMENTOS

À professora Nadia Krieger pela oportunidade de realizar este trabalho, pela orientação e por todo o conhecimento transmitido.

Aos coorientadores Dra. Vivian Rotuno Moure e professor Marcelo Müller dos Santos pela ajuda e orientação nos trabalhos desenvolvidos.

Ao professor David Alexander Mitchel pelas valiosas sugestões e correções feitas neste trabalho.

Aos professores Emanuel Maltempi de Souza e Wanderson Duarte da Rocha pelas sugestões e pelo acompanhamento na realização deste trabalho desde o início através das correções do projeto e dos relatórios.

À professora Viviane de Paula Martini e ao professor Jorge Iulek pela valiosa ajuda na modelagem molecular das proteínas.

A todos os colegas e amigos dos laboratórios LTEB e LTFE (todos os alunos de mestrado, doutorado, pós-doutorado e iniciação científica) que fizeram parte desta trajetória, pela colaboração e companheirismo durante a realização deste trabalho, em especial ao Robson que me auxiliou desde o início do trabalho e pela disposição em me ajudar todas as vezes que precisei.

Aos alunos de iniciação científica Karina e Luís que participaram da realização de várias etapas deste trabalho.

A todos os integrantes do Núcleo de Fixação de Nitrogênio (NFN), onde realizei grande parte do trabalho, pelo auxílio em todas as etapas desenvolvidas.

Ao CNPq pelo auxílio financeiro.

Ao Programa de Pós-graduação em Bioquímica.

À UFPR e ao departamento de Bioquímica e Biologia Molecular.

À minha família, minha mãe Valéria, minha irmã Josiane, meu irmão Alexandre e minhas queridas sobrinhas Ana Carolina e Maria Júlia, por todo suporte que me deram e que mesmo de longe sempre me incentivaram a realizar este doutorado. A Cacilda e Edison por todo carinho e incentivo sempre.

Ao Gerson por todo amor, carinho e dedicação que sempre teve comigo, e pela imensa ajuda na concretização desta estapa da minha vida.

“A ciência serve para nos dar uma ideia de
quão extensa é a nossa ignorância.”
(Félicité Robert de Lamennais)

RESUMO

O uso intensivo de lipases como biocatalisadores em síntese orgânica tem impulsionado a busca por novas lipases e o melhoramento de lipases conhecidas. Neste contexto, o presente trabalho apresenta os estudos realizados com duas lipases isoladas de uma biblioteca metagenômica, construída a partir de solo contaminado com gordura animal (SCGA). A primeira parte do trabalho investigou os efeitos da His-tag na estrutura, atividade, estabilidade e imobilização de LipC12, uma lipase previamente caracterizada. LipC12 foi purificada com a His-tag na região N-terminal por cromatografia de afinidade, em seguida, a His-tag foi removida utilizando a protease do vírus do mosaico do tabaco (TEV). A estrutura geral de LipC12 não foi afetada pela remoção da His-tag, como confirmado por análise de dicroísmo circular. As atividades de hidrólise específicas contra os substratos naturais e artificiais foram significativamente maiores com LipC12 sem His-tag. No entanto, esta variante de LipC12 apresentou menor atividade e estabilidade na presença de solventes orgânicos polares em relação à LipC12 com His-tag. A eficiência de imobilização em Immobead 150 foi de 100% para as duas variantes de LipC12 e estudos de dessorção de proteínas confirmaram que a His-tag não participa de ligações covalentes com o suporte. Para LipC12 imobilizada, a His-tag também influenciou negativamente a atividade de hidrólise, mas influenciou positivamente na atividade de esterificação. Isto abre a possibilidade de modular a atividade de LipC12 para diferentes reações: a His-tag pode ser mantida para reações de hidrólise ou removida para reações de síntese. A segunda parte do trabalho foi a caracterização da nova lipase LipMF3. Esta lipase requer uma foldase para o seu correto enovelamento, de modo que os genes *lipMF3* e *lifMF3,* que codificam para a lipase e sua foldase, respectivamente, foram amplificados e clonados. Estes genes foram co-expressos em *Escherichia coli*, em seguida, o complexo Lip-LifMF3 foi purificado por cromatografia de afinidade e caraterizado bioquimicamente. A estrutura tridimensional do complexo também foi determinada por modelagem por homologia. Através de análise filogenética, LipMF3 foi classificada como pertencente à subfamília I.1 de lipases bacterianas, apresentando identidade de sequência de 68% e 67% com lipases de *Chromobacterium violaceum* e *C. amazonense*, respectivamente. LipMF3 apresenta alta atividade de hidrólise contra triacilgliceróis de cadeia curta, média e longa (1650 ± 46 U mg^{-1} para tributirina, 1314 ± 68 U mg^{-1} para tricaprilina e 862 ± 62 U mg^{-1} para óleo de oliva). A maior atividade de LipMF3 foi a 40 °C e pH 6,5. A enzima foi estável por 3 horas em solventes orgânicos, apresentando atividade residual em torno de 100% na presença de 25% (v/v) de DMSO, isopropanol, metanol, etanol, propanol e butanol. Apresentou estabilidade também em uma ampla faixa de pH (5,5 a 11) com atividade residual acima de 80%. LipMF3 foi imobilizada em um suporte hidrofílico (Immobead 150P) e em um suporte hidrofóbico (Sepabeads FP-BU), com melhores resultados de imobilização obtidos com Sepabeads. Esta preparação apresentou uma conversão de 94% em 5 h de reação para síntese de oleato de etila. Na resolução cinética de (*R,S*)-1-fenil-1-etanol, apresentou um excesso enantiomérico (*ee*) de 90% para o produto (*R*)-1-feniletil acetato. Esta nova lipase possui, portanto, potencial de aplicação em reações biotecnológicas.

Palavras-chave: Lipases. Metagenômica. Estrutura Tridimensional. Biocatálise. Imobilização.

ABSTRACT

The intensive use of lipases as biocatalysts in organic synthesis has driven the search for new lipases and the improvement of known lipases. In this context, the current work presents the studies undertaken with two lipases isolated from a metagenomic library constructed from fat-contaminated soil. The first part of the work investigated the effects of the His-tag on the structure, activity, stability and immobilization of the LipC12, a lipase that has previously been characterized. LipC12 was purified with a His-tag at the N-terminal region by affinity chromatography, then the His-tag was removed using protease from Tobacco Etch Virus (TEV). The overall structure of LipC12 was not affected by the removal of His-tag, as confirmed by circular dichroism analysis. The specific hydrolytic activities against natural and artificial substrates were significantly higher for LipC12 without His-tag. However, this form of LipC12 had a lower activity and stability in the presence of polar organic solvents than LipC12 with His-tag. The efficiency of immobilization on Immobead 150 was 100% for the two LipC12 variants and protein desorption studies confirmed that the His-tag does not participate in covalent bonding with the support. For immobilized LipC12, the His-tag also negatively influenced the hydrolytic activity, but positively influenced the esterification activity. This opens up the possibility of modulating the activity of LipC12 for different reactions: the His-tag can be maintained for hydrolysis reactions or removed for synthesis reactions. The second part of the work was the characterization of the new lipase LipMF3. This lipase requires a foldase for correct folding, so the genes *lipMF3* and *lifMF3*, which code for the lipase and its foldase, respectively were amplified and cloned. These genes were co-expressed in *Escherichia coli,* then LipLifMF3 complex was purified by affinity chromatography and characterized biochemically. The three-dimensional structure of the complex was also determined by homology modeling. Through phylogenetic analysis, LipMF3 was classified as belonging to the subfamily I.1 of bacterial lipases, presenting sequence identities of 68% and 67% with lipases of *Chromobacterium violaceum* and *C. amazonense*, respectively. LipMF3 has high hydrolytic activity against short-, medium- and long-chain triacylglycerols (1650 ± 46 U mg^{-1} for tributyrin, 1314 ± 68 U mg^{-1} for tricaprylin and 862 ± 62 U mg^{-1} for olive oil). The highest activity of LipMF3 was at 40 °C and pH 6.5. The enzyme was stable for 3 hours in organic solvents, with residual activity around 100% in the presence of 25% (v/v) of DMSO, isopropanol, methanol, ethanol, propanol and butanol. It also showed stability over a wide range of pH (5.5 to 11) with residual activity above 80%. LipMF3 was immobilized onto a hydrophilic support (Immobead 150P) and a hydrophobic support (Sepabeads), with better results for immobilization obtained with Sepabeads. This preparation gave 94% conversion in 5 h for the synthesis of ethyl oleate. In the kinetic resolution of (*R,S*)-1-phenyl-1-ethanol, it gave an enantiomeric excess (*ee*) of 90% for the product (*R*)-1-phenylethyl acetate. This new lipase therefore has potential for application in biotechnological reactions.

Keywords: Lipases. Metagenomics. Three-dimensional Structure. Biocatalysis. Immobilization.

LISTA DE FIGURAS

LISTA DE FIGURAS DO CAPÍTULO I

LISTA DE FIGURAS DO CAPÍTULO II

LISTA DE TABELAS

LISTA DE TABELAS DO CAPÍTULO I

LISTA DE TABELAS DO CAPÍTULO II

SUMÁRIO

1 INTRODUÇÃO

As lipases são enzimas de grande interesse biotecnológico e alvo de intensas pesquisas nas últimas décadas, sendo o terceiro grupo de enzimas hidrolíticas mais comercializadas no mercado de biocatalisadores (LI et al., 2012). Este destaque se deve ao fato de que as lipases são enzimas versáteis e catalisam uma ampla gama de reações, entre as quais estão as reações de hidrólise, esterificação, transesterificação, lactonização, entre outras, desempenhando, assim, um papel importante em química orgânica (JAEGER; EGGERT, 2002).

Desta forma, o estudo de novas lipases, assim como a modificação estrutural de lipases já caracterizadas, se faz necessário para viabilizar aplicações destas enzimas em biocatálise. Portanto, esta tese de doutorado teve como objetivo o estudo de duas lipases da biblioteca metagenômica de solo contaminado com gordura animal (SCGA), visando à caracterização de uma nova lipase, denominada de LipMF3 e a modificação estrutural de outra lipase já caracterizada anteriormente (LipC12).

O Capítulo 1 desta tese apresenta os resultados obtidos em relação à LipC12, uma lipase clonada e caracterizada por Glogauer et al. (2011). Esta enzima é considerada uma lipase verdadeira, pois apresenta alta atividade contra triacilgliceróis de cadeia longa (1722 U mg^{-1} para óleo de oliva). Madalozzo et al. (2015) realizaram estudos de imobilização de LipC12 em Immobead 150 e aplicação desta enzima imobilizada em síntese de ésteres de biodiesel. Neste trabalho, os autores propuseram que a cauda de histidina (His-tag) presente na LipC12 poderia influenciar no processo de imobilização, que ocorre em pH 7,5, pois neste pH os resíduos de histidina encontram-se majoritariamente desprotonados (pKa 6,0) e seriam mais reativos ao ataque nucleofílico dos grupos oxirano do suporte. Para confirmar esta hipótese, foram realizados estudos para avaliar a influência da His-tag na atividade, estabilidade e na imobilização de LipC12. Os resultados referentes à LipC12 foram compilados em um manuscrito intitulado: "*Tailoring recombinant lipases: keeping the His-tag favors esterification reactions, removing it favors hydrolysis reactions*", publicado na revista *Scientific Reports*.

No Capítulo 2 estão apresentados os resultados referentes à nova lipase LipMF3, isolada da mesma biblioteca metagenômica, uma enzima dependente de uma foldase, denominada LifMF3, codificada pelo gene *lifMF3*, que está localizado à jusante do gene da lipase (*lipMF3*). Assim, o estudo desta lipase incluiu a predição da

estrutura através de modelagem por homologia das proteínas LipMF3 e LifMF3, clonagem dos genes *lipMF3* e *lifMF3*, superexpressão heteróloga, purificação, caracterização e imobilização desta enzima.

1.1 JUSTIFICATIVA

Não obstante o grande potencial de aplicação de lipases, principalmente na indústria de detergentes, alimentos e síntese orgânica, e as numerosas publicações em relação ao isolamento e seleção destas enzimas descritas nas últimas décadas, relativamente poucas lipases apresentam as propriedades desejadas para aplicação em processos industriais.

Desta forma, existe uma necessidade de lipases com alta atividade, termoestabilidade e estabilidade em meios reacionais não-convencionais, como solventes orgânicos. Esta demanda pode ser suprida utilizando-se além do isolamento de micro-organismos do ambiente e a identificação de suas lipases por métodos convencionais, também a metagenômica. A metagenômica é uma alternativa que vem se mostrando eficiente para isolar novas lipases com as propriedades catalíticas almejadas. Além disso, a modificação estrutural também é uma opção atrativa para melhorar as lipases já conhecidas e com potencial de aplicação em biocatálise, como é o caso de LipC12.

1.2 OBJETIVOS

1.2.1 Objetivo geral

Este trabalho teve como objetivo geral o estudo de duas lipases isoladas da biblioteca metagenômica de solo contaminado com gordura animal (SCGA), envolvendo a verificação do efeito da cauda de histidina (His-tag) nas propriedades catalíticas da lipase LipC12 e a caracterização bioquímica, molecular e estrutural de uma nova lipase (LipMF3).

1.2.1.1 Objetivos específicos

a) LipC12

- Produzir variantes de LipC12 com e sem a His-tag, a partir da clonagem do gene *lipC12* em pET29a(+) (para expressão de LipC12 sem His-tag) e pTEV5 (para expressão de LipC12 com His-tag e um sítio de clivagem da protease TEV), assim como pela expressão de LipC12 em pTE28a(+) previamente clonada por Glogauer et al. (2011) .
- Determinar as propriedades catalíticas das duas variantes de LipC12, com e sem His-tag, quanto à atividade de hidrólise em meio aquoso e em solventes orgânicos, estabilidade à solventes orgânicos, efeito de detergentes e a determinação dos parâmetros cinéticos K_M, k_{cat}, K_M/k_{cat};
- Determinar mudanças na estrutura secundária e temperatura de desenovelamento das duas variantes de LipC12, com e sem His-tag, por dicroísmo circular;
- Imobilizar as duas variantes de LipC12 em Immobead 150 e caracterizar os preparados imobilizados, para verificar o efeito da His-tag na imobilização e nas propriedades catalíticas de LipC12 imobilizada;

b) LipMF3

- Construir um modelo tridimensional do complexo Lip-LifMF3 através de modelagem por homologia;
- Realizar a amplificação e clonagem em vetores de expressão dos genes identificados da lipase (*lipMF3*) e foldase (*lifMF3*);
- Determinar o melhor sistema de expressão para a co-expressão heteróloga dos genes *lipMF3* e *lifMF3* em *E. coli*;
- Purificar e caracterizar LipMF3, determinando-se a massa molecular, ponto isoelétrico (pI), preferência por substratos, estabilidade em solventes orgânicos, efeito da temperatura e do pH na atividade e estabilidade;
- Avaliar o efeito da imobilização de LipMF3 em diferentes suportes hidrofóbicos e hidrofílicos e medir os principais parâmetros de imobilização, como retenção de atividade, atividade de hidrólise e atividade de esterificação;
- Utilizar LipMF3 imobilizada, em reações de síntese de oleato de etila e na resolução cinética do álcool (*R,S*)-1-fenil-1-etanol em solventes orgânicos, para determinar o seu potencial de aplicação em biocatálise.

2 REVISÃO DA LITERATURA

2.1 LIPASES

As lipases (EC 3.1.1.3 - triacilglicerol hidrolases) são enzimas que naturalmente hidrolisam ligações éster de triacilgliceróis, mas podem catalisar uma ampla variedade de reações químicas e reconhecer como substrato muitos outros compostos, o que as tornam importantes em diversas aplicações biotecnológicas como nas indústrias de detergente, alimentos, biodiesel e farmacêutica (JAEGER; EGGERT, 2002; GUPTA; GUPTA; RATHI, 2004).

Lipases possuem em geral uma estrutura tridimensional com elementos em comum, apresentando uma forma globular e uma conformação α/β hidrolase, ou seja, formada por um núcleo central composto por folhas-β, circundadas por α-hélices. Como exemplo, pode-se citar a lipase de *Pseudomonas aeruginosa* (PDB: 1EX9), a primeira lipase da família I.1 a ter a sua estrutura elucidada por cristalografia (FIGURA 1). O sítio ativo das lipases é formado pelos resíduos de Ser, Asp (Glu) e His (JAEGER et al., 1994), sendo que a serina catalítica se encontra no pentapeptídeo altamente conservado GlyXSerXGly (onde X representa qualquer resíduo de aminoácido) (JAEGER; REETZ, 1998).

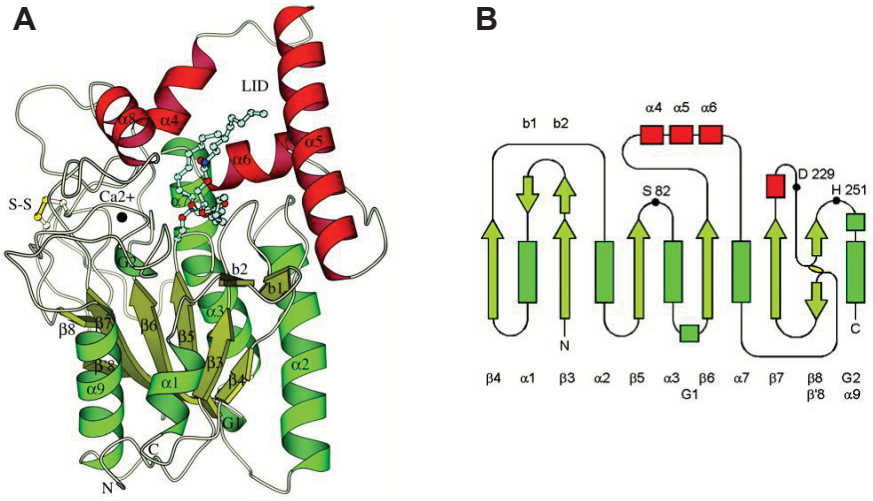

FIGURA 1 - ESTRUTURA DA LIPASE DE *Pseudomonas aeruginosa* (PDB: 1EX9)
LEGENDA: A: representação das estruturas secundárias α-hélices, folhas-β e alças, o domínio *lid* está representado pelas α-hélices em vermelho. B: diagrama de topologia da estrutura secundária α/β hidrolase. A tríade catalítica é composta pelos resíduos Ser82, Asp229 e His251, α-hélices e folhas-β são representados por retângulos e setas, respectivamente. FONTE: Nardini et al. (2000).

Outra característica estrutural interessante das lipases, é a presença de uma tampa hidrofóbica, chamada *lid*, uma cadeia de aminoácidos que recobre o sítio ativo,

que é responsável pelo fenômeno de ativação interfacial. Quando a lipase é colocada em um meio com substratos hidrofóbicos, a *lid* se move, expondo o sítio ativo para a catálise. No entanto, não são todas as lipases que apresentam esse fenômeno, e muitas lipases também não possuem uma *lid*. Khan et al. (2017) classificaram as lipases, de acordo com a estrutura do domínio *lid*, em três grupos diferentes: lipases sem *lid*, lipases com a *lid* composta por apenas uma α-hélice e lipases com duas ou mais α-hélices formando a *lid*, observando-se uma tendência de maior termoestabilidade para lipases com *lids* maiores.

A maioria das lipases utilizadas industrialmente são de origem microbiana, notadamente, fungos e bactérias. Um dos grupos de lipases mais utilizados e estudados são as lipases bacterianas (JAVED et al., 2018), principalmente dos gêneros *Pseudomonas, Burkholderia* e *Bacillus,* que possuem ampla aplicação em biocatálise (GUPTA; GUPTA; RATHI, 2004).

Uma classificação proposta para lipases bacterianas foi realizada por Arpigny e Jaeger (1999). Os autores classificaram as lipases em oito famílias, com base na homologia de sequência de aminoácidos e características estruturais. A TABELA 1 mostra a família I, formada por lipases verdadeiras, que hidrolisam triacilgliceróis de cadeia longa, é a família mais conhecida e abundante, sendo subdividida em 7 subfamílias. As lipases das subfamílias I.1, I.2 e I.3 apresentam um sítio de ligação ao cálcio formado por resíduos de aspartato. Além disso, na maioria das lipases das subfamílias I.1 e I.2, dois resíduos de cisteína formam uma ponte dissulfeto. A subfamília I.2 apresenta lipases com peso molecular maior do que as lipases da subfamília I.1, devido à uma inserção formada por duas β-folhas antiparalelas na superfície das proteínas. A maioria das lipases da subfamília I.1 e I.2 necessita de uma proteína auxiliar denominada de foldase específica para lipases (Lif), que é necessária para obtenção de lipases ativas (ROSENAU; JAEGER, 2000).

A classificação de Arpigny e Jaeger (1999) foi atualizada por Jaeger e Eggert (2002), com a inclusão de outras enzimas descritas posteriormente. No entanto, ao longo do tempo foram adicionadas a essa classificação mais dez famílias (TABELA 2), pois muitas lipases não se enquadravam nas oito famílias *a priori* caraterizadas. Em função disso, atualmente existem 18 famílias de lipases bacterianas. As famílias mais recentes foram caracterizadas principalmente por diferenças em motivos conservados e na cavidade oxiânion.

TABELA 1 - PROPRIEDADES DAS LIPASES DA FAMÍLIA I

Sub-família	Fonte de Lipases	Massa molecular (kDa)	Foldase (Lif)	Sítio de Ca^{2+}	Ponte Dissulfeto	Pentapeptídeo conservado	Lid
I.1	*Pseudomonas aeruginosa* *Pseudomonas fluorescens* C9 *Vibrio cholerae* *Acinetobacter calcoaceticus* *Pseudomonas fragi* *Pseudomonas wisconsinensis* *Proteus vulgaris*	30-32	Sim/Não	Sim	Sim/Não	GXSXG	Sim
I.2	*Burkholderia glumae* *Chromobacterium viscosum* *Burkholderia cepacia* *Pseudomonas luteola*	33	Sim/Não	Sim	Sim	GXSXG	Sim
I.3	*Pseudomonas fluorescens SIKW1* *Serratia marcescens*	50 65	Não	Sim	Não	GXSXG	Sim
I.4	*Bacillus subtilis* *Bacillus pumilus* *Bacillus licheniformis* *Bacillus subtilis* (LipB)	~20	Não	Não	Não	AXSXG	Não
I.5	*Geobacillus stearothermophilus* *Geobacillus thermocatenulatus* *Geobacillus thermoleovorans*	~45	Chaperona intramolecular	Não	Não	AXSXG	Sim
I.6	*Staphylococcus aureus* *Staphylococcus haemolyticus* *Staphylococcus epidermidis* *Staphylococcus hyicus* *Staphylococcus xylosus* *Staphylococcus warneri*	~75	Não	Não	Não	GXSXG	Sim
I.7	*Propionibacterium acnes* *Streptomyces cinnamoneus*	33 50	Não	Não	Não	GXSXG	Sim

FONTE: Arpigny e Jaeger (1999); Rosenau e Jaeger (2000); Borrelli e Trono (2015).

TABELA 2 - NOVAS FAMÍLIAS DE LIPASES

Família	Enzima/Fonte	Referência
IX	Depolimerase PhaZ7/*Pseudomonas lemoignei*	Handrick et al. (2001)
X	Esterase EstD/*Thermotoga marítima*	Levisson, Van Der Oost e Kengen, (2007)
XI	LipG/metagenômica	Lee et al. (2006)
XII	LipEH166/metagenômica	Kim et al. (2009),
XIII	EST30/*Bacillus* sp.	Ewis, Abdelal e Lu (2004); Liu et al. (2004); Rao et al. (2013)
XIV	EstA3/*Thermoanaerobacter tengcongensis* MB4	Rao et al. (2011)
XV	EstDZ2/metagenômica	Zarafeta et al. (2016)
XVI	LipSM54/*Stenotrophomonas maltophilia* GS11	Li et al. (2016)
XVII	LipJ2/*Janibacter* sp. R02	Castilla et al. (2017)
XVIII	LipSm/*Stenotrophomonas maltophilia* Psi-1	Parapoull et al. (2018)

2.2 FOLDASES ESPECÍFICAS PARA LIPASES (LIF)

Muitas proteínas necessitam de outras proteínas auxiliares para tornar sua estrutura biologicamente ativa dentro das células. Existem dois grupos de proteínas auxiliares: as chaperonas moleculares e as foldases (WANG; TSOU, 1998).

As foldases são representadas pelas proteínas PDI (*protein disulfide isomerase*) e PPI (*peptidyl-prolyl isomerase*) que realizam a formação de ligações covalentes como formação de pontes dissulfeto e a isomerização de ligações peptídicas N-terminais à resíduos de prolina, respectivamente (GUPTA; TUTEJA, 2011). Estas foldases são consideradas enzimas, pois apresentam atividade de isomerase, mas também apresentam atividade de chaperona, pois auxiliam no enovelamento das proteínas auxiliadas (WANG; TSOU, 1998).

Por outro lado, o termo chaperona molecular tem como definição proteínas que assistem a correta montagem não-covalente de outras proteínas nascentes, mas não são componentes da proteína enovelada (ELLIS, 1987, 1993). Dentre as chaperonas moleculares estão as proteínas Hsp (*Heat shock proteins*), proteínas auxiliares dependentes de ATP que ajudam no enovelamento correto de muitas proteínas induzidas por choque térmico em bactérias. Outro grupo de chaperonas moleculares são as Lifs, cuja denominação (Lif, *lipase-specific foldase*) foi proposta por Jaeger et al. (1994) e designa chaperonas moleculares específicas para lipases.

As Lifs compõem uma família de chaperonas moleculares estéricas, que ficam ancoradas na membrana interna das células bacterianas voltadas para o periplasma

e têm como função modificar as lipases para sua forma ativa (WILHELM et al., 2007). Além disso, essas Lifs possuem um papel importante no sistema de secreção de muitas lipases, que ocorre via sistema de secreção tipo II, descrito abaixo. Além do seu papel no enovelamento de proteínas, as Lifs aumentam a resistência à degradação das lipases assistidas (EL KHATTABI et al., 2000).

2.2.1 Sistema de secreção de lipases

As lipases bacterianas são enzimas extracelulares e necessitam de um sistema de secreção para transportar as lipases do meio intracelular até o meio extracelular; para isso, precisam passar pela barreira da membrana interna, periplasma e membrana externa em bactérias gram-negativas e membrana citoplasmática para as bactérias gram-positivas. Existem 3 tipos de sistemas de secreção em bactérias gram-negativas para lipases: tipo I, tipo II e tipo III (autotransportador). As lipases pertencentes a subfamília I.1 e I.2 apresentam o sistema de secreção tipo II, enquanto as lipases da subfamília I.3 apresentam o sistema de secreção do tipo I (FIGURA 2) (ROSENAU; JAEGER, 2000).

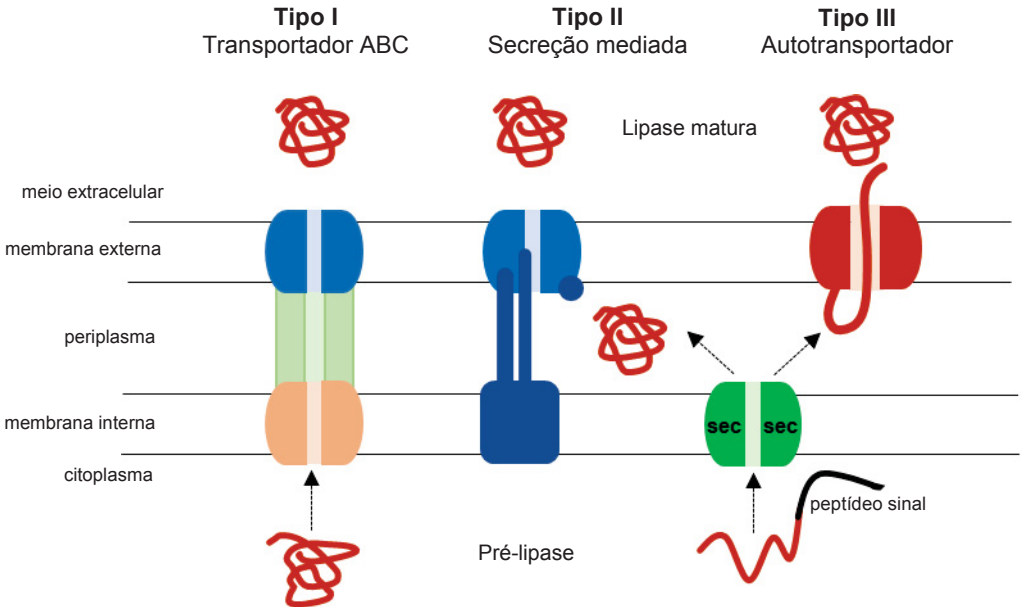

FIGURA 2 - VIAS DE SECREÇÃO DE ENZIMAS LIPOLÍTICAS PRESENTES EM BACTÉRIAS
FONTE: O autor (2019).

O sistema de secreção do tipo I, apresentado por lipases da subfamília I.3, ocorre em um único passo, diretamente do citoplasma para o meio extracelular, com gasto de energia (ANGKAWIDJAJA; KANAYA, 2006). Este sistema é formado por três

componentes: proteína ATP-*binding cassette* (ABC), associada à membrana interna; proteína de fusão de membrana (MFP) associada à membrana interna e externa e proteína OMP, associada somente à membrana externa (AKATSUKA et al., 1997). As lipases transportadas pelo sistema do tipo I não apresentam peptídeo sinal na região N-terminal. Entretanto, é comum a presença de um sinal de secreção na região C-terminal, como observado nas lipases de *P. fluorescens* (DUONG et al., 1994) e *Serratia marcescens* (AKATSUKA et al., 1995).

No sistema de secreção tipo II, a lipase é excretada do citoplasma para o periplasma através do peptídeo sinal presente na região N-terminal da lipase, através do sistema Sec. Na passagem para o espaço periplasmático, a lipase perde o peptídeo sinal e ocorre o correto dobramento da lipase em sua forma ativa, através da ação da foldase. No periplasma existem outras proteínas auxiliares inespecíficas, incluindo proteínas Dsb, que catalisam a formação de ligações dissulfeto. Então, a lipase é excretada para fora da célula através de um intrincado sistema de secreção composto por mais de 12 proteínas diferentes (ROSENAU; JAEGER, 2000; GREEN; MECSAS, 2015). Este sistema de secreção foi descrito para lipases de *P. aeruginosa* e está apresentado na FIGURA 3.

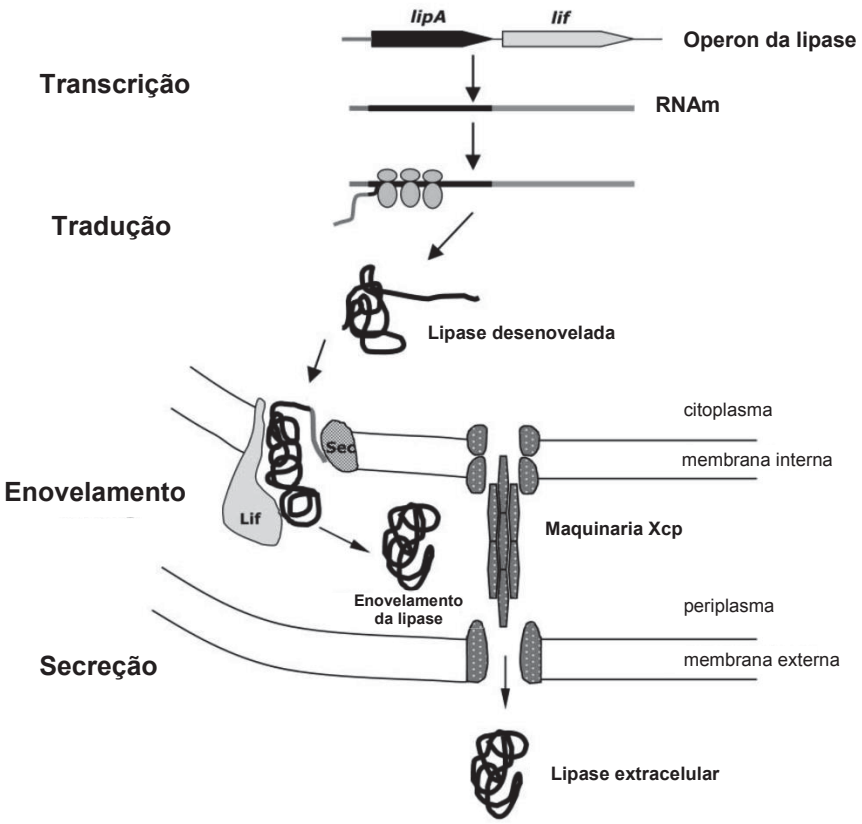

FIGURA 3 - SECREÇÃO E DOBRAMENTO DE LIPASE DE *Pseudomonas aeruginosa*
FONTE: Adaptado de Rosenau; Tommassen e Jaeger (2004).

No sistema do tipo III (autotransportador), as proteínas contendo um peptídeo sinal N-terminal são primeiramente transportadas através da membrana citoplasmática interna pela maquinaria Sec. Após a remoção do peptídeo sinal e liberação no periplasma, as proteínas maturas cruzam a membrana externa, por uma via de secreção autotransportadora, não requerendo nenhuma proteína acessória. Os domínios C-terminais destas lipases se inserem na membrana externa, formando um poro que permite o transporte da região N-terminal para a superfície da célula. A porção matura da proteína é, então, liberada desta estrutura de poro por clivagem proteolítica. Um exemplo de lipase transportada por esse sistema é a lipase PalA de *P. aeruginosa* (ROSENAU; JAEGER, 2000; SANDKVIST, 2001; LEE; BYUN, 2003).

2.2.2 Classificação e estrutura das Lifs

Devido à importância das Lifs no entendimento dos processos de enovelamento e de secreção de muitas lipases, Rosenau, Tommassen e Jaeger (2004) sugeriram uma classificação de Lifs de bactérias gram-negativas em 4 famílias, baseada na homologia de sequência de aminoácidos. A família I é formada por Lifs do gênero *Pseudomonas*, a família II, por Lifs de *Burkholderia*, a família III, por Lifs de *Acinetobacter* e a família IV, por Lifs de *Vibrio*. As Lifs destas famílias, em geral, apresentam baixa similaridade de sequência e exibem apenas um motivo conservado, formado pelos resíduos de aminoácidos RXXFDY(F/C)L(S/T)A (onde X representa qualquer aminoácido).

Além do motivo conservado, as Lifs possuem algumas características em comum, como uma região N-terminal transmembrana composta por aminoácidos hidrofóbicos (FRENKEN et al., 1993). Essa região transmembrana não é requerida para a função biológica da Lif, existindo várias evidências experimentais de Lifs recombinantes sem a região transmembrana N-terminal que exibem normalmente a sua atividade de dobramento de lipases (EL KHATTABI; OCKHUIJSEN, 1999). Apesar de a região transmembrana não ter uma função biológica, a expressão homóloga da Lif de *Burkholderia glumae* sem essa região resultou na secreção da Lif junto com a lipase para a região periplasmática da célula, evidenciando a importância da região N-terminal para ancorar a proteína na membrana interna das bactérias. Por sua vez, a região C-terminal das Lifs é um grande domínio periplasmático, e é a porção responsável pela ação da Lif, sendo que para a Lif de *B. glumae* uma porção de 138

resíduos de aminoácidos da região C-terminal determina a especificidade da interação da Lif com a lipase cognata (EL KHATTABI; OCKHUIJSEN, 1999).

A única Lif a ter a sua estrutura tridimensional elucidada por cristalografia foi a Lif de *B. glumae*, cristalizada complexada com a sua lipase cognata (PAUWELS et al., 2006). A Lif de *B. glumae* é composta por onze α-hélices que englobam a lipase (FIGURA 4). A determinação da estrutura tridimensional dessa Lif trouxe novos conhecimentos sobre estrutura e função das foldases específicas para lipases, como por exemplo, a presença de dois mini-domínios identificados entre as α-hélices 1-3 e 9-11, que fazem parte da região C-terminal e N-terminal, respectivamente. Estes dois mini-domínios são as únicas regiões da Lif que apresentam uma estrutura terciária na forma globular, indicando que provavelmente estas regiões são importantes para o reconhecimento e atividade de dobramento da Lif. O motivo conservado (RXXFDY(F/C)L(S/T)A) está localizado na α-hélice 1 (região em vermelho na FIGURA 4). Além disso, Pauwels et al. (2006) destacam que há uma interação de alta afinidade entre Lip-Lif formada por 20 ligações de hidrogênio e uma ponte salina (Glu63 e Arg343), fazendo com que o complexo seja estável e de difícil dissociação.

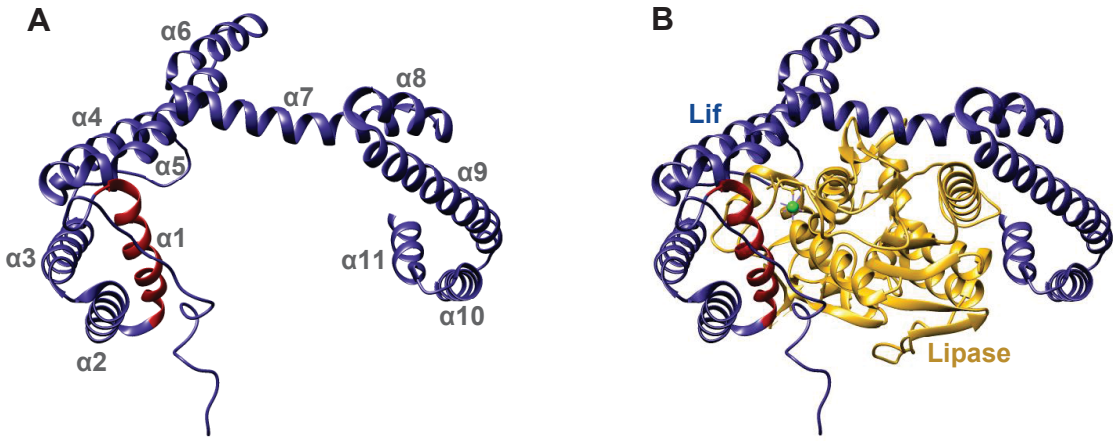

FIGURA 4 - COMPLEXO LIP-LIF DE *Burkholderia glumae*
LEGENDA: A: estrutura da Lif composta pelas α-hélices α1 à α11, o motivo conservado está localizado na α-hélice α1 em vermelho. B: complexo Lip-Lif.
FONTE: Adapatado de Pauwels et al. (2006) (PDB: 2ES4). Estrutura gerada no programa UCSF Chimera.

2.2.3 Expressão de lipases e Lifs em sistema heterólogo

A expressão de lipases em hospedeiro heterólogo é amplamente difundida e visa maximizar a produção destas enzimas, e também evitar o cultivo de organismos

potencialmente patogênicos (WU et al., 2012). Hospedeiros procarióticos são os organismos mais utilizados para expressão de proteínas recombinantes, principalmente a bactéria *Escherichia coli*, pois são fáceis de cultivar e atingem alta densidade celular em pouco tempo (BORRELLI; TRONO, 2015).

A expressão de lipases em *E. coli* muitas vezes pode ser mais eficiente do que a expressão no organismo original, como demonstrado por Ogino et al. (2008), que conseguiram melhorar a produtividade da lipase LST-03 em 807 vezes, em comparação a produção no organismo original *P. aeruginosa*. No entanto, um fator limitante para a superexpressão de muitas lipases na forma ativa é a necessidade da presença da Lif para o seu correto enovelamento (WU et al., 2012). As lipases das subfamílias I.1 e I.2 são codificadas no mesmo operon das suas Lifs, sendo que os genes da lipase e foldase encontram-se em tandem (ROSENAU; TOMMASSEN; JAEGER, 2004).

Apesar de *E. coli* ser o sistema mais utilizado para expressão de proteínas heterólogas, uma grande parte destas proteínas são expressas como corpos de inclusão, que são agregados inativos e insolúveis de proteínas (PALMER; WINGFIELD, 2004; VALLEJO; RINAS, 2004; BETIKU, 2006). Esta característica pode ficar ainda mais acentuada quando é realizada a expressão concomitante de duas proteínas, como é o caso das lipases com suas Lifs cognatas.

Existem três principais técnicas utilizadas para expressão heteróloga de lipases e Lifs (QUYEN; VU; THU LE, 2012). A primeira é a expressão da lipase e Lif separadamente em *E. coli*, para então, com as proteínas purificadas, realizar o processo de dobramento *in vitro,* a fim de recuperar a lipase ativa. Esta técnica já foi utilizada para a expressão das lipases e foldases de *Pseudomonas* sp. cepa 109 (IHARA et al., 1995), *Pseudomonas cepacia* DSM 3959 (HOBSON et al., 1993), *Pseudomonas* sp. KWI 56 e *Chromobacterium viscosum* (TRAUB et al., 2001).

A segunda estratégia de expressão heteróloga é o sistema de co-expressão, no qual os genes da lipase e da foldase são clonados em plasmídeos diferentes e então inseridos conjuntamente em *E. coli* para superexpressão das duas proteínas, obtendo-se lipases ativas *in vivo*. Esta técnica já foi utilizada para a expressão de lipase e foldase de *P. aeruginosa,* cujos genes foram clonados nos vetores pET32Xa/LIC e pET29a(+), respectivamente (MADAN; MISHRA, 2010). Esta estratégia foi utilizada também por Martini et al. (2014) para co-expressão da lipase LipG9 e foldase LifG9, isoladas da mesma biblioteca metagenômica, com os genes

clonados em pET28a(+) e pT7-7, respectivamente, e também para a co-expressão da lipase LipBC e foldase LifBC de *B. contaminans* LTEB11, cujos genes foram clonados em pET28a(+) e pT7-7, respectivamente (ALNOCH et al., 2018). Dentro desta estratégia há a possibilidade de uso de plasmídeos de expressão dual, ou seja, plasmídeos que apresentam dois promotores num único plasmídeo para a expressão de duas proteínas simultaneamente. Esta técnica foi utilizada para expressão dos genes *lipA* (lipase) e *lipB* (foldase) de *Ralstonia* sp. M1 no vetor pELipA-LipB derivado do plasmídeo pET22b(+) (QUYEN; VU; THU LE, 2012). Wu et al. (2012) testaram diferentes plasmídeos para co-expressão de lipases e foldases, incluindo dois plasmídeos de expressão dual (pACYCDuet e pETDuet), e observaram que o tipo de plasmídeo pode influenciar na expressão da lipase ativa, sendo que a atividade de hidrólise observada nas lipases expressas a partir dos plasmídeos duais foram maiores. Em pETDuet-*lipA*-*lipB* a lipase apresentou uma atividade de 3200 U L^{-1} e em pACYCDuet-*lipA*-*lipB* apresentou uma atividade de 8500 U L^{-1}, atividades maiores se comparadas à atividade da lipase e foldase expressas em pET28a-*lipAB* (1300 U L^{-1}).

Outra técnica aplicada para expressão de lipases e foldases é o *autodisplay*, na qual as proteínas são expressas na membrana externa de *E. coli*. Nesta técnica, a proteína recombinante de interesse é transportada via um peptídeo sinal através da membrana interna; ao chegar no periplasma, a região C-terminal dobra-se em uma estrutura semelhante a uma porina na conformação β-barril; em seguida, a porção N-terminal é transportada para a superfície da célula através deste peptídeo β-barril, ficando ancorada na superfície da célula (JOSE; MEYER, 2007). A vantagem desta técnica é a possibilidade de uso das células inteiras ou frações das membranas externas em reações de interesse, além de conferir maior estabilidade à enzima, uma vez que elas ficam aderidas a membrana externa das bactérias (KRANEN et al., 2014; CHANG et al., 2017).

Kranen et al. (2014) co-expressaram a lipase e foldase de *B. cepacia* na superfície de *E. coli* através do método de *autodisplay*, e obtiveram lipases ativas para o substrato palmitato de *p*-nitrofenila, com atividade de 2,7 mU mL^{-1} aplicando as células inteiras, e 4,0 mU mL^{-1} aplicando frações das membranas de *E. coli*. Chang et al. (2017), também através do método de *autodisplay*, expressaram separadamente lipase e foldase de *B. cepacia* na membrana externa de *E. coli*; então, incubaram a fração de membrana contendo as lipases com a fração de membrana contendo as foldases e conseguiram recuperar a atividade da lipase. Os autores também

demonstraram que a atividade pode ser controlada pela razão entre lipase e foldase adicionada ao meio de reação durante o redobramento, sendo que a maior atividade foi alcançada na razão molar 1:3 (lipase:foldase) com atividade de 149 mU mg^{-1}, enquanto que na razão molar de 1:1(lipase:foldase) a atividade foi de 43 mU mg^{-1}.

Apesar das inúmeras técnicas de expressão de lipases com foldases existentes, a expressão heteróloga eficiente ainda é problemática, uma vez que, além da necessidade do mesmo nível de expressão de lipases e foldases, os hospedeiros bacterianos são incapazes de realizar muitas modificações pós-traducionais, como o correto dobramento das proteínas, fosforilação, glicosilação, e a correta formação de pontes dissulfeto (BORRELLI; TRONO, 2015).

2.2.4 Mecanismo de ação das Lifs

Para obtenção de uma grande quantidade de lipases ativas é necessário a compreensão de como essas lipases são ativadas pelas suas Lifs cognatas. No entanto, o mecanismo molecular de ação das Lifs ainda não é bem conhecido (PAUWELS et al., 2012). Os estudos sobre as interações de lipases e Lifs são escassos, pois determinar essas interações experimentalmente é algo complexo. Os estudos existentes são geralmente restritos às lipases e Lifs de *P. aeruginosa* e *B. glumae*. Apesar disso, é possível estabelecer alguns parâmetros sobre o mecanismo de interação Lip-Lif, a partir de alguns trabalhos que alcançaram com sucesso o redobramento *in vitro* de lipases a partir de lipases inativas ou presentes em corpos de inclusão.

As primeiras evidências de que as Lifs desempenham um papel crucial para obtenção de lipases ativas de *Pseudomonas* sp. e *B. glumae* foram dadas por Jørgensen, Skov e Diderichsen (1991) e Frenken et al. (1993), que obtiveram lipases inativas na ausência das Lifs.

Para estudar a especificidade das Lifs, El Khattabi e Ockhuijsen, (1999), realizaram a co-expressão da lipase de *B. glumae* e Lif de *P. aeruginosa*, e vice-versa, e ainda a co-expressão de Lif de *P. aeruginosa* com lipase de *Acinetobacter calcoaceticus*. Os autores não detectaram atividade das lipases, indicando a alta especificidade das Lifs, que não agem em lipases de espécies diferentes.

Uma característica observada foi que as Lifs não alteram a estrutura secundária nem a estrutura terciária das lipases, uma vez que, análises de dicroísmo

circular revelaram que não houve diferenças significativas no conteúdo de estrutura secundária das lipases inativas livres sem a presença de Lif e das lipases ativas depois da incubação com as Lifs (EL KHATTABI et al., 2000). Através de dados cristalográficos, observou-se que a lipase livre (não complexada com a Lif) de *B. glumae* é idêntica estruturalmente à lipase no complexo Lip-Lif, apresentando uma ponte dissulfeto, um íon cálcio ligado e uma ligação *cis*-peptídica. Porém, uma característica interessante é que a Lif apresenta uma mudança na estrutura secundária depois que se liga à lipase, ou seja, na região entre os minidomínios uma ou mais α-hélices se formam na Lif durante a formação do complexo (PAUWELS et al., 2006).

Desta forma, acredita-se que a ação das Lifs é semelhante à ação dos propeptídeos de algumas proteases, como a protease α-lítica e a subtilisina. Estas proteases são sintetizadas com um propeptídeo na região N-terminal, este propeptídeo age como uma chaperona intramolecular, contribuindo basicamente com informação estérica. Na presença dos propeptídeos, as proteases inativas conseguem ultrapassar a barreira energética, adotando uma conformação nativa com menor energia livre do que a sua conformação inicial não nativa (JASWAL et al., 2005).

Portanto, as Lifs são consideradas chaperonas estéricas, ou seja, elas provavelmente modificam o ambiente das nuvens eletrônicas da molécula da lipase. As Lifs auxiliam as lipases a diminuírem a barreira energética, fazendo com que elas entrem em uma via produtiva de dobramento para a forma ativa. Desta forma, as lipases que necessitam de Lifs não possuem a informação necessária na sua sequência de aminoácidos para realizar o auto dobramento na sua forma ativa (EL KHATTABI et al., 2000), e, devido a isto, ficam presas por uma barreira energética em uma conformação não-nativa. Assim, o papel das chaperonas moleculares é conferir estabilidade cinética às proteínas. O desdobramento térmico da lipase de *B. glumae* nativa é dependente da velocidade de aquecimento, provando que a lipase nativa é uma conformação cineticamente controlada, assim como as proteases dependentes de seus propeptídeos (PAUWELS et al., 2012).

Uma hipótese levantada em relação à ação das Lifs é que as moléculas de água estabilizam os intermediários não nativos das lipases e quando as Lifs se ligam a estes intermediários elas expelem as moléculas de água, principalmente das regiões hidrofóbicas da lipase, fazendo com que a interação entre Lif e lipase seja melhor estabelecida, e isso diminui a barreira energética necessária para alcançar a

conformação ativa (EL KHATTABI et al., 2000; PAUWELS et al., 2012). No entanto, faltam ainda evidências experimentais para comprovar esse mecanismo.

2.3 LIPASES E SUAS APLICAÇÕES EM BIOCATÁLISE

Os recentes avanços em biocatálise, com o uso de enzimas em diferentes bioprocessos, têm intensificado a busca por enzimas de interesse industrial. Isso ocorre porque a utilização destes biocatalisadores apresenta vantagens em relação aos catalisadores químicos, como maior qualidade do produto, menores custos de produção, menor desperdício e consumo de energia (SARROUH, 2012). Além disso, há uma tendência ao desenvolvimento de processos ambientalmente corretos, seguros e sustentáveis, e a utilização de enzimas é um caminho para alcançar este objetivo (ALBARRÁN-VELO; GONZÁLEZ-MARTÍNEZ; GOTOR-FERNÁNDEZ, 2018; SARMAH et al., 2018). Até 2030, espera-se que 40% dos processos de síntese química sejam substituídos por processos enzimáticos (FERRER et al., 2015).

Dentre os biocatalisadores, as lipases compõem um dos grupos enzimáticos mais importantes utilizados em biotecnologia, devido a sua multifuncionalidade na catálise de diferentes tipos de reações como esterificação, interesterificação e transesterificação, (JAEGER et al., 1994; JAEGER; EGGERT, 2002). A grande versatilidade desta classe de enzimas se deve ao fato de que, além de naturalmente hidrolisarem ligações do tipo éster em triacilgliceróis, gerando ácidos graxos livres e glicerol, as lipases podem aceitar como substrato uma ampla gama de compostos, dependendo do meio e condições em que atuam. As lipases apresentam ainda quimio, regio e enantiosseletividade (GUPTA; GUPTA; RATHI, 2004). Além disso, algumas lipases apresentam características imprescindíveis para aplicação industrial como termoestabilidade, estabilidade em uma ampla faixa de pH, estabilidade em solventes orgânicos, entre outras (SARMAH et al., 2018).

As lipases pertencem ao terceiro grupo de enzimas hidrolíticas mais comercializadas mundialmente, atrás somente das carboidrases e proteases (LI et al., 2012). O mercado de lipases microbianas (bacterianas e fúngicas) foi avaliado em USD 400,6 milhões em 2017 e está projetado para atingir USD 590,2 milhões até 2023, crescendo a uma taxa composta anual de 6,8% a partir de 2018. As principais áreas de aplicação das lipases comerciais são na indústria de detergentes, na produção de ração animal, produtos lácteos, produtos de panificação, produtos de

confeitaria, biocombustíveis e papel e celulose (TABELA 3) (MICROBIAL lipases market worth 590.2 million USD by 2023, 2018).

TABELA 3 - PRINCIPAIS ÁREAS DE APLICAÇÃO DE LIPASES

Áreas	Aplicações	Referências
Indústria de detergentes	Composição de detergentes, sabões e outros agentes de limpeza, agindo em reações de hidrólise de gorduras e óleos	Hasan, Shah e Hameed (2006)
Indústria de alimentos	Hidrólise de gorduras do leite e maturação de queijo Modificação de gorduras para a produção de manteigas Melhoria de aromas e sabores de bebidas e produtos de panificação Fabricação de produtos nutracêuticos por reações de hidrólise e transesterificação de óleos e gorduras Síntese de ésteres de aromas a partir de ácidos graxos de cadeias curtas e médias	Aravindan (2007); Ferreira-Dias et al. (2013)
Indústria de papel e celulose	Controle do *pitch* (depósitos de composição graxa derivados do processamento da madeira) na fabricação de papel	Bajpai (1999)
Indústria de biodiesel	Reações de esterificação de ácidos graxos e transesterificação de óleos	Tan et al. (2010)
Indústria farmacêutica	Síntese assimétrica, como resolução cinética de compostos racêmicos (álcoois, ácidos, ésteres, aminas), e dessimetrização de compostos pró-quirais	Gotor-Fernández, Brieva e Gotor (2006); García-Urdiales, Alfonso e Gotor (2005)

Basicamente, as reações catalisadas por lipases são divididas em dois grupos: reações de hidrólise, que ocorrem em meio aquoso, e reações de síntese, que ocorrem na presença de solventes orgânicos ou em outros ambientes aquo-restritos. As reações de síntese são classificadas em reações de esterificação, aminólise e transesterificação, sendo a última dividida em reações de interesterificação, alcoólise, acidólise e lactonização (KAGEYAMA; NIHIRA; YAMADA, 1990; VILLENEUVE et al., 2000).

Uma das áreas de maior interesse para aplicação de lipases é na indústria farmacêutica com as reações enantiosseletivas (RAY, 2012). A produção de compostos enantiomericamente puros é a área mais importante no desenvolvimento de drogas, pois em torno de 80% de todos os medicamentos desenvolvidos são moléculas quirais (BHARDWAJ; GUPTA, 2017).

Além disso, nas últimas décadas, é crescente a aplicação de lipases em reações não convencionais, como condensação aldólica, reação de Hantzsch, reação de Canizzaro, reação de Mannich, reação de Baylis-Hillman, condensação

Knoevenagel, adição Michael, reação de Ugi, oxidação (DWIVEDEE et al., 2018) e reação de amidação (LIU; NAG; SHAW, 2001).

Todas estas características tornam as lipases cada vez mais interessantes, revelando novas aplicações e ampliando o interesse científico e industrial neste grupo de biocatalisadores (DWIVEDEE et al., 2018). A TABELA 4 traz alguns exemplos de reações catalisadas por lipases, dentre elas, algumas reações não convencionais.

Apesar da grande variedade de reações que podem ser catalisadas por lipases, a diversidade destas enzimas que efetivamente são aplicadas é baixa. Como observado na TABELA 4, é mais comum o uso de lipases comerciais ou lipases já bem conhecidas, como as lipases A e B de *C. antarctica* e lipases de *Pseudomonas* sp. e *Burkholderia* sp. Isso evidencia o potencial existente de exploração de lipases mais eficientes para aplicação em determinadas reações.

Para a prospecção e isolamento de novas lipases, existem algumas estratégias modernas, como a exploração da biodiversidade através da metagenômica, utilizada neste trabalho, e que será descrita a seguir.

2.4 METAGENÔMICA COMO FERRAMENTA DE PROSPECÇÃO DE LIPASES

O termo metagenômica surgiu em 1998 e foi proposto por Handelsman e colaboradores (HANDELSMAN et al., 1998), com o intuito de obter acesso global da biodiversidade do solo, através do isolamento direto do DNA dos organismos contidos neste ambiente. A metagenômica maximiza as chances de isolamento de sequências de DNA, codificadoras de enzimas e moléculas bioativas, provenientes de micro-organismos não cultiváveis em laboratório, uma vez que menos de 0,1% dos micro-organismos presentes no solo são passíveis de isolamento e cultivo em laboratório (TORSVIK; SØRHEIM; GOKSØYR, 1996). Técnicas clássicas para obtenção de culturas puras são muitas vezes demoradas, difíceis e desafiadoras para micro-organismos que possuem requisitos metabólicos complexos (YARZA et al., 2014).

TABELA 4 - EXEMPLOS DE REAÇÕES CATALISADAS POR LIPASES

Lipase/organismo	**Reação**	**Meio reacional**	**Referência**
Lipase A / *Candida antarctica* Lipase / *Rhizopus niveus*	Aminólise para resolução cinética de (*R,S*) 1-fenil-etilamina	*n*-Hexano	De Castro; Gago (1998)
Lipase B / *Candida antarctica* (Novozym 435 - Novozyme)	Amidação de ácidos graxos com dietanolamina	Acetonitrila	Liu, Nag e Shaw (2001)
LipL / *Pseudomonas* sp.	Lactonização para transesterificação de ésteres de ácidos graxos ω-hidroxi para formar lactonas macrocíclicas	*n*-Hexano	Omori et al. (2005)
Lipase / *Pseudomonas cepacia*	Transesterificação para resolução cinética de (*R,S*)-2-alcanol	Acetato de isopropenila	Kanamori et al. (2005)
LipB68 / *Pseudomonas fluorescens*	Transesterificação de óleo de soja para produção de biodiesel	*n*-Heptano	Luo et al. (2006)
Lipase / *Pseudomonas stutzeri* LC2-8	Transesterificação para resolução cinética de (*R,S*)-1-feniletanol	*n*-Hexano	Cao et al. (2012)
Lipase / *Burkholderia cepacia* Lipase / *Mucor javanicus*	Reação Morita-Baylis–Hillman entre 4-nitrobenzaldeído e 2-ciclohexeno-1-ona, estabelecendo ligação C-C	Água/DMSO	Kapoor; Majumder; Gupta (2014)
Lipase A / *Aspergillus niger* (Amano)	Acetilação de celulose nanofribilada	DMSO	Božič et al. (2015)
PPL / Lipase pancreática de porco	Adição 1,2-tiol para a síntese de *N,S*-acetal	Dimetoxietano	Albuquerque et al. (2018)
Lipase / pancreática de porco tipo II, *Candida rugosa*, *Pseudomonas fluorescens*, *Burkholderia cepacia*, *Rhizopus oryzae*, *C. cylindracea*, *C. antarctica*, *Mucor miehei*	Reação de Mannich com cetona, aldeído e amina para formar compostos β-amino-cetona	Água	Li et al. (2009)
Lipase B / *Candida antarctica* (Novozym 435 - Novozyme)	Oxidação de álcoois salicílicos a salicilaldeídos	Acetonitrila	Zhao et al. (2017)
Lipase B / *Candida antarctica* (Novozym 435 - Novozyme)	Oxidação Baeyer-Villiger de levoglucosenona derivada de celulose em (*S*)-γ-Hidroximetil-α,β-Butenolídeo	Tampão/Peróxido de hidrogênio	Teixeira et al. (2016)

Na técnica de metagenômica, os fragmentos de DNA obtidos são inseridos em vetores e expressos em hospedeiro heterólogo, geralmente *E. coli*, gerando assim uma coleção de clones, denominada de biblioteca metagenômica (FIGURA 5). Essa biblioteca metagenômica pode então ser submetida a identificação de genes de interesse, através de triagem baseada em sequência de DNA, ou, os clones podem ser submetidos a triagem funcional para identificação de clones com produção de moléculas de interesse como enzimas, biosurfactantes e antibióticos (HANDELSMAN et al., 1998; HANDELSMAN, 2004; SOLIMAN et al., 2007).

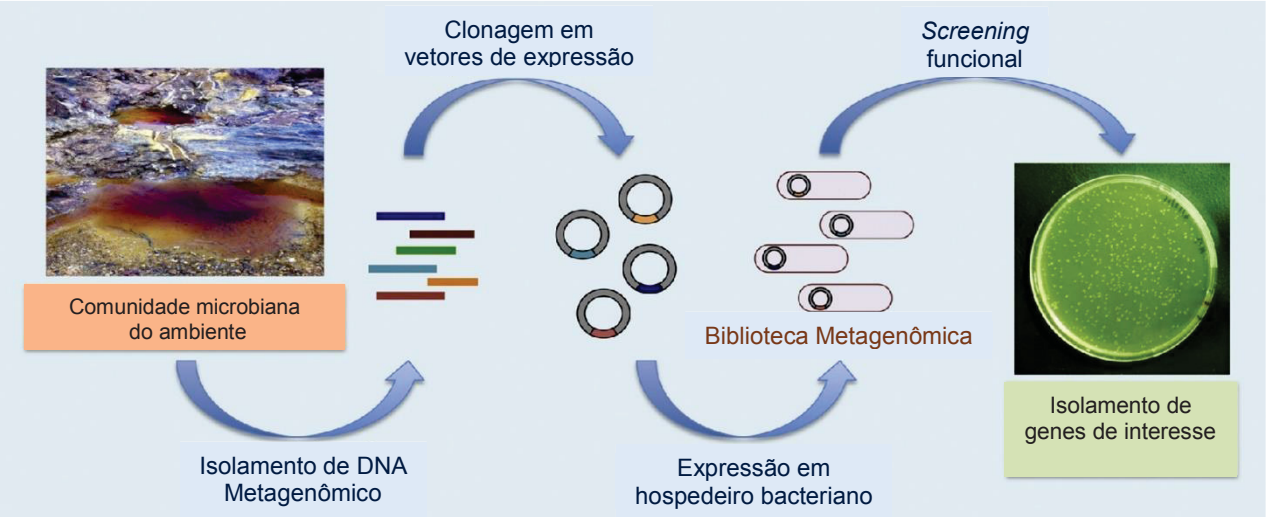

FIGURA 5 - ESQUEMA DA CONSTRUÇÃO DE UMA BIBLIOTECA METAGENÔMICA
FONTE: Adaptado de Mirete, Morgante e González-Pastor (2016).

Atualmente a metagenômica é aplicada para isolamento de DNA de diversos ambientes, sendo que o conteúdo metagenômico de aproximadamente 2192 diferentes ambientes ao redor do mundo já foi analisado, dentre os quais estão diversos ambientes terrestres, marinhos, água doce, além de ambientes extremos como lagos salinos não marinhos e alcalinos, sistemas de drenagem de minas ácidas, lamas de tratamento de águas residuais e microbiomas associados a eucariotos (esponja marinha, intestinos de cupins e minhocas, guelras de camarão, rúmen e microbiota humana) (FERRER et al., 2015). Assim, a maior parte dos ambientes representativos de diferentes *habitats* já foram amostrados. No entanto, enzimas foram isoladas e parcialmente caracterizadas em apenas 256 (11,6%) dos ambientes amostrados, comprovando que, embora os ambientes naturais sejam ricos em biodiversidade, eles ainda precisam ser mais bem estudados para obtenção de novas enzimas (FERRER et al., 2015).

As enzimas lipolíticas (lipases e esterases) são as enzimas mais representativas de bibliotecas metagenômicas. De acordo com Ferrer et al. (2015), de um total de 6038 clones ativos, enzimas ou sequências codificadoras, isolados e caraterizados dos 256 ambientes onde enzimas foram encontradas por prospecção metagenômica, 68% destas enzimas são lipases ou esterases, sendo que do total, 4034 foram selecionadas por triagem funcional e 77 por triagem baseada em sequência. Esta característica também foi confirmada pelo trabalho de revisão de Berini et al. (2017), que avaliaram 332 enzimas isoladas de metagenômica no período de janeiro de 2014 a março de 2017, e desse total, 161 enzimas (48%) eram lipases e esterases.

Os ambientes mais comuns onde lipases e esterases foram encontradas, a partir de um estudo com a análise de 288 sequências destas enzimas derivadas de diferentes bibliotecas metagenômicas, foram em ambiente de solo (35,7%), ambientes marinhos (31,7%), microbiota de diversos hospedeiros (16,4%), água doce (8%), composto (adubo) (5,1%) e águas residuárias 2,9%. Foi possível observar uma diversidade nas sequências, tendo sido encontrados representantes das 14 famílias até então documentadas (FERRER et al., 2016).

2.4.1 Métodos de triagem de bibliotecas metagenômicas

A descoberta de novas enzimas por meio da metagenômica está atrelada a dois principais fatores: a eficiência dos métodos de triagem e a diversidade genética da amostra coletada (XING; ZHANG; HUANG, 2012). A etapa de identificação de clones contendo genes de interesse é um dos desafios da metagenômica, pois encontrar um método de triagem de alta eficiência para a atividade desejada não é simples. Uma vez que as bibliotecas metagenômicas são, em geral, grandes (milhares de sequências de DNA), é necessário o desenvolvimento de métodos de triagem em grande escala e economicamente viáveis (CHOI et al., 2014). Estima-se que são encontrados apenas aproximadamente 0,08% de clones positivos em relação ao total de clones em uma biblioteca metagenômica, através de protocolos de triagem simples (FERRER et al., 2015).

A identificação de clones com genes de interesse em uma biblioteca metagenômica é realizado principalmente através de dois métodos: triagem funcional

e triagem baseada em sequência, sendo que ambos apresentam vantagens e desvantagens.

2.4.1.1 Triagem funcional

A triagem funcional é o método mais utilizado, pois permite a detecção da atividade de novos catalizadores não sendo necessário conhecer a sequência do gene *a priori* (ALMA'ABADI; GOJOBORI; MINETA, 2015; MADHAVAN et al., 2017). É uma abordagem baseada no fenótipo, onde a atividade desejada pode ser detectada por métodos simples, principalmente por desenvolvimento de coloração resultante de clivagem de determinados substratos (GUAZZARONI; SILVA-ROCHA; WARD, 2015).

Uma das desvantagens dessa estratégia é a possível falha na expressão gênica, dependendo do organismo heterólogo utilizado (MADHAVAN et al., 2017), podendo apresentar baixos níveis de expressão devido à incompatibilidade da expressão heteróloga (CHOI et al., 2014). Essas incompatibilidades na expressão são devidas, principalmente, a dificuldades no reconhecimento do promotor, tradução ineficiente da proteína e falta de modificações pós-traducionais necessárias para a obtenção de proteínas ativas (UCHIYAMA et al., 2005).

Atribui-se o fato de lipases e esterases serem os biocatalisadores mais encontrados em bibliotecas metagenômicas principalmente à facilidade de se proceder a triagem funcional (KENNEDY et al., 2011; SIMON; DANIEL, 2011). Técnicas de triagem funcional já foram utilizadas com sucesso para detectar genes que codificam para várias lipases em estudos funcionais metagenômicos (GLOGAUER et al., 2011; REYES-DUARTE; FERRER; GARCÍA-ARELLANO, 2012; FERRER et al., 2015).

Existem muitos métodos de triagem para detecção de atividade de lipases e esterases, nos quais já foram testadas mais de 200 diferentes moléculas de substratos (TABELA 5) (PEÑA-GARCÍA et al., 2016).

Um dos métodos mais simples e utilizados para detecção de lipases é o cultivo dos clones em placa de Petri, com meio sólido enriquecido com diferentes substratos oleosos para verificação de halo de hidrólise. Também há a utilização de microplacas para as reações com diferentes substratos e identificação de atividade por reação colorimétrica (HOSOKAWA et al., 2015). No entanto, estas abordagens quando utilizadas na forma tradicional são limitadas pela baixa quantidade de clones positivos

encontrados, e por serem métodos trabalhosos e demorados (HOSOKAWA et al., 2015).

TABELA 5 - MÉTODOS DE TRIAGEM FUNCIONAL PARA LIPASES

Método	**Base do método**	**Substrato**	**Referência**
Formação de halo de hidrólise	Formação de halo de hidrólise ao redor das colônias em placas com ágar	Triacilgliceróis naturais: tributirina, tricaprilina, trioleína, azeite de oliva	Glogauer et al. (2011)
Ensaio cromogênico	Formação de colônia com coloração. Hidrólise de esteres de *p*-nitrofenil em microplaca	1-naptil palmitato Ésteres de *p*-nitrofenila	Korman et al. (2013)
Ensaio fluorimétrico	Formação de halo fluorescente laranja ao redor das colônias em placas com ágar e corante fluorescente Rodamina B; Medida da fluorescência	Triacilgliceróis naturais: tributirina, tricaprilina, trioleína, azeite de oliva Ésteres de umbeliferil e resorufina para reações de hidrólise e enantiosseletivas.	Kouker; Jaeger (1987) De Monpezat et al. (1990) Shimura; Tsuzuki; Suzuki, (1991)
Espectrometria de massa	Uso de substratos isotopicamente marcados na forma de pseudo-enantiômeros ou compostos pseudo-proquirais	Compostos enantioméricos	Reetz et al. (1999)
Ensaio de adrenalina	Retrotitulação com adrenalina para detectar, por colorimetria 1,2-dióis, 1,2-aminoálcoois e α-hidroxicetonas, produtos da reação de catálise enzimática	Polióis acetatos	Wahler et al. (2004)
Seleção de crescimento *in vivo*	Mistura de ésteres pseudo-racêmicos, com um composto servindo de fonte de carbono e outro servindo como composto tóxico	Compostos enantioméricos	Fernández-Álvaro et al. (2011)
Ensaio específico para ácido acético	Hidrólise de um éster acetato liberando ácido acético	Compostos racêmicos acetato/ ésteres quirais	Baumann; Stürmer; Bornscheuer (2001)
Atividade por pH indicador	Produção de ácido carboxílico após a hidrólise do éster, utiliza um indicador, tipicamente *p*-nitrofenol, vermelho de fenol ou azul de bromotimol	Compostos enantioméricos Ácidos carboxílicos β-arilalquil	Janes; Kazlauskas (1997) Fernández-Álvaro (2010)
Ensaio de atividade de síntese	Transesterificação de um éster de vinila e um álcool	Ésteres de vinila	Konarzycka-Bessler; Bornscheuer (2003)
Microfluídico baseado em gotas	Co-encapsulamento de células produzindo moléculas alvo com uma molécula repórter como uma substância fluorescente	Dicaprilato de fluoresceína Compostos enantioméricos	Hosokawa et al. (2015) Ma et al. (2018)
Sistema genético	Baseados em circuitos genéticos artificiais, o acúmulo de fenol dentro das células pela ação das lipases, induzem uma cascata de eventos genéticos produzindo um sinal de fluorescência celular.	Substratos-fenil sintéticos	Choi et al., (2014)

Assim, os métodos de triagem de alto desempenho (*High throughput screening*, HTS) têm sido estudadas e desenvolvidas. Estes métodos baseiam-se na

automação dos processos tradicionais de triagem (XIAO; BAO; ZHAO, 2015). Um método de alto desempenho deve permitir a determinação rápida e confiável de forma a ser reprodutível principalmente com uma frequência de 10^3 a 10^4 amostras por dia (SCHMIDT; BORNSCHEUER, 2005). Desta forma, melhorar as técnicas de triagem de alto desempenho para enzimas pode trazer vantagens significativas (PEÑA-GARCÍA et al., 2016).

Dentre os métodos citados na TABELA 5, podemos destacar os métodos de sistema genético de triagem de enzimas e microfluídico baseado em gotas, pois são métodos de alto desempenho que se apresentam como uma ferramenta eficiente para a avaliação do comportamento celular em células únicas.

O sistema genético de triagem de enzimas ocorre por detecção de fluorescência de células únicas, e quando combinado com citometria de fluxo, permite explorar mais de 10^7 células por hora (CHOI et al., 2014). Foi confirmado que dois substratos marcados com fenol (fenil fosfato e organofosfatos) e três substratos marcados com *p*-nitrofenol (*p*-nitrofenil butirato, *p*-nitrofenil celotriosídeo e metil paration) podem ser usados para rastrear enzimas de metagenômica (KIM et al., 2015).

No método microfluídico baseado em gotas, as células são co-encapsuladas com o substrato, produzindo as proteínas-alvo com uma molécula repórter, como por exemplo, uma substância fluorescente. Essa compartimentalização das células pode ser usada para isolar reações individuais, eliminar o risco de contaminação cruzada e promover a mistura uniforme dos reagentes existentes dentro da gota (HOSOKAWA et al., 2015). Recentemente este método foi utilizado para seleção de mutantes da esterase de *Archaeoglobus fulgidus* de uma biblioteca de evolução dirigida. A seleção, realizada para reações enantioseletivas, baseou-se na avaliação de dois canais de reação simultaneamente. Este método permite a triagem de aproximadamente 10^7 variantes de enzimas por dia e pode ser usado para identificação de lipases enantioespecíficas, quimioespecíficas e regioespecíficas (MA et al., 2018).

2.4.1.2 Triagem baseada em sequência

Na triagem baseada em sequência, os genes são identificados por PCR ou hibridização utilizando *primers* e sondas derivadas de regiões conservadas de genes conhecidos (HANDELSMAN, 2004). Como essa técnica tem como alvo regiões

internas dos genes, como domínios e motivos conservados, as regiões que flanqueiam estes motivos precisam ser clonadas para se obter o gene inteiro. Caso a biblioteca já tenha sido sequenciada, utilizam-se *primers* para regiões próximas ao gene de interesse (UCHIYAMA; MIYAZAKI, 2009). A triagem baseada em sequência não requer a expressão dos genes clonados em hospedeiro heterólogo. Portanto, consegue contornar as limitações de expressão neste sistema (YUN; RYU, 2005).

A consolidação das técnicas de sequenciamento de DNA de nova geração, como sequenciador de genoma 454, plataforma SOLiD, o analisador de genoma *Illumina*, a plataforma *Ion Torrent*, PacBio e Oxford Nanopore, permitiu a análise de um enorme volume de dados de bibliotecas metagenômicas, dos mais variados ambientes. Isso gerou uma grande expansão dos bancos de dados de genes de proteínas funcionais hipotéticas (AMBARDAR et al., 2016; PEÑA-GARCÍA et al., 2016; KUSNEZOWA; LEICHERT, 2017; MADHAVAN et al., 2017).

No entanto, a triagem baseada em sequência também apresenta algumas desvantagens. Apenas novas variantes das mesmas classes funcionais de enzimas podem ser encontradas, pois o método está baseado em homologia de sequência (SCHLOSS; HANDELSMAN, 2003; LEE et al., 2010; SIMON; DANIEL, 2011). Além disso, nas bibliotecas metagenômicas, o DNA das espécies mais abundantes fica melhor representado do que dos membros mais raros da comunidade, o que diminui ainda mais a probabilidade de encontrar novas enzimas e aumenta as chances de se encontrar produtos gênicos com alta homologia (entre 50% a 98%) com sequências já conhecidas (TUFFIN et al., 2009).

Um outro grande problema desta abordagem é a baixa qualidade das informações das sequências de metagenomas depositadas, com erros de sequenciamento (MARTÍNEZ-MARTÍNEZ et al., 2013) e dados incompletos sobre a função das proteínas (FERNÁNDEZ-ARROJO et al., 2010; MARTÍNEZ-MARTÍNEZ et al., 2013). Isso faz com que a análise de bibliotecas metagenômicas em busca de enzimas pelas vias funcional e sequencial resultem em dados divergentes (TUFFIN et al., 2009).

A expansão do uso da triagem baseada em sequência depende de uma revisão criteriosa das informações dos bancos de dados de genes e do desenvolvimento de novas ferramentas de bioinformática, capazes de predizer a estrutura da proteína e atividade catalítica com base na sequência primária do gene (TUFFIN et al., 2009).

Finalmente, é importante ressaltar que a triagem baseada em sequência não dispensa a caracterização experimental da função das proteínas (KUSNEZOWA; LEICHERT, 2017). Porém, como a velocidade de geração de dados de novas sequências é muito grande, necessita-se de uma abordagem combinada dos dois tipos de triagem, a funcional e a sequencial (TUFFIN et al., 2009).

2.4.2 Biblioteca metagenômica SCGA e as lipases LiC12, LipG9 e LipMF3

A biblioteca metagenômica SCGA foi construída por Glogauer et al. (2011), a partir de amostras de solo contaminado com gordura animal, presente nas margens de uma lagoa de tratamento de efluentes de uma indústria de processamento de carnes e laticínios, na cidade de Carambeí - PR. Esta biblioteca foi construída com fragmentos de DNA com cerca de 36 kb, clonados no vetor pCC2FOS, gerando uma biblioteca metagenômica com aproximadamente 500.000 clones em *E. coli* EPI300. A biblioteca está depositada no Departamento de Bioquímica e Biologia Molecular da Universidade Federal do Paraná.

Esta biblioteca foi submetida a uma triagem funcional através do cultivo dos clones em placas de Petri com meio LB (Luria Bertani) enriquecido com diferentes triacilgliceróis para identificação de halos de hidrólise. Essa seleção foi realizada em três etapas subsequentes com os substratos tributirina, tricaprilina e trioleína. Na primeira etapa, com tributirina, foram identificados 2661 clones; destes,127 clones apresentaram halo de hidrólise contra tricaprilina, e por último, dos 127 clones, apenas 32 apresentaram halo de hidrólise para trioleína.

Os clones foram selecionados de acordo com o tamanho do halo de hidrólise. A partir do último grupo de 32 clones foram isolados os clones C12 e G9, sendo que o clone C12, que codifica para a lipase LipC12, foi objeto de estudo de Glogauer et al. (2011) e o clone G9, que codifica para a lipase LipG9 foi estudado por Martini et al. (2014).

LipC12 possui uma massa molecular de 33 kDa e apresenta 72% de identidade com a lipase putativa de *Yersinia enterocolitica* subsp. *palearctica* Y11. A análise filogenética classificou LipC12 como pertencente à família I.1 (GLOGAUER et al., 2011). Além disso, LipC12 já teve a sua estrutura tridimensional determinada por cristalografia (MARTINI et al., 2012). Outra característica fundamental é que LipC12 se dobra em sua forma nativa sem a necessidade de uma Lif, facilitando a sua

expressão. LipC12 apresenta altos níveis de expressão em *E. coli* atingindo 20% do total de proteínas expressas e é de fácil purificação (>95% de pureza).

A caracterização de LipC12 livre em meio aquoso revelou que a enzima apresenta elevada atividade de hidrólise (1722 U mg^{-1} em óleo de oliva) e mantém atividade e estabilidade em uma ampla faixa de pH (6,5 - 11) e temperatura (0 ºC – 60 ºC). A enzima também se mostrou estável em soluções aquosas contendo diferentes solventes orgânicos polares (metanol, etanol, propanol, acetona, DMSO) quando incubada por 48 h em concentrações de até 30% dos solventes, mantendo 100% da atividade inicial em todas as soluções (GLOGAUER et al., 2011).

Nos estudos de imobilização de LipC12, através de ligação covalente ao suporte Immobead 150, foram alcançadas altas conversões na produção de biodiesel (99% de conversão em oleato de etila em 1 h de reação) (MADALOZZO et al., 2015a). LipC12 imobilizada em Immobead apresenta enantiosseletividade e é *sn*-1,3-específica, portanto, pode ser utilizada em aplicações mais nobres, como a resolução de misturas racêmicas para a produção de compostos quirais e para a síntese de lipídeos estruturados. A capacidade de produção de lipídeos estruturados de LipC12 imobilizada foi verificada pela transesterificação ácida do azeite de oliva com ácido caprílico, com produção de um lipídeo de baixa caloria do tipo MLM contendo 23% de ácido caprílico nas posições *sn*-1 e *sn*-3 (MADALOZZO et al., 2016).

A segunda enzima caracterizada da biblioteca SCGA, a lipase LipG9, necessita de uma Lif para seu correto enovelamento; portanto, foi realizada a co-expressão dos genes *lipG9* e *lifG9* para caraterização desta enzima por Martini et al. (2014). LipG9 e LifG9 apresentam 96% de identidade com a lipase de *Aeromonas veronii* B565 e 77% de identidade com a foldase do mesmo microrganismo. Através de análise filogenética LipG9 foi classificada na família I.1.

LipG9 apresenta alta atividade de hidrólise com 1800 U mg^{-1} em tributirina, 1500 U mg^{-1} em tricaprilina e 820 U mg^{-1} em trioleína; portanto, caracteriza-se como uma lipase verdadeira. A enzima livre mantém atividade em uma ampla faixa de pH (6,0 a 9,0) e temperatura (10 ºC a 50 ºC). LipG9 já foi aplicada para reações de esterificação e resolução de compostos racêmicos, comprovando o seu potencial para aplicação em biocatálise (ALNOCH et al., 2015; BANDEIRA et al., 2016).

A biblioteca SCGA revelou duas lipases promissoras que serviram de base para diversos estudos. Além destas lipases, a triagem funcional desta biblioteca ainda apresentou outros clones com atividade lipolítica. Um deles, denominado D12,

apresentou halo de hidrólise para tributirina e tricaprilina. Devido à ausência de halo para a trioleína, inicialmente pensou-se que D12 estaria relacionado à produção de uma esterase. Posteriormente, verificou-se que este clone codifica para uma lipase denominada LipMF3, e não uma esterase, e os resultados referentes à clonagem, expressão e caracterização desta nova enzima estão detalhados no Capítulo 2 desta tese.

2.4.3 Outras lipases isoladas de bibliotecas metagenômicas

Além das lipases da biblioteca SCGA, outras lipases isoladas de bibliotecas metagenômicas apresentam caraterísticas interessantes para aplicações em processos industriais. No entanto, a maioria dos artigos que reportam lipases de metagenômica trazem apenas a caracterização bioquímica destas enzimas, sendo que poucos trabalhos são realizados com o intuito de aplicar estas enzimas em reações de biocatálise. Isto foi apontado por Ferrer et al. (2016), que reportaram que, dentre as 288 sequências de lipases e esterases estudadas, apenas 5 foram testadas em reações de síntese.

Na TABELA 6 estão descritas algumas lipases e esterases provenientes de metagenômica que foram aplicadas em diferentes reações e, que, portanto, possuem um potencial de aplicação industrial. Esta tabela foi elaborada com base em uma busca no portal *Web of Science*. Através desta pesquisa, foi possível identificar 24 lipases ou esterases de metagenômica que foram aplicadas em reações de biocatálise, com a finalidade de demonstrar a possibilidade de aplicação biotecnológica. Dentre elas, 11 são lipases e 13 são esterases.

Algumas observações podem ser feitas a partir dos dados apresentados na TABELA 6. Em relação à biodiversidade, nota-se que a maioria das enzimas possui menos de 50% de identidade com enzimas de organismos já conhecidos e somente 3 enzimas apresentaram identidade >90% (2 lipases e 1 esterase) com lipases de micro-organismos conhecidos. Em relação às famílias, poucas enzimas (5 lipases) pertencem à família I, de lipases verdadeiras, sendo a maioria (12 esterases) pertencentes às famílias IV, V, VII e VIII. Isso mostra que a abordagem metagenômica é eficiente em isolar novas enzimas. Além disso, a maioria das enzimas foram isoladas de amostras de solo, com algumas sendo de solo contaminado (com petróleo e gordura animal), ou sedimentos (marinho, costeiro e zona entremarés).

TABELA 6 - ENZIMAS LIPOLÍTICAS OBTIDAS POR METAGENÔMICA COM APLICAÇÃO EM BIOCATÁLISE

(continua)

Área Farmacêutica

Enzima	Fonte de DNA	Identidade	Classificação filogenética	Atividade de hidrólise	Imobilização	Aplicação	Referência
Esterase Est25	Solo	48% com esterase de *Bacillus subtilis*	Não informado	103 U mg^{-1} em acetato de *p*-nitrofenila	Não fez	Hidrólise do isômero (*R*) de Cetoprofeno (eep -4,6%). Est25 mutante – aumento do *E* de 1 para 60 para o isômero (*S*)	Kim et al. (2006, 2017)
Lipase LipCE	Solo contaminado com petróleo	91% com lipase de *Pseudomonas fluorescens* B68	Família I.3	2021 U mg^{-1} em caprato de *p*-nitrofenila	Não fez	Hidrólise do isômero (*R*) de Ibuprofeno (ee>91% e *E* de 55)	Elend et al. (2006)
Esterases EstAT1 EstAT11	Sedimentos costeiros do Ártico	EstAT1 - 43,3% com lipase de *Geobacter* sp. EstAT11 - 38,8% com lipase de *Geobacter* sp.	Família IV	EstAT1 - 200 U mg^{-1} em butirato de *p*-nitrofenila EstAT11 - 60 U mg^{-1} em caproato de *p*-nitrofenila	Não fez	Hidrólise de (*S*) ofloxacina (levofloxacina) EstAT1 - 2,6% de conversão, eep 11,9%. EstAT11 - 12,9% de conversão, eep 70,3%	Jeon et al. (2009)
Esterase EstCS2	Composto	45% com carboxilesterase de *Haliangium ochraceum*	Família VII	Maior atividade relativa em caproato de *p*-nitrofenila	Não fez	Hidrólise do isômero (*R*) de Cetoprofeno (eep -0.07%) Hidrólise de linalil acetato analisada por TLC. Degradação de poliuretano em placa com ágar	Kang et al. (2011)
Lipase LipS	Solo	100% com esterase de *Symbiobacterium thermophilum*	Família desconhecida	12 U mg^{-1} em caprilato de *p*-nitrophenila	Enzima liofilizada	Hidrólise de (*R*)-fenil-éster de ibuprofeno (ee 99%) Síntese de 1-propil laurato e 1-tetradecil miristato	Chow et al. (2012)
Esterase EstEH112	Sedimentos de zona entremarés	48% com esterase de *Marine gamma proteobacterium*	Família IV	Atividade relativa em butirato de *p*-nitrofenila	Não fez	Síntese de 8 álcoois terciários *E* variando de 1 a 4	Oh et al. (2012)
Esterase Est22	Chorume	46% com esterase de *Methylobacterium* sp.	Família VIII	60 U mg^{-1} em butirato de *p*-nitrophenila	Não fez	Hidrólise de derivados de cefalosporina	Mokoena et al. (2013)

(continuação)

Enzima	Fonte de DNA	Identidade	Classificação filogenética	Atividade de hidrólise	Imobilização	Aplicação	Referência
Esterases EstP2K EstF4K	Solo e água de rio contaminado	EstF4K - 83% com EstA3 de organismo não cultivado de solo EstP2K - 37% com lipase de *Neisseria elongata*	Família VIII	EstF4K - ~700 U mg^{-1} em butirato de *p*-nitrofenila e EstP2K - ~40 U mg^{-1} em caprilato de *p*-nitrofenila	Não fez	EstF4K - Hidrólise de (−)-Metil 3-fenilglicidato (ee de 64,3% e conversão de 49,0%). EstP2K - Hidrólise de (+)-Metil 3-fenilglicidato (ee de 70,8% e conversão de 69,9%)	Ouyang et al. (2013)
Lipase LipG9	Solo contaminado com gordura	96% e 84% com lipase e foldase de *Aeromonas veronii* B565	Subfamília I.1	1200 U mg^{-1} em óleo de oliva	Imobilizada em Accurel	Transesterificação de (*R,S*) 1-fenil-1-etanol e hidrólise do éster análogo acetato de 1-feniletila, (ee > 95%) para o produto (*R*)-acetato de 1-feniletila e para o substrato (*S*)-1-fenil-1-etanol e (*E*) >200 Transesterificação de 6 álcoois alifáticos secundários, apresentando conversões de 19–59% e ee de 26%-88% para os álcoois e ee de 30%-96% para os ésteres, *E* de 4-63	Alnoch et al.(2015), Bandeira et al. (2016)
Lipase LipC12	Solo contaminado com gordura	72% com lipase de *Yersinia enterocolitica*	Subfamília I.1	1722 U mg^{-1} em óleo de oliva	Imobilizada em Epoxi-agarose funcionalizada com aldeído C18	Hidrólise para desacetilação regioseletiva de D-glucal peracetilado, com 69% de monodeacetilado C-3 e 81% de conversão	Alnoch et al. (2016)
Lipase LipR1	Solo	Não informado	Não informado	8756 U mg^{-1} em laurato de *p*-nitrofenila	Não fez	Transesterificação de 5 álcoois secundários: (*R,S*)-1-Indanol, (*R,S*)-α-Metil-4 piridina metanol, (*R,S*)-α-(trifluorometil) benzil álcool, (*R,S*)-1-(1-Nafitill)-etanol, (*R,S*)-3-Benziloxi-1,2 Propanediol	Kumar et al. (2017)

(continuação)

Esterase Est3-14	Lama marinha	*51%* com esterase de *Acidimicrobium sp*	Família V	292 U mg^{-1} em butirato de *p*-nitrofenila	Enzima liofilizada	Hidrólise para preparação de all-trans-astaxantina livre, conversão de 99,3% em 36 h	Lu et al. (2018)
Esterase EST4	Lama marinha	48% com esterase de *Cupriavidus metallidurans*	Família V	1389 U mg^{-1} em butirato de *p*-nitrofenila	Célula inteira liofilizada	Transesterificação de 16 álcoois secundários (*E* de 35 a >200) Síntese de ésteres de aroma de cadeia curta	Gao et al. (2016b, 2016a)

Biodiesel

Enzima	Fonte de DNA	Identidade	Classificação filogenética	Atividade de hidrólise	Imobilização	Aplicação	Referência
Lipase LipZ03	Solo	78% com lipase de *Pseudomonas fluorescens*	Família III	44 U mL^{-1} em óleo de oliva	Enzima liofilizada	Produção de biodiesel com 74% de conversão de óleo de oliva em 36 h	Zheng et al. (2012)
Lipase LipC12	Solo contaminado com gordura	72% com lipase de *Yersinia enterocolitica*	Subfamília I.1	1722 U mg^{-1} em óleo de oliva	Imobilizada em Immobead	Síntese de oleato de etila, com conversão em éster de 99% em 1 h	Madalozzo et al. (2015)
Lipase LipG9	Solo contaminado com gordura	96% e 84% com lipase e foldase de *Aeromonas veronii* B565, respectivamente	Subfamília I.1	1200 U mg^{-1} em óleo de oliva	Imobilizada em Accurel	Síntese de oleato de etila, com conversão em éster de 95% em 7 h. Síntese de caprilato de etila, miristato de etila e palmitato de etila com conversões >95% em 3 h	Alnoch et al. (2015)
Lipase Lip479	Fonte termal	Não consta	Família I.5	597 U mg^{-1} em laurato de *p*-nitrofelina	Não fez	Produção de biodiesel com 76,8% de conversão de óleo de gergelim em 12h	Sahoo et al. (2017)
Lipase Lip-1	Fonte termal	Não consta	Não informado	Não fez	Imobilizada em oleosina	Transesterificação de óleo de oliva e metanol	Yan et al. (2017)

Síntese de Aromas e Lipídeos Estruturados

Enzima	Fonte de DNA	Identidade	Classificação filogenética	Atividade de hidrólise	Imobilização	Aplicação	Referência
Lipase #8	Não consta	Não consta	Não informado	0,76 U mg^{-1} em tributirina	Imobilizada em Celite	Síntese dos lipídeos estruturados 1,2-oleoil-3-palmitoil-sn-glicerol (OOP) e 1,3-oleoil-2-palmitoil-sn-glicerol (OPO	Bertram et al. (2008)

(conclusão)

Lipase LipIAF5-2	Biomassa enriquecida em reator de batelada	52% com lipase de *Acidovorax delafieldii*	Família I	160 U mg^{-1} em miristato de *p*-nitrofelina	Células inteiras liofilizadas	Síntese de acetato de isoamila com 100% de conversão de gliceril triacetato e metanol em após 24 h	Brault et al. (2014)
Esterase Est_p6	Sedimentos marinhos	59% com esterase de *Vibrio splendidus*	Família IV	2500 U mg^{-1} em butirato de *p*-nitrofenila	Não fez	Hidrólise de miristato (C14) e palmitato (C16)	Peng et al. (2014)
Lipase LipC12	Solo contaminado com gordura	72% com lipase de *Yersinia enterocolitica*	Subfamília I.1	1722 U mg^{-1} em óleo de oliva	Imobilizada em Immobead	Produção de butil-caprilato com 62% de conversão em 6 h Transesterificação do óleo de oliva com ácido caprílico, para produção de lipídeo de baixa caloria (MLM), formação de óleo de oliva modificado com a presença de cadeias médias de ácido caprílico nas posições *sn*-1 e *sn*-3. Conteúdo de 23% de ácido caprílico em 72 h de reação	Madalozzo et al. (2016)

Outras áreas

Enzima	Fonte de DNA	Identidade	Classificação filogenética	Atividade de hidrólise	Imobilização	Aplicação	Referência
Lipase Lip906	Solo de mangue	34% com lipase de *Streptomyces* sp.	Família desconhecida	220 U mg^{-1} em *p*-NPM (C14)	Não fez	Teste de detergência com óleo vermelho em pedaços de *cotton*	Tang et al. (2017)
Esterases EstB3 EstC7	Comunidades associadas ao musgo *Sphagnum magellanicum*	63% com serina hidrolase de *Tardiphaga* sp. e 53% com 1,4 butanediol diacrilato esterase de *Thermorudis peleae*	Família VIII	EstB3 ~85 U mg^{-1} e EstC7 ~95 U mg^{-1} em caproato de *p*-nitrofenila	Lisado livre de células liofilizado	Degradação de plástico	Müller et al. (2017)

ee: excesso enantiomérico, eep: excesso enantiomérico do produto, ees: excesso enantiomérico do substrato, *E*: coeficiente de anantiosseletividade.
A lista foi criada através da pesquisa no banco de dados *Web of Scince* (acesso em 20/10/18) com as seguintes palavras-chave: (lipase OR esterase) AND (metagenom∗) AND (applicat* AND synthe*) em tópico, data de publicação de 1945 – 2018. Os resultados foram manualmente checados para selecionar somente os artigos que realizaram a aplicação das enzimas em reações de biocatálise, excluindo os artigos que fizeram apenas a caracterização da enzima.

Em relação à atividade de hidrólise, não é possível estabelecer comparações, pois foram utilizados diferentes métodos e condições para determinação da atividade de hidrólise. Nota-se que a maioria dos trabalhos utilizaram substratos sintéticos baseados em *p*-nitrofenila, somente 4 trabalhos utilizaram substratos naturais (óleo de oliva e triburitina)

Dentre todas as enzimas citadas na TABELA 6, apenas uma lipase (LipG9) apresenta uma Lif (LifG9), evidenciando a escassez de trabalhos que reportam a clonagem de lipases e foldases simultaneamente. Isso ocorre provavelmente pela dificuldade em se encontrar os genes da lipase e foldase no mesmo fragmento de DNA em uma biblioteca metagenômica (MARTINI et al., 2014). LipG9 foi a primeira lipase de metagenômica co-expressa com sua foldase cognata reportada até o momento.

Outra característica interessante mostrada na TABELA 6 é que a maioria das enzimas (15 enzimas) foram aplicadas na área farmacêutica, principalmente em reações enantiosseletivas, demonstrando uma tendência de aplicação nesta área, devido à grande relevância do desenvolvimento de drogas por síntese enzimática e ao alto valor agregado dos compostos enantiomericamente puros. Os trabalhos mais representativos apresentaram resultados de transesterificação de diversos álcoois secundários e terciários. Além disso, duas aplicações distintas da resolução racêmica foram a hidrólise para a desacetilação regioseletiva de D-glucal peracetilado, que pode ser utilizado como bloco construtor de fármacos, catalisada pela lipase LipC12 (ALNOCH et al., 2016), e a hidrólise de astaxantina esterificada com ácidos graxos para liberação de *all-trans*-astaxantina livre, um terpenóide com várias aplicações farmacêuticas, catalisada pela esterase Est3-14 (LU et al., 2018).

A TABELA 6 mostra ainda que a maior parte das lipases foi aplicada de forma livre em solução ou liofilizadas, sendo que apenas 6 artigos reportam a imobilização em suportes específicos. Dentre os suportes utilizados estão o Accurel (adsorção), Immobead (ligação covalente), Epoxi-agarose com aldeído C18 (ligação covalente e adsorção) e celite (adsorção).

A segunda área de aplicação mais utilizada para lipases e esterases de metagenômica foi a síntese de biodiesel, com 5 enzimas, sendo que o melhor resultado foi apresentado por LipC12 imobilizada com conversão de 99% em oleato de etila em 1h de reação em presença de *n*-hexano (MADALOZZO et al., 2015a). Além disso, 3 enzimas (EST4, LipIAF5-2 e Est_p6) foram aplicadas na síntese de aromas

(BRAULT et al., 2014; PENG et al., 2014; GAO et al., 2016b), e 2 lipases foram aplicadas na síntese de lipídeos estruturados (Lipase #8 e LipC12) (BERTRAM et al., 2008; MADALOZZO et al., 2016). Aplicação das enzimas em detergentes (Lip906) (TANG et al., 2017) e para degradação de plástico (EstB3 e EstC7) (MÜLLER et al., 2017) também foram encontradas (TABELA 6).

Notadamente, as lipases LipC12 e LipG9 foram as enzimas mais aplicadas em diferentes reações em comparação com as demais enzimas listadas, sendo que LipC12 foi aplicada em reações na área farmacêutica, biodiesel e síntese de aromas e lipídeos estruturados (MADALOZZO et al., 2015b, 2016; ALNOCH et al., 2016) e LipG9 foi aplicada na área farmacêutica (transesterificação de álcoois secundários) e na síntese de biodiesel (ALNOCH et al., 2015; BANDEIRA et al., 2016).

2.5 EFEITO DE TAGS DE AFINIDADE NA ATIVIDADE DE LIPASES

A busca por novas lipases que possam ser aplicadas em biocatálise depende não apenas de um método eficiente de prospecção, como a metagenômica, mas também da facilidade em que essas enzimas podem ser expressas em sistema heterólogo, para obtenção de enzimas ativas e puras.

Uma ferramenta eficiente para purificação de enzimas recombinantes são as *tags* de afinidade, que são sequências de aminoácidos exógenas à proteína original, com alta afinidade por um ligante biológico ou químico específico. Existe uma grande variedade de *tags* de afinidade (TABELA 7) e elas são adicionadas à proteína de interesse de acordo com o vetor utilizado na expressão heteróloga. Em geral, essas fusões são utilizadas para purificação da proteína por afinidade, melhoramento da solubilidade ou para secreção das proteínas de interesse (ARNAU et al., 2006). Em alguns casos, as *tags* podem aumentar a produção de algumas enzimas recombinantes (WAUGH, 2005) e ajudar no empacotamento durante a cristalização da proteína (MAJOREK et al., 2014).

As *tags* de poli-histidina (His-tags) são amplamente utilizadas para a purificação de proteínas por cromatografia de afinidade por íons metálicos imobilizados (IMAC), uma vez que a os grupos doadores de elétrons presentes no anel imidazólico da histidina estabelecem facilmente ligações de coordenação com um metal de transição como o Co^{2+}, Ni^{2+}, Cu^{2+}, Zn^{2+} presentes nas matrizes de purificação (TERPE, 2003). As tags de afinidade do tipo His-tag podem conter, além

dos resíduos de histidina, dependendo do vetor, um local de reconhecimento de protease para clivagem ou um *linker* para a região C e N-terminal (CARSON et al., 2007).

TABELA 7 - EXEMPLOS DE TAGS DE AFINIDADE

Tag	Sequência	Aminoácidos	Tamanho (kDa)
Poli-histidina	HHHHHH	2-10	0,84
Arg-tag	RRRRR	5-6	0,80
FLAG-tag	DYKDDDDK	8	1,01
Strep-tag II	WSHPQFEK	8	1,06
c-Myc	EQKLISEEDL	11	1,20
S-tag	KETAAAKFERQHMDS	15	1,75
HAT-tag	KDHLIHNVHKEFHAHAHNK	19	2,31
Peptídeo de ligação à calmodulina	KRRWKKNFIAVSAANRFKKISSSGAL	26	2,96
SBP-tag	MDEKTTGWRGGHVVEGLAGELEQL RARLEHHPQGQREP	38	4,03
Domínio de ligação à quitina	TNPGVSAWQVNTAYTAGQLVTYNGKT YKCLQPHTSLAGWEPSNVPALWQLQ	51	5,59
Tioredoxina	Domínio	109	12
Domínio de ligação à celulose	Domínio	27-189	3,00 a 20
Glutationa S-transferase	Proteína	211	26
Proteína de ligação à maltose	Proteína	396	40
NusA	Proteína	495	54

FONTE: Terpe (2003), Abdullah; Chase (2005), Arnau et al. (2006).

No entanto, as *tags* podem interferir na estrutura e, consequentemente, na função das enzimas (TERPE, 2003). O efeito que as proteínas de fusão exercem sobre a estrutura terciária e a atividade das proteínas recombinantes está relacionado principalmente à sequência de aminoácidos e à localização em que a *tag* será adicionada (N- ou C-terminal da proteína) (BUCHER; EVDOKIMOV; WAUGH, 2002). Portanto, qualquer proteína de fusão, independentemente do tamanho, apresenta potencial de alterar a atividade, interferir no processo de cristalização ou causar alterações no comportamento catalítico das proteínas (WAUGH, 2005).

A atividade das lipases está profundamente relacionada às suas propriedades estruturais. Assim, pequenas variações na estrutura como a troca de um aminoácido, a presença de ponte dissulfeto ou a adição de uma *tag* de afinidade podem causar efeitos catalíticos significativos. Poucos trabalhados relatam a influência de *tags* de afinidade sobre a atividade de lipases, como exemplo, pode-se citar o estudo de Horchani et al. (2009), com uma lipase recombinante de *Staphylococcus aureus*,

expressa em *E. coli* com uma His-tag na região N-terminal (His_6-SAL3). Esta lipase apresentou atividades de hidrólise específicas menores (1300 U mg^{-1} para óleo de oliva e 4000 U mg^{-1} para tributirina) do que a lipase selvagem sem His-tag (wt-SAL3) que apresentou 3500 U mg^{-1} para óleo de oliva e 4500 U mg^{-1} para tributirina. Além disso, a lipase selvagem foi mais termoestável, mantendo 95% da atividade após 60 min à 55 ºC, enquanto nas mesmas condições His_6-SAL3 foi inativada em poucos minutos. Também foi observada uma diferença de atividade para a lipase imobilizada em carbonato de cálcio, sendo que para a síntese de oleato de butila, a conversão foi de 71% para wt-SAL3 e 17% para His_6-SAL3, após 24 h de reação.

Outro trabalho que apresentou a influência da His-tag em lipases foi realizado com a lipase de *Staphylococcus simulans* (SSL e rSSL) e lipase de *Staphylococcus xylosus* (SXL e rSXL). Os autores demonstraram que ambas as lipases nativas sem a His-tag (SSL e SXL) foram mais termoestáveis. A lipase SSL apresentou 50% de atividade residual após 40 min de incubação à 50 ºC, enquanto que a lipase rSSL com His-tag apresentou meia vida de 15 min à 50 ºC. Da mesma forma, a lipase SXL apresentou meia vida de 135 min enquanto a lipase rSXL (com His-tag) exibiu meia vida de 100 min na mesma temperatura. A presença da His-tag na região N-terminal também alterou a regioseletividade das lipases rSSL e rSXL contra isômeros dicaprina (SAYARI et al., 2007).

Madalozzo et al. (2015) sugeriram que a His-tag poderia ter um efeito sobre a imobilização da lipase LipC12 no suporte Immobead 150. Os autores propuseram que as histidinas seriam alvos preferenciais ao ataque nucleofílico dos grupos oxirano do suporte. Assim, confirmar o efeito da His-tag sobre a imobilização e as propriedades catalíticas de LipC12 foi objeto de estudo deste trabalho e os resultados encontram-se no Capítulo I.

3 CAPÍTULO I

Manuscrito publicado na revista:
Scientific Reports

Tailoring recombinant lipases: keeping the His-tag favors esterification reactions, removing it favors hydrolysis reactions

Scientific Reports (2018) 8:10000 DOI:10.1038/s41598-018-27579-8

Tailoring recombinant lipases: keeping the His-tag favors esterification reactions, removing it favors hydrolysis reactions

Janaina Marques de Almeida[1#], Vivian Rotuno Moure[1#], Marcelo Müller-Santos[1], Emanuel Maltempi de Souza[1], Fábio de Oliveira Pedrosa[1], David Alexander Mitchell[1] and Nadia Krieger[2*].

[1]Departamento de Bioquímica e Biologia Molecular, Universidade Federal do Paraná, Cx.P. 19046 Centro Politécnico, Curitiba 81531-980, Paraná, Brazil.

[2]Departamento de Química, Universidade Federal do Paraná, Cx.P. 19081 Centro Politécnico, Curitiba 81531-980, Paraná, Brazil.

[*] To whom correspondence should be addressed. E-mail: nkrieger@ufpr.br; Telephone: +55-41-33613470. [#] J.M.A and V.R.M. contributed equally to this work

Abstract

We determined the effect of the His-tag on the structure, activity, stability and immobilization of LipC12, a highly active lipase from a metagenomic library. We purified LipC12 with a N-terminal His-tag and then removed the tag using tobacco etch virus (TEV) protease. Circular dichroism analysis showed that the overall structure of LipC12 was largely unaffected by His-tag removal. The specific hydrolytic activities against natural and artificial substrates were significantly increased by the removal of the His-tag. On the other hand, His-tagged LipC12 was significantly more active and stable in the presence of polar organic solvents than untagged LipC12. The immobilization efficiency on Immobead 150 was 100% for both forms of LipC12 and protein desorption studies confirmed that the His-tag does not participate in the covalent binding of the enzyme. In the case of immobilized LipC12, the His-tag negatively influenced the hydrolytic activity, as it had for the free lipase, however, it positively influenced the esterification activity. These results raise the possibility of tailoring recombinant lipases for different applications, where the His-tag may be retained or removed, as appropriate for the desired activity.

3.1 INTRODUCTION

Affinity tags have gained importance over the last decades as a purification tool for recombinant proteins[1]. Such tags include arg-tags, the calmodulin-binding peptide, cellulose-binding domains, DsbA, the c-myc-tag, glutathione S-transferase, the FLAG-tag, the HAT-tag, the maltose-binding protein, NusA, the S-tag, the SBP-tag, the Strep-tag, thioredoxin and His-tags[2]. Of these, His-tags (i.e. the polyhistidine affinity tag) are the most used, with approximately 25% of all protein structures in the Protein Data Bank (PDB) having been obtained for His-tagged proteins[3]. His-tagged proteins are purified by metal affinity chromatography, since the imidazole ring of the histidine establishes coordination bonds with immobilized ions (such as Co^{2+}, Ni^{2+}, Cu^{2+} or Zn^{2+})[2]. His-tags can be used for purifying proteins, under either non-denaturing or denaturing conditions, and the recombinant proteins can be eluted under mild conditions[4,5]. In addition to simplifying purification, His-tags are designed to optimize protein expression and therefore result in high yields. They also allow the detection of the recombinant protein[6,7].

His-tags are bulky and might affect the conformation of the enzyme. The polyhistidine region typically consists of six consecutive histidine residues, but it can vary from two to ten histidine residues. In addition, His-tagged heterologous proteins that are expressed in *Escherichia coli* using the pET vector series[8] contain several other amino acid residues. For example, use of the vector pET28a leads to the addition of a total of 20 residues at the N-terminal, of which only six are histidine residues.

His-tags are often used in the expression of recombinant lipases. Lipases are of great industrial interest due to their diverse biotechnological applications. They are efficient catalysts not only in conventional aqueous media, but also in non-conventional media, such as organic solvents, ionic liquids, supercritical fluids, and eutectic solvents[9,10]. Depending on the medium, they catalyze reactions of hydrolysis, esterification, transesterification, acetylation and lactonization[11].

Despite the potential that His-tags have to affect conformation and activity, to date, few studies have assessed their influence on the properties of lipases. In one study, the His-tagged *Staphylococcus xylosus* lipase (His-SXL), overexpressed in *E. coli*, had altered kinetic parameters, altered stereo- and regioselectivity and altered thermostability, compared to the native lipase (SXL)[12,13]. In another study, *S. aureus*

lipase (SAL), expressed in *E. coli* with a His-tag at the N-terminal, had a lower specific activity for the hydrolysis of tributyrin than the native lipase[14].

In our laboratory, LipC12, a recombinant lipase containing a His-tag at the N-terminal, was originally isolated from a metagenomic library and characterized by Glogauer et al.[15]. Later, LipC12 was immobilized on Immobead 150. One immobilized preparation was obtained using the crude extract obtained after expression of the enzyme and cell breakage, while another was obtained using a preparation that had been purified from the crude extract using a nickel affinity column[16,17]. During these immobilization studies, Madalozzo et al.[16] suggested that the presence of the His-tag might contribute to selective immobilization of His-LipC12 from the crude extract onto Immobead 150. Their argument was that, at the pH of 7.5 used for the immobilization, the histidine residues in the tag would be mostly deprotonated (the pKa of the histidine side chains in the His-tag is reported as 6.0)[18] and this would favor nucleophilic attack by these side chains on the oxirane group of the support. However, they did not undertake studies to confirm that the His-tag was actually involved in immobilization.

In this work, we systematically investigated the effects of the His-tag on the structure, activity, stability and immobilization of LipC12. We used two strategies for the expression and removal of the His-tag from LipC12: (1) the *lipC12* gene was cloned into pET28a for the expression of the His-tag on the N-terminal of the enzyme[15] and this homolog was compared with the other recombinant form of LipC12, which was produced by cloning the *lipC12* gene into pET29a for the expression of recombinant LipC12 (denominated rLipC12) without the His-tag; (2) the *lipC12* gene was cloned into pTEV5 for the expression of the His-tag at the N-terminal of the enzyme, with the inclusion of a tobacco etch virus (TEV) cleavage site, enabling posterior His-tag removal[19].

3.2 RESULTS

All results in this section are presented as mean of triplicate determinations ± standard deviation of the mean.

3.2.1 Properties of LipC12 expressed with and without His-tag

Although previous reports have suggested that the His-tag negatively affects the hydrolytic activity of lipases[12,13], it is not a consensus. In this work, we compared the activities and the immobilization behavior of LipC12 expressed with and without the His-tag. In order to do so, the *lipC12* gene was cloned into pET28a(+) and pET29a(+), producing CSF-His-LipC12 (crude soluble fraction containing LipC12 with His-tag) and CSF-rLipC12 (crude soluble fraction containing LipC12 without His-tag), respectively, through overexpression in *E. coli* BL21(DE3). In each case, the cell pellet was disrupted by sonication, the crude extract was then centrifuged, and the crude soluble fraction, containing either His-LipC12 or rLipC12, was used for activity and immobilization tests.

The specific hydrolytic activities of these crude soluble fractions were determined in a pHStat against olive oil. The crude soluble fraction containing rLipC12 had a significantly higher specific activity (1938 ± 82 U mg^{-1}) than did the crude soluble fraction containing His-LipC12 (1469 ± 63 U mg^{-1}) ($P < 0.05$). This difference in specific hydrolytic activity was not due to differences in protein expression: densitometry analysis of SDS-PAGE gels of the two crude soluble fractions showed that the lipases contributed similar percentages of the overall protein. In the case of His-LipC12, the lipase band (at ~33 kDa) contributed 18.6% ± 0.8% of the overall protein, while in the case of rLipC12, the lipase band (at 31 kDa) contributed 18.0% ± 0.3% (Supplementary Fig. S2).

Subsequently, we investigated the suggestion that the covalent immobilization of CSF-His-LipC12 on the commercial support Immobead 150 involves the His-tag[16]. We used previously established conditions[16] (i.e. a loading of 200 mg of protein per gram of support) for immobilization of CSF-His-LipC12 and CSF-rLipC12. The kinetics of immobilization were followed by monitoring the residual olive-oil-hydrolyzing activity of the supernatant. The profiles were very similar (Fig. 1), with immobilization efficiencies of 80% being obtained at 8 h for both preparations (Supplementary Table S1). Hereafter, the immobilized preparations are referred to as I-CSF-His-LipC12 and I-CSF-rLipC12.

After immobilization, the olive-oil-hydrolyzing activities of the two LipC12 preparations were determined in the pHStat. As had occurred with the soluble preparations of LipC12, I-CSF-rLipC12 had a significantly higher hydrolytic activity (421 ± 24 U g^{-1} support) than I-His-LipC12 (303 ± 21 U g^{-1} support) ($P < 0.05$).

Both immobilized preparations were then used to esterify oleic acid with ethanol in *n*-hexane. The esterification activities for both preparations were not significantly different, 66 ± 0 U g^{-1} for I-CSF-rLipC12 and 61 ± 1 U g^{-1} for I-CSF-His-LipC12 ($P > 0.05$).

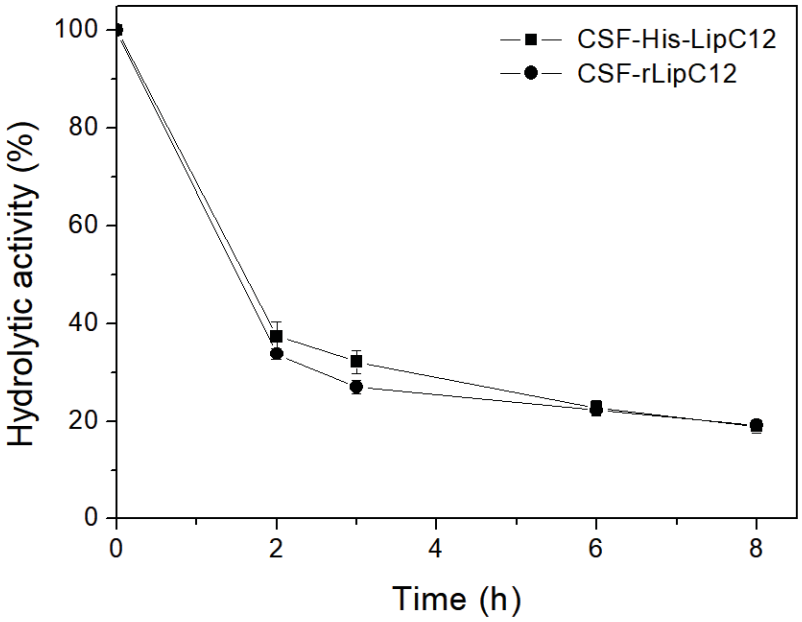

Figure 1. Kinetics of immobilization of CSF-His-LipC12 and CSF-rLipC12 on Immobead 150. The residual hydrolytic activities of the supernatants in aqueous medium were measured against olive oil by the titrimetric method, at 30°C and pH 7.0.

Together, these results suggest that the His-tag decreases the hydrolytic activity of both the free and immobilized LipC12. Further studies using purified untagged and His-tagged LipC12 were needed to confirm these results, they are reported in the next subsection.

3.2.2 Properties of purified LipC12 with and without cleavable His_{TEV}-Tag

We cloned *lipC12* into the vector pTEV5, which introduces the TEV protease cleavage site between the His-tag and the target protein. The resulting LipC12 variant, denominated His_{TEVS}-LipC12, was overexpressed in *E. coli* BL21(DE3) and purified using immobilized metal affinity chromatography. The His-tag was later cleaved by TEV protease, with 100% efficiency, as confirmed by western blot (Fig. 2). The cleaved variant was denominated cLipC12. This strategy allowed the cost-effective production of both His_{TEVS}-LipC12 and untagged cLipC12, with high purity being obtained in a one-step affinity process (Supplementary Fig. S1).

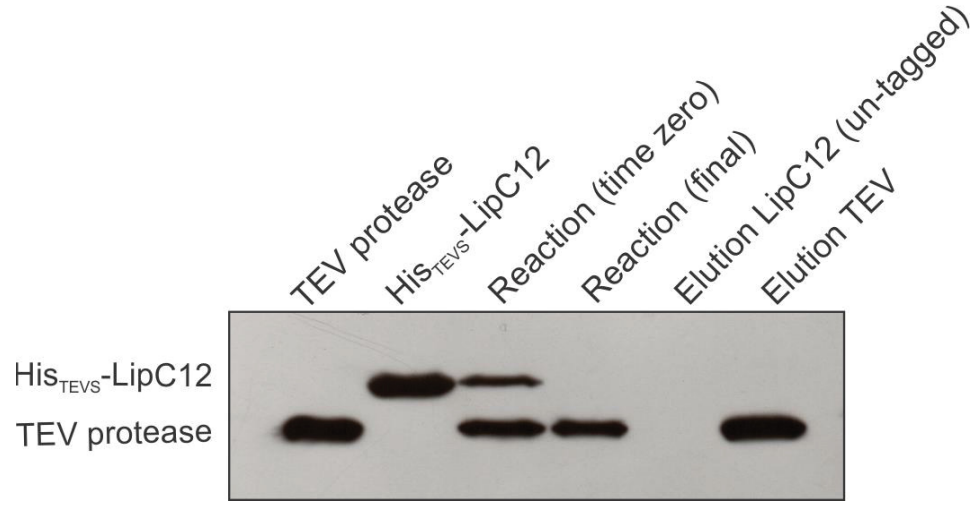

Figure 2. Cleavage of His$_{TEVs}$-LipC12 by TEV protease. The substrate His$_{TEVS}$-LipC12, containing a TEV protease cleavage site, was mixed with the TEV protease at mass ratio 10:1 of substrate: TEV. 1 µg of TEV and 2 µg of other fractions were analyzed by 12% SDS-PAGE followed by western blotting and incubation with Ni-NTA HPR. The full-length blot is reported in Supplementary Figure S6.

The *lipC12* gene encodes 293 amino acids and rLipC12 has a theoretical molecular weight of 31.2 kDa. His$_{TEVS}$-LipC12 has 27 additional residues at its N-terminal (MSYYHHHHHHDYDIPTSENLYFQGASH) and has a theoretical molecular weight of 34.5 kDa. After TEV protease cleavage, four of these additional residues (GASH) remain at the N-terminal, such that cLipC12 has a theoretical molecular weight of 31.6 kDa. These theoretical molecular weights were confirmed by SDS-PAGE (Supplementary Fig. 3S).

Several authors have used TEV protease to cleave the His-tag from different target proteins. The amount of TEV required is usually empirically determined, with ratios of target protein to TEV between 100:1 and 5:1 being tested[20]. Our results showed complete cleavage under mild conditions (8 °C for 20 h) using a ratio of 10:1.

3.2.3 Structural analysis of His$_{TEVS}$-LipC12 and cLipC12 by circular dichroism

The far-UV CD spectra of both His$_{TEVS}$-LipC12 and cLipC12 showed typical negative absorption signals of α-helices at about 208 nm and 222 nm, as well as negative absorption signals of antiparallel β-sheets at 215 nm (Fig. 3A). Positive absorption peaks at about 190 nm were not seen because the dynode voltage was above 600 V, resulting in unreliable data[21]. This CD profile is similar to those shown by other lipases[22,23,24,25]. The CD spectra for His$_{TEVS}$-LipC12 and cLipC12 overlap completely in the far-UV (250-200 nm) and near-UV (350-250 nm) regions, indicating

that the His-tag does not induce structural rearrangements in LipC12. The CD spectra of His_{TEVS}-LipC12 and LipC12 were further analyzed by K2D3 online software; for each protein, the estimate was an α-helix content of 36% and a β-sheet content of 20%. There is no previous study in which CD spectra have been used to characterize the structural changes of lipases due to the presence of a His-tag, but CD spectra have been used to show that a His-tag induces structural changes in zinc finger protein ZNF191 (243-368)[26].

We also compared the thermal stabilities of His_{TEVS}-LipC12 and LipC12 by recording CD data at 222 nm to determine the melting temperature (Tm) (Fig. 3B). The Tm decreased by only 1°C in the presence of the His-tag, which suggests the His-tag has a minimum impact on the thermal stability of LipC12.

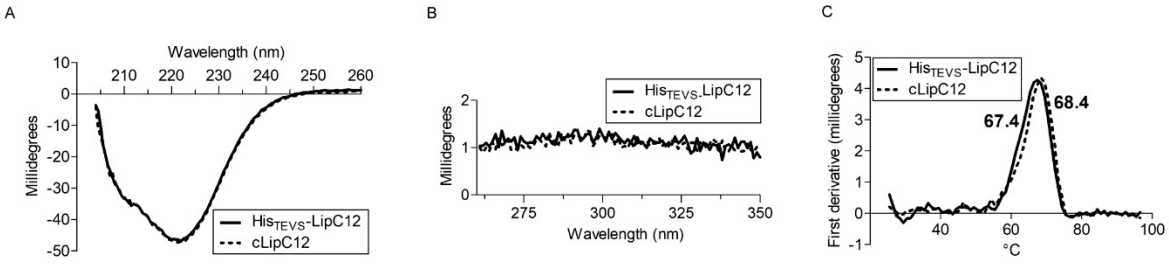

Figure 3. Circular dichroism analysis of His_{TEVS}-LipC12 and LipC12. Proteins were diluted to 5 μM in a 10-mM sodium phosphate buffer, pH 7.4, containing 100 mM NaCl. (A) CD spectra of His_{TEVS}-LipC12 and LipC12 were recorded at 25 °C. (B) CD spectra of His_{TEVS}-LipC12 and LipC12 in the near-UV (350-250 nm) regions. (C) Determination of the melting temperatures (Tm) of His_{TEVS}-LipC12 and LipC12. The Tm was calculated by measuring the CD signal at 222 nm with increasing temperature (from 25 to 98 ºC) in a continuous ramp mode (1 ºC/2 min). The Tm was determined from the first derivative (GraphPrism 6.0).

3.2.4 Hydrolytic activity of His_{TEVS}-LipC12 and cLipC12

The specific olive-oil-hydrolyzing activities were 2555 ± 17 U mg^{-1} for His_{TEVS}-LipC12 and 4590 ± 101 U mg^{-1} for cLipC12. The significantly lower hydrolytic activity in the presence of the His-tag ($P < 0.05$) confirms the results obtained above, where the hydrolytic activity of CSF-His-LipC12 was lower than that of CSF-rLipC12 and the hydrolytic activity of I-CSF-His-LipC12 was lower than that of I-CSF-rLipC12 (see the first subsection of the results). We also evaluated the activities of His_{TEVS}-LipC12 and cLipC12 in the hydrolysis of natural substrates with a range of acyl chain lengths. For all substrates, the activity of His_{TEVS}-LipC12 was significantly lower than that of cLipC12 ($P < 0.05$) (Table 1).

Table 1. Relative hydrolytic activities of His_{TEVS}-LipC12 and cLipC12 against different triacylglycerols.

Substrate	Relative hydrolytic activities	
	His_{TEVS}-LipC12	**cLipC12**
Olive oil	100 ± 4	173 ± 4
Triolein (C18)	109 ± 5	170 ± 6
Tricaprylin (C8)	188 ± 2	345 ± 9
Tributyrin (C4)	304 ± 8	611 ± 10

Measurements were performed by the titration method using an automatic titrator pHStat. Values represent the mean of triplicates ± standard deviations of the mean.

3.2.5 Hydrolytic activity of His_{TEVS}-LipC12 and cLipC12 against *p*NPD

Under the standard reaction conditions (see methods section) for the hydrolysis of *p*-nitrophenyl decanoate (*p*NPD), cLipC12 had a specific activity of 325 ± 20 U mg^{-1}, which is 1.7-fold higher than that of His_{TEVS}-LipC12 (192 ± 5 U mg^{-1}).

The effect of the *p*NPD concentration on the initial hydrolysis rate was determined for both His_{TEVS}-LipC12 and cLipC12 under the standard reaction conditions (Supplementary Fig. S4). The Michaelis-Menten equation was fitted to the data obtained with both enzymes using non-linear regression. In both cases, the coefficient of determination was greater than 0.99. Table 2 shows the parameter values that gave the best fits.

The K_M values obtained for His_{TEVS}-LipC12 and cLipC12 were different (their 95% confidence intervals did not overlap). On the other hand, the k_{cat} values were essentially the same (their 95% confidence intervals overlap almost completely). Due to the difference in the K_M, the values of k_{cat}/K_M were also different for the two enzymes, with that for His_{TEVS}-LipC12 being only 75% of the value obtained for cLipC12. In other words, the presence of the His-tag decreases the catalytic efficiency of LipC12 with *p*NPD as the substrate.

Table 2. Apparent kinetic constants for *p*-nitrophenyl decanoate hydrolysis of His_{TEVS}-LipC12 and LipC12.

Enzyme	K_M (mM)	k_{cat} (min^{-1})	k_{cat}/K_M (mM^{-1} min^{-1})
His_{TEVS}-LipC12	1.77	152	86
	(1.56-2.02)[a]	(143-162)	(80-92)
cLipC12	1.33	151	114
	(1.17-1.51)	(144-160)	(105-123)

[a]The values between parentheses are the 95% confidence intervals.

3.2.6 Activity and stability in organic solvents of His_{TEVS}-LipC12 and cLipC12

The use of organic solvents instead of water in biocatalytic processes involving lipases has intensified over the last few decades[9]. Lipases must therefore have both high activity and high stability in organic solvents if they are to be useful biocatalytic tools[27]. Based on the difference in activity found in aqueous media using untagged LipC12 (CSF-rLipC12, cLipC12 and I-CSF-rLipC12) and His-tagged LipC12 (His-LipC12, His_{TEVS}-LipC12 and I-His-LipC12), we investigated His_{TEVS}-LipC12 and cLipC12 with respect to their *p*NPD-hydrolyzing activity and stability in various concentrations of different polar organic solvents (ethanol, isopropanol, methanol, propanol, acetone, acetonitrile, DMF and DMSO). The activities were expressed as relative activities, in other words, as percentages of the corresponding activity in 50 mM Tris-HCl buffer (pH 7.5) used in the standard reaction.

His_{TEVS}-LipC12 showed significantly higher activity in the presence of acetone, DMF and DMSO than cLipC12. For both variants of LipC12, the relative activities were lower than 50% for all organic solvents and at all concentrations tested, except for DMSO (Fig. 4A). For this solvent, concentrations up to 40% activated both enzymes, with His_{TEVS}-LipC12 being activated to a greater extent than cLipC12. It is well known that polar organic solvents like methanol, ethanol, propanol and butanol inhibit lipase activity[28]. On the other hand, DMSO has been shown to activate lipases several-fold[22,29]. Although the mechanism of this activation has not been elucidated, it has been suggested that DMSO stabilizes the transition state by replacing water in the enzyme-substrate complex[30,31].

To evaluate the stability in organic solvents, His_{TEVS}-LipC12 and cLipC12 were incubated for 3 h at 25 °C in two concentrations (20% and 40% (v/v)) of the polar organic solvents (Fig. 4B). The hydrolytic activity against *p*NPD was then determined under standard conditions (using final enzyme concentrations of 7 nM for His_{TEVS}-LipC12 and 5 nM for cLipC12). In most cases, His_{TEVS}-LipC12 was more stable than cLipC12 (Fig. 4B). However, in 20% ethanol, 40% methanol, 40% acetone, 40% acetonitrile and 40% DMF, the residual activities of the two enzymes were not significantly different ($P > 0.05$). The activity of His_{TEVS}-LipC12 increased approximately 1.2-fold after incubation in 20% methanol, 20% acetonitrile and 20% DMF. The stability of His_{TEVS}-LipC12 in DMSO was not higher than in the other hydrophilic solvents, since its residual activity was 80% after incubation in 40% DMSO

(Fig. 4B). Both His_{TEVS}-LipC12 and cLipC12 were more stable in polar organic solvents than lipase P21 of *Pseudomonas fluorescens*, which had residual activities below 50% after incubation for 2 h at 30 °C in 3:1 (v/v) solutions of methanol, ethanol, acetone, isopropanol and butanol in water[32].

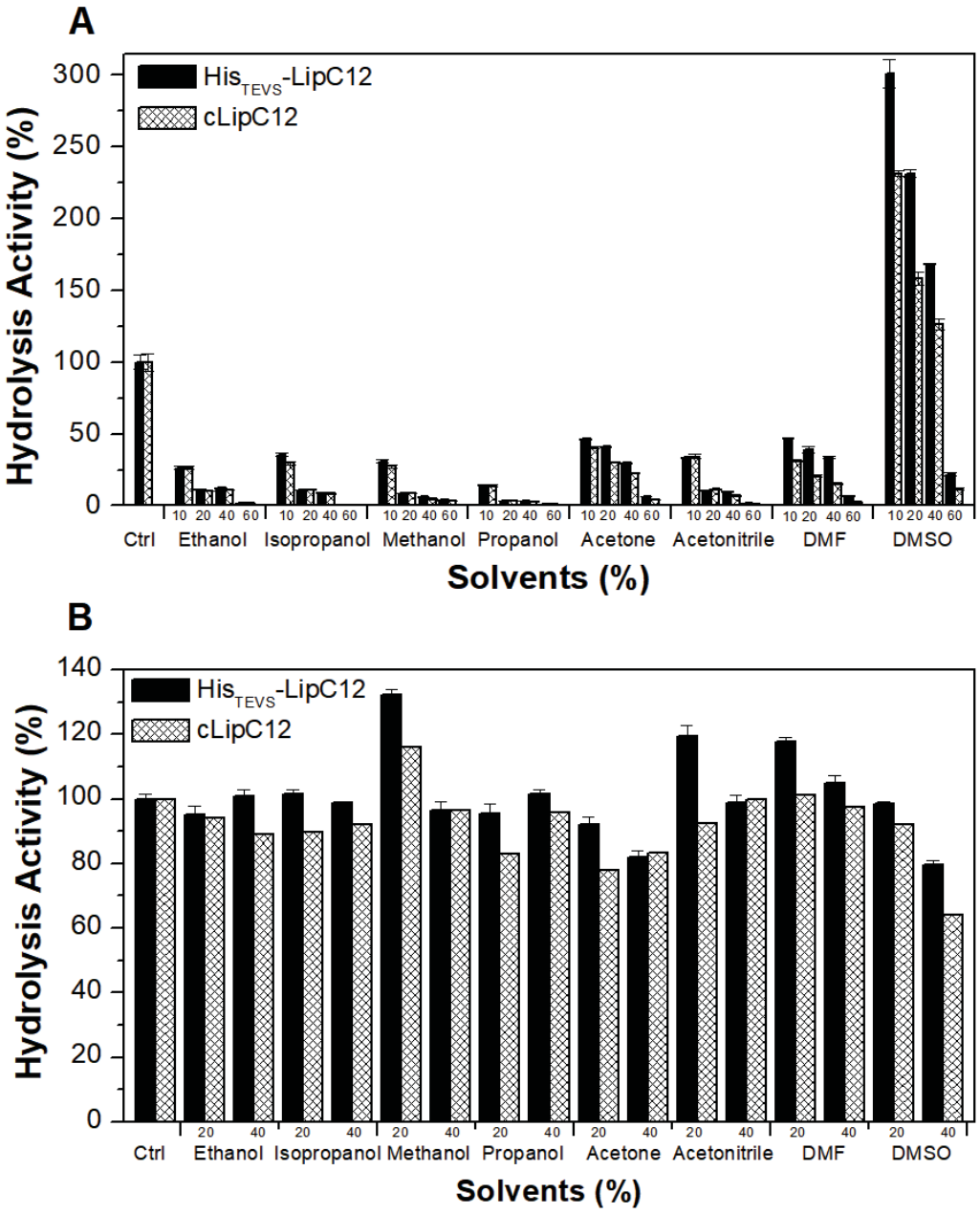

Figure 4. Relative activities (A) and stabilities (B), compared to the control, of His_{TEVS}-LipC12 and LipC12 in the presence of different concentrations of polar organic solvents. Activities were determined by the spectrophotometric method using the hydrolysis of *p*-nitrophenyl decanoate. The stability in organic solvents was determined after 3 h incubation at 25 °C.

3.2.7 Immobilization of His_{TEVS}-LipC12 and cLipC12

Purified His-LipC12 was immobilized on Immobead 150 in previous work[16]. The authors proposed that the His-tag was involved in the covalent bonding with the support. To investigate this question, we immobilized His_{TEVS}-LipC12 and cLipC12 onto the same support.

For both His_{TEVS}-LipC12 and cLipC12, an immobilization efficiency of 100% was obtained using a protein loading of 10 mg g^{-1}. Despite this high immobilization efficiently, the retention of hydrolytic activity in aqueous medium, measured using triolein, was low (0.21% for His_{TEVS}-LipC12 and 0.27% for cLipC12). A possible explanation for the poor triolein-hydrolyzing activities of the immobilized preparations is that triacylglycerols like triolein form droplets in aqueous media, with these droplets being bigger than the pores of the support, such that the substrate is only accessible to the enzyme immobilized at the outer surface of the support. This can cause the immobilized lipases to have much lower activities against triacylglycerols than that of the free enzyme or that obtained in organic medium[33,34].

To confirm covalent immobilization, these immobilized preparations were boiled for 30 min in a solution containing SDS. After SDS-PAGE, in both cases, approximately 8% of the immobilized protein desorbed. This shows that, for both immobilized enzymes, most of the protein was covalently attached to Immobead 150. Since both variants produced the same results, it can be deduced that the His-tag does not favor the binding covalent of LipC12 to Immobead 150.

In accordance with the findings for the variants of LipC12 that had been immobilized from the crude soluble fraction (I-CSF-His-LipC12 and I-CSF-rLipC12), the olive-oil-hydrolyzing activity of I-cLipC12 (123 ± 2 U g^{-1}) was higher than that of I-His_{TEVS}-LipC12 (54 ± 1 U g^{-1}). On the other hand, the presence of the His-tag increased esterification activity for the substrates octanoic acid, lauric acid, palmitic acid and oleic acid (Table 3). At longer reaction times, the performance of I-His_{TEVS}-LipC12, with conversions at 9 h above 90%, was also higher than that of I-cLipC12, which gave conversions at 9 h below 68%. To verify the stability of I-His_{TEVS}-LipC12 and I-cLipC12 throughout the reaction, the immobilized preparations were recovered after 10 h by filtration, washed with *n*-hexane, dried, and the residual hydrolytic activities against olive oil were measured. The losses of olive-oil-hydrolyzing activity were about 50% for I-His_{TEVS}-LipC12 and 74% for I-cLipC12, showing that the removal of the His-tag

decreases the stability of I-cLipC12 in the reaction medium, which initially contains ethanol and *n*-hexane, with ethyl caprylate, ethyl laurate, ethyl palmitate or ethyl oleate being produced during the reactions. This result is in agreement with the lower stability found for cLipC12 when it was incubated in polar organic solvents (Fig. 4B).

Table 3. Esterification activity of I-cLipC12 and I-His$_{TEVS}$-LipC12 with fatty acids of different chain lengths and ethanol as the alcohol.

	I-cLipC12		**I-His$_{TEVS}$LipC12**	
Fatty acid	Activity (U g^{-1})	Conversion (%)*	Activity (U g^{-1})	Conversion (%)*
Octanoic acid (C8:0)	1.51 ± 0.03	26.1 ± 0.5	5.90 ± 0.03	90.8 ± 1.7
Lauric acid (C12:0)	1.65 ± 0.08	26.4 ± 2.5	6.84 ± 0.15	100.0 ± 0.7
Palmitic acid (C16:0)	2.32 ± 0.19	42.2 ± 2.2	7.88 ± 0.22	97.5 ± 0.2
Oleic acid (C18:1)	5.26 ± 0.03	67.9 ± 0.3	9.21 ± 0.01	96.8 ± 0.4

*Conversion of free fatty acids in 9 h of the esterification reactions. Values represent the mean of triplicates ± standard deviations of the means.

3.3 DISCUSSION

Our work represents the first time that a His-tagged lipase (I-His$_{TEVS}$-LipC12) has shown to have lower hydrolytic activity but higher esterification activity, when compared to a similar recombinant enzyme without the His-tag (I-cLipC12). Since lipases are used both for hydrolysis and synthesis reactions, this opens up the possibility of removing the His-tag or not, after expression, in order to tailor the enzyme for the specific application that is intended.

Various previous studies have reported the effects of affinity tags on hydrolytic and esterification activities, as we discuss below. In our comparisons with the literature, we will use the prefix “wt” to indicate a wild type lipase, indicating that the lipase was not produced using molecular biology techniques. The prefix “r” will be used to indicate a recombinant lipase without a His-tag. Since His-tag proteins are recombinant proteins, where possible, we will compare the His-tagged lipases with similar recombinant lipases. Where the authors did not give results for a recombinant lipase, we will undertake comparisons with the wild type lipase.

The most important result of our work is that a His-tag on LipC12 negatively affected hydrolytic activity but promoted esterification activity. His-tagged variants of LipC12 consistently gave lower hydrolytic activities in aqueous media. Both free (CSF-His-LipC12 and His$_{TEVS}$-LipC12) and immobilized (I-CSF-His-LipC12 and I-His$_{TEVS}$-LipC12) enzymes had lower specific olive-oil-hydrolyzing activities than their non-His-

tagged counterparts in free (CSF-rLipC12 and cLipC12) and immobilized (I-CSF-rLipC12 and I-cLipC12) forms. Likewise, for the hydrolysis of *p*NPD, the value of k_{cat}/K_M for His_{TEVS}-LipC12 was 75% of the value obtained for cLipC12. The situation was different for esterification of oleic acid with ethanol in *n*-hexane. In this case, I-CSF-His-LipC12 and I-CSF-rLipC12 had similar activities, but, on the other hand, I-His_{TEVS}-LipC12 had both a significantly higher activity and a better stability in the reaction medium than did I-cLipC12.

We suggest that these results might be explained as follows: the His-tag is highly flexible in aqueous medium and some of its movements may temporarily block access of substrates to the active site. There are two possibilities: the flexible His-tag may interfere with the opening of the lid or it might interact with the active site of other lipases in the reaction medium, as has been shown for Majoreck et al.[3]. To investigate the second possibility, we added two non-ionic detergents (Triton X-100 and Nonidet P-40) to reaction media during the hydrolysis of *p*NPD, with the aim of separating aggregates of enzyme molecules. For both detergents, we used concentrations both above and below the critical micellar concentration (CMC), which is 0.24 mM for Triton X-100 and 0.08 mM for Nonidet P-40. The effects of the detergents on the two lipases were similar, although the activity of the LipC12 variant without the His-tag (cLipC12) was higher than that of the variant with the His-tag (His_{TEVS}-LipC12) at all detergent concentrations (Supplementary Figure S7). This result suggests that there is no interaction between different lipase molecules and, therefore, that the second possibility does not occur.

On the other hand, proteins tend to be less flexible in hydrophobic organic solvents of relatively high log P values, such as the *n*-hexane[35] that was used in the esterification reactions. In this medium, the His-tag would also be less flexible, for example, it might be trapped within the solvation layer, and therefore unable to interfere with the access of substrates to the active site. NMR analysis or molecular dynamics studies of LipC12 with and without His-tag in aqueous solution and in the presence of organic solvents would be needed to confirm these suggestions. We recognize that our explanation does not explain why I-His_{TEVS}-LipC12 had a significantly higher esterification activity than I-cLipC12. However, His-tags can have subtle effects on protein structure[6]. For example, although a His-tag did not affect the overall structure of myoglobin, it did alter the picosecond-scale dynamic of the protein; this change can affect the recognition of ligands[36].

The effects of His-tags on lipases have been most studied with respect to their effects on hydrolytic activities (Table 4). Various authors have compared specific activities of lipases with and without His-tags, using several different substrates. Results are variable, with His-tags having been reported to have no effect or to cause decreases and increases of specific hydrolytic activity. In our case, the His-tag decreased the specific olive-oil-hydrolyzing activities (values were 2555 U mg^{-1} for His_{TEVS}-LipC12 and 4590 U mg^{-1} for cLipC12). Decreases in specific hydrolytic activity due to the His-tag have been reported previously. For example, for *Staphylococcus aureus* lipase 3 (SAL3), the specific activity of His-SAL3 against tributyrin (4000 U mg^{-1}) was lower than that of the recombinant untagged enzyme (r-SAL3, 4500 U mg^{-1})[14]. Likewise, for the hydrolysis of tributyrin (TC4) and olive oil by the lipase of *S. xylosus,* His-SXL had lower specific activities (1500 and 850, respectively, for TC4 and olive oil) than did r-SXL (2000 and 1400, respectively, for TC4 and olive oil)[37]. However, in some cases, the specific hydrolytic activity was higher with the His-tag. For example, in the case of SAL3, the specific activity against olive oil of His-SAL3 (1300 U mg^{-1}) was higher than that of r-SAL3 (1100 U mg^{-1}). Similar results were obtained for the hydrolysis of TC4 and olive oil by the lipase of *S. simulans* (SSL). The specific activities of His-SSL against both these substrates (980 and 940 U mg^{-1}, respectively, for TC4 and olive oil) were higher than those of r-SSL (850 U mg^{-1}, for both TC4 and olive oil)[37]. In some cases, the His-tag caused no significant difference in specific hydrolytic activities. This has been reported for the hydrolysis of *p*NPB, *p*NPL and carboxyfluorescein diacetate by Lipase B of *Candida antarctica* (CALB)[38], for the hydrolysis of olive oil and TC4 by turkey pancreatic lipase (TPL)[39] and for the hydrolysis of TC4, trioctanoin (TC8) and olive oil by the lipase of *Fusarium solani*[40] (Table 4).

Some authors have analyzed the effect of the His-tag on kinetic parameters (Table 4). Again, the results are quite variable. In our case, the His-tag did not have any effect on k_{cat} for hydrolysis of *p*-nitrophenyl decanoate, but increased K_M 1.3-fold, such that k_{cat}/K_M for His_{TEVS}-LipC12 was 75% of the value obtained for cLipC12. In other words, the presence of the His-tag decreases the catalytic efficiency of LipC12 with *p*NPD as the substrate. Decreases in k_{cat}/K_M with the presence of the His-tag have been reported previously: for SAL3 with TC4 as the substrate, k_{cat}/K_M for His-SAL3 was 74% of the value obtained with r-SAL3[14]; for SXL with TC8 as the substrate, k_{cat}/K_M was 80% of the value obtained for wt-SXL[12] and for various variants of CALB with a fusion protein at the N-terminus and a His-tag at the C-terminus, the His-tagged

proteins had values of k_{cat}/K_M for the hydrolysis of *p*-nitrophenyl butyrate (*p*NPB) that were from 85 to 98% of the value for the unmodified CALB[41]. Increases in k_{cat}/K_M have also been reported for His-tagged lipases with TC8 as the substrate: for SAL3, the value of k_{cat}/K_M for His-SAL3 was 1.5-fold higher than that for r-SAL3[14] while for SXL, the value of k_{cat}/K_M for His-SXL was 1.2-fold greater than that for wt-SXL[12]. There are also some reports of no significant differences in the kinetic parameters between the His-tagged and non-tagged forms: this was the case for a CALB, for both *p*NPB and *p*-nitrophenol laurate (*p*NPL) as substrates[38] and for TPL with TC4 as the substrate[39].

Significantly, our work represents the first report of a His-tag leading to an increase in esterification activity of a lipase: for the synthesis of ethyl-oleate in *n*-hexane, the specific activity of I-His_{TEVS}-LipC12 (9.21 ± 0.01 U g^{-1}) was significantly higher than that of I-cLipC12 (5.26 ± 0.03 U g^{-1}). The only previous study of the effects of His-tags on esterification activity, undertaken by Horchani et al.[14], involved the synthesis of butyl oleate in *n*-hexane with three immobilized variants of *S. aureus* lipase 3: I-wt-SAL3, I-r-SAL3 and I-His-SAL3. Based on the conversions at the first sampling time of that study, 4 h, one can infer that r-SAL3 and His-SAL3 gave similar initial esterification rates, which were much lower than that obtained with I-wt-SAL3. Horchani et al.[14] followed the reaction profiles over 24 h, with I-wt-SAL3 giving a conversion of around 70% in 20 h and both r-SAL3 and His-SAL3 giving much lower conversions at this time, of around 20%[14]. The key difference from our work is that the presence of the His-tag did not improve the esterification performance of SAL3.

Our study is also the first study of the effect of a His-tag on the stability of a lipase in polar organic solvents. Our key result was that, after a 3-h incubation, His_{TEVS}-LipC12 had activities around 1.2-fold greater than cLipC12 in the cases of 20% methanol, 20% acetonitrile, 20% DMF and 40% DMSO. The only previous direct study of the effect of a His-tag on the stability of a lipase in solvents was undertaken by Horchani et al.[14]. They incubated immobilized variants of SAL3 in non-polar solvents, including *n*-hexane, the solvent that they had used in their esterification studies. After a 24-h incubation in *n*-hexane, both free and immobilized wt-SAL3 and r-SAL3 retained 100% activity, while free and immobilized His-SAL3 had lower residual activities, of 70 and 80%, respectively. The key difference from our work is that, in the case of SAL3, the presence of the His-tag decreased stability in the solvents tested, although it should be noted than *n*-hexane is much less polar than the solvents that we used in our stability studies. The results of Horchani et al.[14] suggest, indirectly, that both I-r-SAL3

and I-His-SAL3 are denatured by polar solvents. The low final conversions that they obtained at 20 h must have been caused by denaturation, as the reaction profiles had leveled out. Since both I-r-SAL3 and I-His-SAL3 had given residual activities above 80% after 24-h incubations in *n*-hexane in their stability study, the loss of activity of these preparations in the esterification reaction was not due to the presence of *n*-hexane. It is possible to infer, then, that both I-r-SAL3 and I-His-SAL3 were denatured by one of the reaction species involved in the synthesis of butyl oleate, possibly the butanol, with the presence of the His-tag not improving stability. Contrary to these results of Horchani et al.[14], in our case the presence of the His-tag did improve stability within the esterification reaction medium, with the residual activity after 10 h being 54% for I-His_{TEVS}-LipC12 against only 24% for I-cLipC12.

In the case of immobilization of lipases, only one previous study has addressed the effect of His-tags. In this study, Horchani et al.[14] immobilized wt-SAL3, r-SAL3 and His-SAL3 on $CaCO_3$. The immobilization yield was high for wt-SAL3 (79%). It was significantly lower for r-SAL3 (22%) and much lower still for His-SAL3 (2.5%), suggesting that the His-tag did interfere somehow with immobilization. This effect of the His-tag is different from the effect in the current work, in which the His-tag did not affect immobilization.

Our study demonstrates that the His-tag decreases the specific hydrolytic activities of both the free and immobilized forms of LipC12 against triacylglycerols. However, in several polar solvents, both the *p*NPD-hydrolyzing activity and the stability were favored by the presence of the His-tag. Importantly, our study represents the first time that a His-tag has increased esterification action. Our work gives insights into tailoring lipases for specific applications: for hydrolysis reactions, the His-tag should be removed from LipC12, while for esterification reactions, it should be retained.

3.4 METHODS

3.4.1 Bacterial strains, plasmids and protein expression

LipC12 is a lipase isolated by Glogauer et al.[15] from a metagenomic library prepared from DNA extracted from fat-contaminated soil of a waste treatment plant. The gene *lipC12* was cloned into pET28a(+) (this plasmid is referred to as pET28lipC12) to produce an N-terminal His-tagged protein (denominated His-LipC12)

that has a theoretical molecular weight of 33.4 kDa. The *lipC12* gene was also cloned into pET29a(+). This was done by digesting pET28lipC12 with *NdeI* and *BamHI* and ligating the *lipC12* coding region into the pET29a vector (Novagen, Hertfordshire, United Kingdom), which had been previously digested with the same restriction enzymes. The resulting plasmid was called pET29lipC12. It was used to produce recombinant LipC12 without a His-tag (denominated named rLipC12).

Additionally, the *lipC12* gene was cloned into the pTEV5 vector to obtain the plasmid named pTEV5lipC12. This was done by digesting pET28lipC12 with *NdeI* and *BamHI* and ligating the *lipC12* coding region into the pTEV5 vector, which had been previously digested with the same restriction enzymes. The LipC12 produced in cells harboring pTEV5lipC12 is named His_{TEVS}-LipC12 and contains a His-tag at the N-terminal and a TEV protease site (TEVS) to allow His-tag cleavage with TEV. After TEV cleavage, the protein is named cLipC12, which is an un-tagged LipC12 that contains 4 extra amino acids (GASH).

His-LipC12, rLipC12, His_{TEVS}-LipC12 and TEV protease were overexpressed in *Escherichia coli* strains harboring the plasmids listed in Supplementary Table S2. The *E. coli* strains and expression conditions are also described in Supplementary Table S2. The overexpression and cells disruption by ultrasonication were done as previously described[15,16].

3.4.2 Protein purification

His_{TEVS}-LipC12 was purified using a 5-mL HiTrap Chelating column (GE Healthcare, Uppsala, Sweden) preequilibrated with buffer A (20 mM Tris-HCl pH 7.5, 150 mM NaCl, 10% (v/v) glycerol and 20 mM imidazole). The protein was eluted stepwise, using increasing concentrations (from 50 to 500 mM) of imidazole in buffer A, with 2 column volumes of buffer being passed at each concentration. Fractions with purity over 95%, as judged by SDS-PAGE (Supplementary Fig. S1), were pooled. Imidazole was removed in a HiTrap Desalting column (GE Healthcare, Uppsala, Sweden) using a 20-mM Tris-HCl buffer at pH 7.5 that contained 150 mM NaCl and 5% (v/v) glycerol. TEV protease was purified as previously described[42].

3.4.3 Cleavage of the His-tag with TEV protease

Purified His_{TEVS}-LipC12 and TEV protease were mixed in 2 mL of buffer (20 mM Tris-HCl pH 7.5 and 150 mM NaCl), in a mass ratio of His_{TEVS}-LipC12 to TEV protease of 10:1. The mixture was maintained at 8 °C, 90 rpm for 20 h. It was then passed through a 5-mL HiTrap Chelating column (GE Healthcare). cLipC12 was eluted with 100 mM imidazole and TEV protease was eluted with 300 mM imidazole. Imidazole was removed from the LipC12 preparation in a desalting column, using a 20 mM Tris-HCl buffer at pH 7.5 that contained 150 mM NaCl and 5% (v/v) glycerol.

The efficiency of cleavage of the His-tag was confirmed by 12% (w/v) SDS-PAGE followed by western blotting and incubation with the anti-His antibody Ni-NTA HPR (Qiagen, Hilden, Germany).

3.4.4 Titrimetric determination of triacylglycerol-hydrolyzing activity

The triacylglycerol-hydrolyzing activities of the soluble fractions of crude extracts and of purified lipase preparations were determined by the titrimetric method using an automatic titrator (Metrohm 718 STAT Titrino potentiometric titrator, Metrohm, Herisau, Switzerland) with 0.05 M NaOH during 5 min. The conditions have been previously described[16,43]. The reactions were performed at 30 °C using 20 mL of emulsion at pH 7.0. One unit of hydrolytic activity in aqueous medium corresponds to the release of 1 µmol of fatty acid per min, under the assay conditions.

3.4.5 Spectrophotometric determination of *p*NPD-hydrolyzing activity

The *p*NPD-hydrolyzing activities of the lipases in aqueous solution were determined by monitoring the release of *p*-nitrophenol from *p*-nitrophenyl decanoate (Sigma, St. Louis, USA) at 410 nm at 25 °C in an iMark™ Microplate Absorbance Reader (Bio-Rad, Hercules, USA).

The standard assay conditions have been previously described[15]. The final volume of the reaction mixture was 250 µL. It contained 50 mM Tris-HCl buffer, pH 7.5, 1 mM $CaCl_2$, 0.6% (v/v) Triton X-100, 1 mM *p*NPD, 4% (v/v) isopropanol, 1% (v/v) acetonitrile and an enzyme concentration of 172 nM when His_{TEVS}-LipC12 was assayed and of 123 nM when LipC12 was assayed. One unit of lipase activity was defined as 1 µmol of *p*-nitrophenol produced per min. Linear regressions to determine initial reaction velocities were performed with Microsoft Excel.

The *p*NPD-hydrolyzing activities of the lipases in the presence of polar organic solvents were determined at concentrations varying from 10 to 60% (v/v) of the solvent (ethanol, isopropanol, methanol, propanol, acetone, acetonitrile, dimethylformamide (DMF) or dimethylsulfoxide (DMSO)) in water. The activity was determined in a 96-well plate by monitoring the release of *p*-nitrophenol from *p*NPD, according to standard assay conditions with the addition of the stated solvent concentrations.

The stability of the lipases was determined by measuring the residual activity after incubation (at final concentrations of 1.72 µM for His_{TEVS}-LipC12 and 1.23 µM for LipC12) for 3 h at 25 °C in the same polar organic solvents described for activity. The enzymes were then diluted in 50-mM Tris-HCl buffer at pH 7.5, 150 mM NaCl and 2-mM $CaCl_2$ in the reaction media to reach the protein concentrations of 172 nM and 123 nM used in the standard assay of *p*NPD-hydrolyzing activities.

3.4.6 Determination of kinetic parameters

The kinetic parameters were determined using concentrations of *p*NPD ranging from 0.1 to 3.5 mM and 10 µL of enzyme (enzyme concentration in the reaction medium of 6.9 µM for His_{TEVS}-LipC12 and 4.9 µM for LipC12). The reaction was followed for 5 min with the absorbance at 410 nm being read every 30 s. The values of K_M and k_{cat} were determined by non-linear regression, in GraphPad Prism 7, of the data of initial velocity versus substrate concentration, using the Michaelis-Menten equation. The program was used to calculate 95% confidence intervals.

3.4.7 Circular dichroism

CD spectra of proteins were recorded between 250 and 350 nm using a JASCO J-815 spectropolarimeter (Easton, USA) fitted with a Jasco Peltier-type temperature controller (CDF-426S/15). The optical pathlength was 2 mm and the concentration of the protein solution was 5 µM in a pH 7.4 buffer containing 10 mM sodium phosphate and 100 mM NaCl. The spectra were recorded at 25°C. The percentages of secondary structures (α-helices and β-sheets) were determined with the software K2D3[44], after conversion of the data to delta epsilon values (Δε), also referred as the molar circular dichroism[21].

The melting temperatures (Tm) were determined by measuring the CD signal at 222 nm with increasing temperature in a continuous ramp mode (1 ºC/2 min). The temperature was increased from 25 to 98 ºC. The Tm was determined from the first derivative using GraphPrism 6.0.

3.4.8 Lipase immobilization

The covalent immobilization of LipC12 preparations was performed using Immobead 150 (Sigma–Aldrich, St. Louis, USA) according to Madalozzo et al.[16]. The immobilization kinetics of crude soluble fractions containing His-LipC12 and rLipC12 were determined with protein loadings of 200 mg g^{-1} during 8-h incubations at 4 °C in an orbital shaker at 150 rpm. Purified His_{TEVS}-LipC12 and cLipC12 were also immobilized on Immobead 150 with protein loadings of 10 mg g^{-1}, with incubation for 6 h at 4 °C in an orbital shaker at 150 rpm.

A desorption test was done after immobilization. Twenty mg of the support was added to 200 µL of a 2% (m/v) SDS solution. The mixture was heated at 100 ºC for 30 min. After that, samples were loaded onto a 12% SDS-PAGE gel for analysis. The percentage of desorption was calculated based on the protein contents of the samples (which were estimated using the protein standards supplied by the manufacturer, GE Healthcare).

3.4.9 Determination of the esterification activity

The esterification activities of the immobilized preparations of LipC12 were determined based on ethyl-oleate synthesis[16]. The reactions were carried out in 25-mL Erlenmeyer flasks, with 5 mL of reaction medium (210 mmol L^{-1} ethanol and 70 mmol L^{-1} oleic acid in *n*-hexane). The flasks were placed in an orbital shaker at 40 °C and 250 rpm. The reaction was started with the addition of 110 mg of the immobilized enzyme. At each sampling time, a 100-µL sample was collected and analyzed to quantify free fatty acids by the colorimetric Lowry-Tinsley method[45]. One unit of lipase esterification activity (U) corresponds to the consumption of 1 µmol of fatty acid per min, under the assay conditions.

3.4.10 Protein analysis

The molecular weight of the proteins was determined using the ProtParam tool of the online program Expasy. Protein electrophoresis was carried out by 12% SDS-PAGE[46] and gels were stained with Coomassie Blue. Densitometry analysis of the protein bands from the SDS-PAGE gel was performed using the LabWorks Software Version 4.0 (UVP BioImaging Systems, Upland, CA). Protein concentrations were determined by the Bradford assay using bovine serum albumin as the standard[47].

3.4.11 Statistical analysis

For all assays, the standard deviation of the mean was calculated. The two-tailed unpaired *t* test was used to compare activities and stability values of LipC12 variants with and without His-tags. Differences were evaluated for significance at the 5% level (i.e. $P < 0.05$). The difference of the kinetic parameters was obtained by 95% confidence intervals (profile-likelihood).

3.4.12 Data availability

The datasets generated and analyzed during the current study are available from the corresponding author on reasonable request.

Table 4. Effects of His-tags on lipases.

Lipase	Tag	Aspect studied	Key results for His-tagged protein relative to untagged protein	Article
Metagenomic lipase LipC12, expressed in *Escherichia coli*	N-terminal His-tag (Six histidine residues)	Specific hydrolytic activities against TC4, TC8, TC18, olive oil, *p*NPD	Lower	This work
		Hydrolytic activities against *p*NPD in presence of polar organic solvents	Higher in acetone, DMF and DMSO	
		Stability in polar organic solvents	Higher in methanol, acetonitrile and DMF	
		Kinetic parameters for *p*NPD hydrolysis	K_M and k_{cat}/K_M higher	
		Synthesis of ethyl oleate over 10 h with immobilized lipase	Higher	
Staphylococcus xylosus Lipase (SXL)	N-terminal His-tag (Six histidine residues)	Kinetic parameters for hydrolysis of TC4 and TC8	K_M and k_{cat} lower; k_{cat}/K_M higher for TC4, but not affected for TC8	Mosbah et al (2006)[12]
Lipase B of *Candida antarctica* (CALB) expressed in *Escherichia coli*	N-terminal FLAG and C-terminal His-tag	Specific hydrolytic activities against *p*NPB, *p*NPL and CFDA	No difference	Blank et al (2006)[38]
		Kinetic parameters for hydrolysis of *p*NPB and *p*NPL	No difference	
Lipase B of *Candida antarctica* (CALB	Fusion proteins (Mdh, PotD, SlyD, GST, MBP) on the N-terminal and C-terminal His-tag	Kinetic parameters for hydrolysis of *p*PNB	K_M, k_{cat} and k_{cat}/K_M lower for all tags	Seo et al (2009)[41]
Staphylococcus aureus Lipase (SAL)	N-terminal His-tag (Six histidine residues)	Specific hydrolytic activities	Lower in tributyrin, higher in olive oil	Horchani et al (2009)[14]
		Kinetic parameters for hydrolysis of TC4	k_{cat}/K_M lower	
		Immobilization on $CaCO_3$	Immobilization efficiency lower	
		Synthesis of butyl oleate with immobilized lipase over 24 h	Lower conversion of oleic acid to ester	
		Stability in organic solvents	Lower stability in organic solvents (*n*-hexane, *tert*-butanol and chloroform) for both free and immobilized forms	
Lipases of *Staphylococcus simulans* (SSL & rSSL), *S. xylosus* (SXL & rSXL) and	N-terminal His-tag (Six histidine residues)	Specific hydrolytic activities	Lower with TC4 and with olive oil for HisSXL, higher with TC4 and with olive oil for HisSSL	Horchani et al (2010)[37]

S. aureus (SAL & rSAL)				
Turkey pancreatic lipase (TPL)	N-terminal His-tag (Six histidine residues	Specific hydrolytic activities against olive oil and TC4	No significant difference	Bou Ali et al (2014)[39]
		Kinetic parameters for hydrolysis of olive oil and TC4	No significant difference in k_{cat} and k_{cat}/K_M	
Yarrowia lipolytica Lipase YlLip11	N-terminal His-tag (Six histidine residues)	Activity against *p*NPP	Tagged proteins were produced, but inactive	Kumari et al (2015)[48]
Fusarium solani lipase expressed in *Pichia pastoris*	N-terminal His-tag (Six histidine residues)	Specific activities against TC4, TC8, olive oil, phospholipids (egg-yolk PC) and galactolipids (1,2-octanoyl-3-O-α-D-galactosyl-sn-glycerol (DiC8-MGDG)	No difference	Jallouli et al (2016)[40]

3.5 REFERENCES

1. Arnau, J., Lauritzen, C., Petersen, G. E. & Pedersen, J. Current strategies for the use of affinity tags and tag removal for the purification of recombinant proteins. *Protein Expr. Purif.* **48,** 1–13 (2006).
2. Terpe, K. Overview of tag protein fusions: from molecular and biochemical fundamentals to commercial systems. *Appl. Microbiol. Biotechnol.* **60,** 523–533 (2003).
3. Majorek, K. A., Kuhn, M. L., Chruszcz, M., Anderson, W. F. & Minor, W. Double trouble-Buffer selection and His-tag presence may be responsible for nonreproducibility of biomedical experiments. *Protein Sci.* **23,** 1359–1368 (2014).
4. Costa, S., Almeida, A., Castro, A. & Domingues, L. Fusion tags for protein solubility, purification, and immunogenicity in *Escherichia coli*: The novel Fh8 system. *Frontiers in Microbiology* **5,** 63 (2014).
5. Kimple, M. E., Brill, A. L. & Pasker, R. L. in *Current Protocols in Protein Science* **73,** 9.9.1-9.9.23 (John Wiley & Sons, Inc., 2013).
6. Carson, M., Johnson, D. H., McDonald, H., Brouillette, C. & DeLucas, L. J. His-tag impact on structure. *Acta Crystallogr. Sect. D Biol. Crystallogr.* **63,** 295–301 (2007).
7. Waugh, D. S. Making the most of affinity tags. *Trends in Biotechnology* **23,** 316–320 (2005).
8. Studier, F. W. & Moffatt, B. A. Use of bacteriophage T7 RNA polymerase to direct selective high-level expression of cloned genes. *J. Mol. Biol.* **189,** 113–130 (1986).
9. Adlercreutz, P. Immobilisation and application of lipases in organic media. *Chem. Soc. Rev.* **42,** 6406–36 (2013).
10. Kumar, A., Dhar, K., Kanwar, S. S. & Arora, P. K. Lipase catalysis in organic solvents: advantages and applications. *Biol. Proced. Online* **18,** 2 (2016).
11. Schmid, R. D. & Verger, R. Lipases: interfacial enzymes with attractive applications. *Angew. Chemie Int. Ed.* **37,** 1608–1633 (1998).
12. Mosbah, H., Sayari, A., Bezzine, S. & Gargouri, Y. Expression, purification, and characterization of His-tagged *Staphylococcus xylosus* lipase wild-type and its mutant Asp 290 Ala. *Protein Expr. Purif.* **47,** 516–523 (2006).

13. Sayari, A., Mosbah, H., Verger, R. & Gargouri, Y. The N-terminal His-tag affects the enantioselectivity of staphylococcal lipases: A monolayer study. *J. Colloid Interface Sci.* **313,** 261–267 (2007).
14. Horchani, H., Ouertani, S., Gargouri, Y. & Sayari, A. The N-terminal His-tag and the recombination process affect the biochemical properties of *Staphylococcus aureus* lipase produced in *Escherichia coli*. *J. Mol. Catal. B Enzym.* **61,** 194–201 (2009).
15. Glogauer, A. *et al.* Identification and characterization of a new true lipase isolated through metagenomic approach. *Microb. Cell Fact.* **10,** 54 (2011).
16. Madalozzo, A. D. *et al.* Immobilization of LipC12, a new lipase obtained by metagenomics, and its application in the synthesis of biodiesel esters. *J. Mol. Catal. B Enzym.* **116,** 45–51 (2015).
17. Madalozzo, A. D. *et al.* Synthesis of flavor esters and structured lipids by a new immobilized lipase, LipC12, obtained from metagenomics. *Biocatal. Agric. Biotechnol.* **8,** 294–300 (2016).
18. Qiagen. *The QIAexpressionist. A handbook for high-level expression and purification of 6xHis-tagged proteins*. (2003).
19. Gräslund, S. *et al.* Protein production and purification. *Nat. Methods* **5,** 135–146 (2008).
20. Waugh, D. S. An overview of enzymatic reagents for the removal of affinity tags. *Protein Expr. Purif.* **80,** 283–293 (2011).
21. Greenfield, N. J. Using circular dichroism spectra to estimate protein secondary structure. *Nat. Protoc.* **1,** 2876–2890 (2007).
22. Kamal, Z., Yedavalli, P., Deshmukh, M. V. & Rao, N. M. Lipase in aqueous-polar organic solvents: Activity, structure, and stability. *Protein Sci.* **22,** 904–915 (2013).
23. Kumar, V., Yedavalli, P., Gupta, V. & Rao, N. M. Engineering lipase A from mesophilic *Bacillus subtilis* for activity at low temperatures. *Protein Eng. Des. Sel.* **27,** 73–82 (2014).
24. Shariff, F. M., Rahman, R. N. Z. R. A., Basri, M. & Salleh, A. B. A newly isolated thermostable lipase from *Bacillus* sp. *Int. J. Mol. Sci.* **12,** 2917–34 (2011).
25. Bertoldo, J. B. *et al.* Structural stability of *Staphylococcus xylosus* lipase is modulated by Zn^{2+} ions. *Biochim. Biophys. Acta - Proteins Proteomics* **1814,**

1120–1126 (2011).

26. Zhao, D. & Huang, Z. Effect of His-Tag on expression, purification, and structure of zinc finger protein, ZNF191(243-368). *Bioinorg. Chem. Appl.* **2016,** (2016).
27. Carrea, G. & Riva, S. Properties and Synthetic Applications of Enzymes in Organic Solvents. *Angew. Chemie Int. Ed.* **39,** 2226–2254 (2000).
28. Tsuzuki, W., Ue, A. & Nagao, A. Polar organic solvent added to an aqueous solution changes hydrolytic property of lipase. *Biosci. Biotechnol. Biochem.* **67,** 1660–1666 (2003).
29. Tsuzuki, W., Ue, A. & Kitamura, Y. Effect of Dimethylsulfoxide on Hydrolysis of Lipase. *Biosci. Biotechnol. Biochem.* **65,** 2078–2082 (2001).
30. Inagami, T. & Sturtevant, J. M. The trypsin-catalyzed hydrolysis of benzoyl-l-arginine ethyl ester. *Biochim. Biophys. Acta* **38,** 64–79 (1960).
31. Rammler, D. H. The effect of DMSO on several enzyme systems. *Ann. N. Y. Acad. Sci.* **141,** 291–299 (1967).
32. Cadirci, B. H. & Yasa, I. An organic solvents tolerant and thermotolerant lipase from *Pseudomonas fluorescens* P21. *J. Mol. Catal. B Enzym.* **64,** 155–161 (2010).
33. Montero, S. *et al.* Immobilization of *Candida rugosa* lipase and some properties of the immobilized enzyme. *Enzyme Microb. Technol.* **15,** 239–47 (1993).
34. Bosley, J. A. & Peilow, A. D. Immobilization of lipases on porous polypropylene: Reduction in esterification efficiency at low loading. *J. Am. Oil Chem. Soc.* **74,** 107–111 (1997).
35. Wang, S. *et al.* Enzyme stability and activity in non-aqueous reaction systems: a mini review. *Catalysts* **6,** 32 (2016).
36. Thielges, M. C., Chung, J. K., Axup, J. Y. & Fayer, M. D. Influence of histidine tag attachment on picosecond protein dynamics. *Biochemistry* **50,** 5799–5805 (2011).
37. Horchani, H. *et al.* Heterologous expression and N-terminal His-tagging processes affect the catalytic properties of staphylococcal lipases: A monolayer study. *J. Colloid Interface Sci.* **350,** 586–594 (2010).
38. Blank, K., Morfill, J., Gumpp, H. & Gaub, H. E. Functional expression of *Candida antarctica* lipase B in *Eschericha coli*. *J. Biotechnol.* **125,** 474–483 (2006).

39. Bou Ali, M., Ben Ali, Y., Aissa, I. & Gargouri, Y. Eukaryotic expression system *Pichia pastoris* affects the lipase catalytic properties: A monolayer study. *PLoS One* **9,** 1–8 (2014).
40. Jallouli, R. *et al.* Heterologous overexpression and biochemical characterization of the (galactophospho)lipase from *Fusarium solani* in *Pichia pastoris* that is expressed in planta. *Int. J. Biol. Macromol.* **84,** 94–100 (2016).
41. Seo, H. S. *et al.* Functional fusion mutant of *Candida antarctica* lipase B (CalB) expressed in *Escherichia coli*. *Biochim. Biophys. Acta - Proteins Proteomics* **1794,** 519–525 (2009).
42. Van Den Berg, S., Löfdahl, P. Å., Härd, T. & Berglund, H. Improved solubility of TEV protease by directed evolution. *J. Biotechnol.* **121,** 291–298 (2006).
43. Tiss, A., Carrière, F. & Verger, R. Effects of gum arabic on lipase interfacial binding and activity. *Anal. Biochem.* **294,** 36–43 (2001).
44. Louis-Jeune, C., Andrade-Navarro, M. A. & Perez-Iratxeta, C. Prediction of protein secondary structure from circular dichroism using theoretically derived spectra. *Proteins Struct. Funct. Bioinforma.* **80,** 374–381 (2012).
45. Lowry, R. R. & Tinsley, I. J. Rapid colorimetric determination of free fatty acids. *J. Am. Oil Chem. Soc.* **53,** 470–472 (1976).
46. Laemmli, U. K. Cleavage of structural proteins during the assembly of the head of bacteriophage T4. *Nature* **227,** 680–685 (1970).
47. Bradford, M. M. A rapid and sensitive method for the quantitation of microgram quantities of protein utilizing the principle of protein-dye binding. *Anal. Biochem.* **72,** 248–254 (1976).
48. Kumari, A., Baronian, K., Kunze, G. & Gupta, R. Extracellular expression of YlLip11 with a native signal peptide from *Yarrowia lipolytica* MSR80 in three different yeast hosts. *Protein Expr. Purif.* **110,** 138–144 (2015).

3.5.1 Acknowledgments

This research was supported by Universal grants (Projects 441015/2016-6 and 303079/2015-0) from CNPq (Conselho Nacional de Desenvolvimento Científico e Tecnológico), a Brazilian government agency for the advancement of science and technology. Research scholarships were granted to J.M.A, N.K, D.A.M., F.O.P, and E.M.S. by CNPq and to V.R.M. by CAPES (Coordenação de Aperfeiçoamento de

Pessoal de Nível Superior), a Brazilian government agency for the development of personnel in higher education.

3.5.2 Author Contributions

J.M.A. and V.R.M. designed, performed the experiments, analyzed the data, wrote and revised the manuscript. D.A.M. and N.K. contributed to data analysis, wrote and revised the manuscript. M.M.S., E.M.S. and F.O.P. reviewed the manuscript.

3.5.3 Additional Information

Competing Interests: The authors declare that they have no competing interests.

3.6 SUPPLEMENTARY MATERIAL

Tailoring recombinant lipases: keeping the His-tag favors esterification reactions, removing it favors hydrolysis reactions

Janaina Marques de Almeida[1#], Vivian Rotuno Moure[1#], Marcelo Müller-Santos[1], Emanuel Maltempi de Souza[1], Fábio de Oliveira Pedrosa[1], David Alexander Mitchell[1] and Nadia Krieger[2*].

[1]Departamento de Bioquímica e Biologia Molecular, Universidade Federal do Paraná, Cx.P. 19046 Centro Politécnico, Curitiba 81531-980, Paraná, Brazil.
[2]Departamento de Química, Universidade Federal do Paraná, Cx.P. 19081 Centro Politécnico, Curitiba 81531-980, Paraná, Brazil.
[*] To whom correspondence should be addressed. E-mail: nkrieger@ufpr.br; Telephone: +55-41-33613470. [#] J.M.A and V.R.M. contributed equally to this work

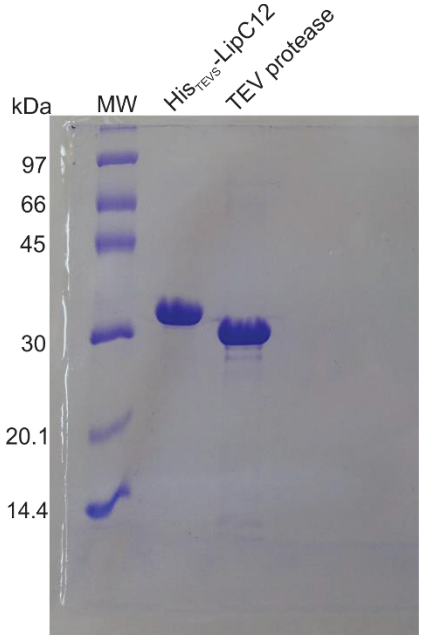

Supplementary Figure S1. Purified fraction of His_{TEVS}-LipC12 and TEV protease. 5 μg of each protein was analyzed on 15% SDS-PAGE and the gel was stained with Coomassie blue. The molecular weight standard (MW) ladder is shown as kDa. For purification of His_{TEVS}-LipC12, the cellular pellet was resuspended in 30 mL of 20 mM Tris-HCl buffer (pH 7.5) containing 150 mM NaCl, 10% (v/v) glycerol and 20 mM imidazole. The soluble fraction was loaded onto a 5-mL HiTrap chelating column. After washing in buffer containing 50 mM imidazole, protein was eluted with a stepwise gradient of imidazole. The target protein was eluted in 300 mM imidazole. Fractions were pooled and loaded onto a 5-mL desalting column (2×) and eluted in a 20 mM Tris-HCl buffer (pH 7.5) containing 150 mM NaCl and 5% (v/v) glycerol. For purification of TEV protease, the cellular pellet was resuspended in 30 mL of 50 mM sodium phosphate buffer (pH 7.4) containing 300 mM NaCl. The soluble fraction was loaded onto a 1-mL HisTrap column. After washing in buffer containing 20 mM imidazole, protein was eluted with a stepwise gradient of imidazole. TEV was eluted in 250 mM imidazole. Fractions were pooled and loaded onto a 5-mL desalting column (2×) and eluted in a 25 mM sodium phosphate buffer (pH 7.5) containing 200 mM NaCl, 2 mM EDTA, 2 mM DTT and 10% (v/v) glycerol.

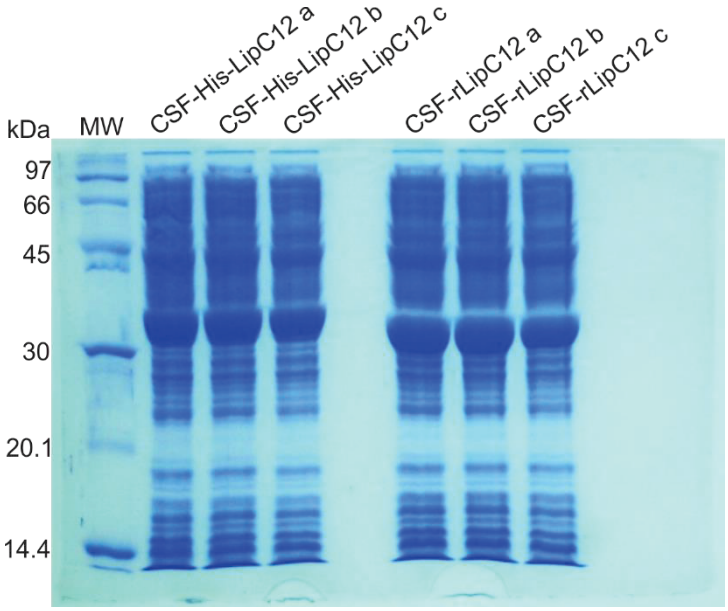

Supplementary Figure S2. Expression of His-LipC12 and rLipC12. Replicates of crude soluble fractions (CSF) containing His-LipC12 and LipC12 (61 and 64 µg of protein respectively) were analyzed on 12% SDS-PAGE and the gel was stained with Coomassie blue. The molecular weight standard (MW) is shown as kDa. The target proteins in the gel were analyzed by densitometry using the LabWorks program.

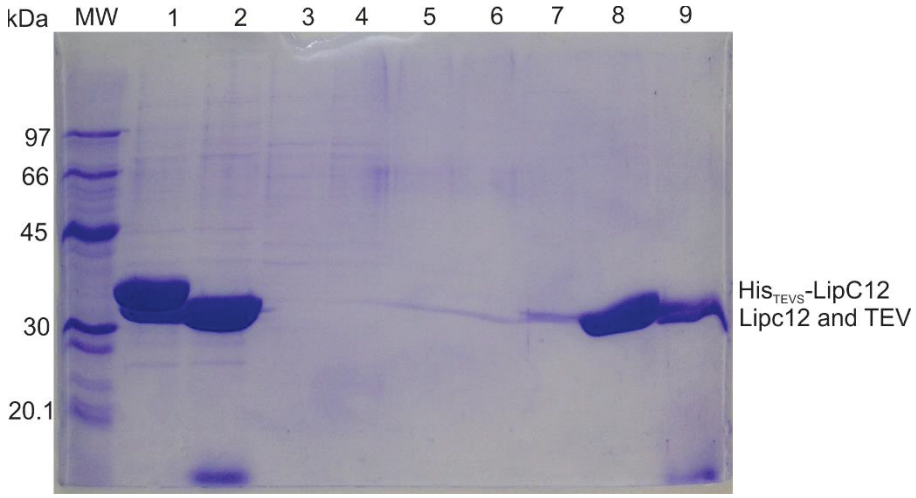

Supplementary Figure S3. Representative profile of His-tag cleavage of LipC12 with TEV. The substrate His$_{TEVS}$-LipC12 was mixed with TEV protease at a substrate:TEV ratio of 10:1. After incubation at 8 °C and 90 rpm for 20 h, the mixture was loaded onto a 5-mL HiTrap Chelating column and eluted with buffer containing 100 and 300 mM imidazole. Lane 1: Reaction at time zero. Lane 2: Reaction at 20 h. Lane 3-7: elution in buffer without imidazole. Lane 8: elution in buffer containing 100 mM imizadole. Lane 9. elution in buffer containing 300 mM imidazole. The molecular weight standard (MW) is shown as kDa.

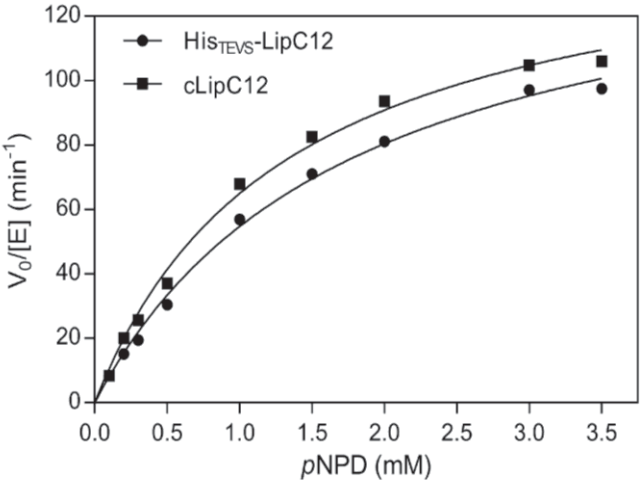

Supplementary Figure S4. Determination of the K_M for *p*NPD using His_{TEVS}-LipC12 and LipC12. The enzyme concentrations were 6.88 nM for HisTEVS-LipC12 and 4.92 nM for LipC12. A control reaction was performed in the absence of enzyme. The K_M, k_{cat} and k_{cat}/K_M values were determined by non-linear regression using GraphPad Prism. V_0 was measured in terms of µmol of product formed per minute.

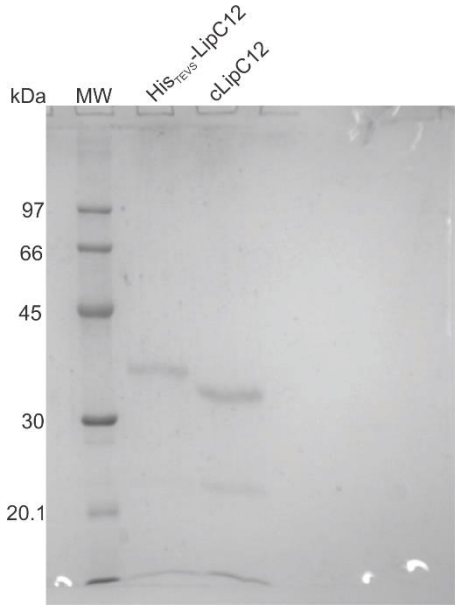

Supplementary Figure S5. Analysis of the desorption of His_{TEVS}-LipC12 and LipC12 after immobilization on Immobead 150. 20 mg of each derivative was incubated with 200 µL of a solution containing 2% SDS at 100 °C for 30 min. Samples of 30 µL were loaded onto a 12% SDS-PAGE gel. The gel was stained with Coomassie blue. Molecular weight standards (MW) are shown as kDa.

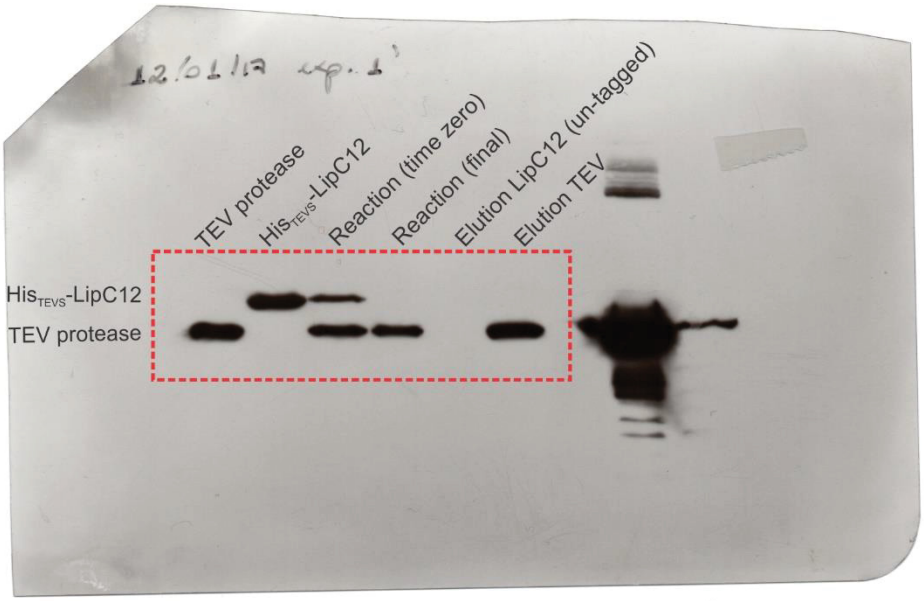

Supplementary Figure S6. Full-length blot of cleavage of His$_{TEVs}$-LipC12 by TEV protease.

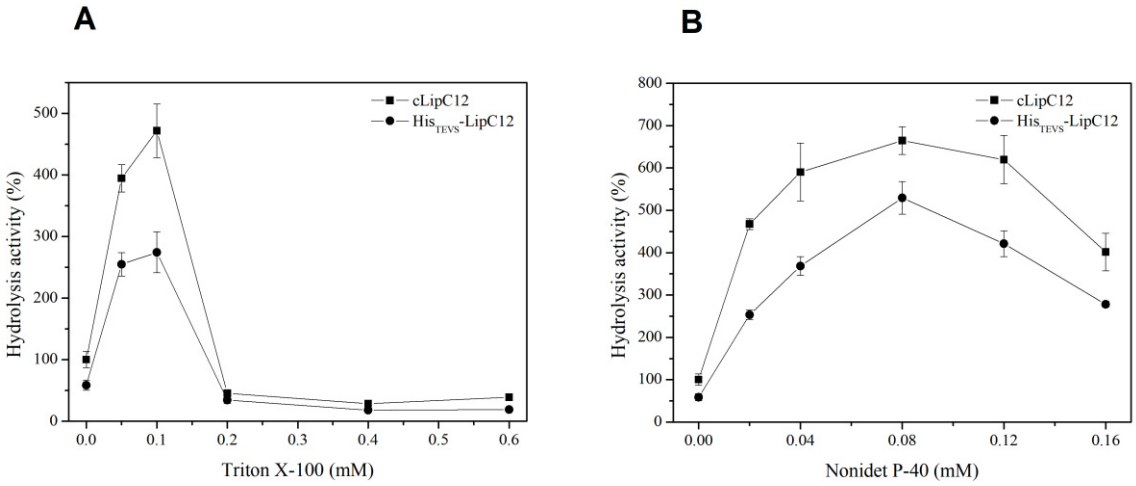

Supplementary Figure S7. (A) Effects of Triton X-100 on the hydrolysis activity of cLipC12 and His$_{TEVS}$-LipC12. (B) Effects of Nonidet P-40 on the hydrolysis activity of cLipC12 and His$_{TEVS}$-LipC12. Activities were determined by the spectrophotometric method using the hydrolysis of *p*-nitrophenyl decanoate. The enzyme concentrations were 172 nM for His$_{TEVS}$-LipC12 and 123 nM for cLipC12. The assays were done in triplicate. The error bars represent the standard deviations of the means.

Supplementary Table S1. Efficiency of immobilization of His-LipC12 and rLipC12 on Immobead 150.

Time (h)	His-LipC12 (%)	rLipC12 (%)
0	0 ± 0	0 ± 0
2	63 ± 3	66 ± 1
3	68 ± 2	73 ± 1
6	77 ± 1	78 ± 1
8	81 ± 1	81 ± 1

Activities were measured by the titration method using an automatic titrator pHStat and olive oil as the substrate. The values are the mean ± the standard deviation of the means

Supplementary Table S2. Plasmids, *Escherichia coli* strains used for protein expression and expression conditions.

Plasmid	Genotype	Reference	*E. coli* strains	Expression conditions
pET28lipC12	Km^r (pET28a). Expresses His-LipC12	Glogauer *et al.*[15]	BL21 (DE3)	0.5 mM IPTG at 18 °C for 16 h
pET29lipC12	Km^r (pET29a). Expresses rLipC12	This work	BL21 (DE3)	0.5 mM IPTG at 18 °C for 16 h
pTEV5lipC12	Amp^r (pTEV5). Expresses His_{TEVS}-LipC12	This work	BL21 (DE3)	0.4 mM IPTG at 16 °C for 16 h
$pTEV_{SH}$	Amp^r (pTH24). Expresses TEV_{SH} protease	van den Berg et al.[42]	Rosetta (DE3) pLysS	1 mM IPTG at 20 °C for 22 h

4 CAPÍTULO II

Manuscrito a ser submetido para a revista:
International Journal of Biological Macromolecules

Biochemical characterization and application of a new lipase and its cognate foldase from fat-contaminated soil metagenomic library

Biochemical characterization and application of a new lipase and its cognate foldase from fat-contaminated soil metagenomic library

Janaina Marques de Almeida[a], Viviane Paula Martini[b], Jorge Iulek[c], Robson Carlos Alnoch[a], Vivian Rotuno Moure[a], Marcelo Muller dos Santos[a], Emanuel Maltempi de Souza[a], David Alexander Mitchell[a] and Nadia Krieger[d*].

[a] Departamento de Bioquímica e Biologia Molecular, Universidade Federal do Paraná, Cx. P. 19046, Centro Politécnico, Curitiba 81531-980, Paraná, Brazil.

[b] Instituto Federal do Paraná, Campus Irati, Irati 84500-000, Paraná, Brazil.

[c] Departamento de Química, Universidade Estadual de Ponta Grossa, Av. Carlos Cavalcanti, 4748, Ponta Grossa 84030-900, Paraná, Brazil.

[d] Departamento de Química, Universidade Federal do Paraná, Cx. P. 19032 Centro Politécnico, Curitiba 81531-980, Paraná, Brazil. * To whom correspondence should be addressed. E-mail: nkrieger@ufpr.br; Telephone: +55-41-33613470

Abstract

LipMF3 is a new lipase isolated from a metagenomic library derived from a fat-contaminated soil. It belongs to the lipase subfamily I.1 and has identities of 68% and 67% with lipases of *Chromobacterium violaceum* and *C. amazonense*, respectively. Genes encoding LipMF3 and its cognate foldase LifMF3 were cloned and co-expressed in *Escherichia coli.* Purified LipMF3 had high hydrolytic activity against triacylglycerols (1650 U mg^{-1} with tributyrin, 1314 U mg^{-1} with tricaprylin and 862 U mg^{-1} with olive oil). The highest activity of LipMF3 was at 40 °C and pH 6.5. It was stable in hydrophilic organic solvents (25%, v/v in water) with residual activity around 100%. It also showed stability over a wide pH range (5.5 to 11) with residual activity above 80%. LipMF3 was immobilized by covalent bonding onto Immobead 150P and by adsorption onto Sepabeads FP-BU. Better results were obtained with the latter preparation. LipMF3 immobilized on Sepabeads gave a 94% conversion after 5 h for the synthesis of ethyl oleate and a 90% enantiomeric excess of the product (*R*)-1-phenylethyl acetate for the kinetic resolution of (*R,S*)-1-phenyl-1-ethanol. The results obtained in this work provide a basis for the development of applications of LipMF3 in biocatalysis.

Keywords: Lipase, metagenomics, foldase, co-expression, immobilization

4.1 INTRODUCTION

Lipases (EC 3.1.1.3 triacylglycerol lipases) act upon carboxylic esters, promoting their hydrolysis in aqueous media or synthesis in water-restricted media. They can accept a wide range of compounds as substrates with high regio- and stereoselectivity [1] and have been applied in esterification, interesterification and transesterification reactions [2,3]. Due to this versatility, they find many applications in the food, agrochemical, pulp and paper, nutrition, cosmetic and pharmaceutical sectors. The pharmaceutical sector is of particular importance, given that about 80% of all drugs developed are chiral molecules [4]: lipases are used in this sector to produce enantiomerically pure compounds [5].

Despite the great potential for the use of lipases, many of them lack the stability and activity required for application in industrial processes and relatively few lipases are produced on an industrial scale [6]. It is, therefore, desirable to find new lipases that have high activities and stabilities at high temperatures and extremes of pH and in the presence of organic solvents.

New lipases can be obtained through metagenomics, which allows enzymes to be obtained non-cultivable microorganisms through the direct isolation of genomic DNA from environmental samples [7]. Glogauer et al. [8] constructed a metagenomic library containing 500 000 clones from a fat-contaminated soil. The clones were screened for lipase activity by culturing them in solid medium enriched with different triacylglycerols and measuring the diameters of the hydrolysis halos. Two positive clones expressed lipases that have been purified and characterized by our group, LipC12 and LipG9. These lipases have important characteristics for application in biocatalysis, such as activity and stability in organic solvents, high regioselectivity and high enantioselectivity [8–11]. They were immobilized and used in the synthesis of biodiesel [10,11], flavor esters and structured lipids [12], in the kinetic resolution of secondary alcohols [10,13] and in the regioselective hydrolysis of carbohydrate derivatives [14].

The current work deals with a third clone from the metagenomic library of Glogauer et al. [8]: clone *pCC2FOS-lipMF3-lifMF3*, which presented hydrolysis halos with both tributyrin and tricaprylin. We describe the expression and characterization of the new lipase, named LipMF3, expressed by this clone. LipMF3 has a lipase-specific foldase (LifMF3), therefore, LipMF3 and LifMF3 were co-expressed in *Escherichia coli*

and characterized. Furthermore, LipMF3 was also immobilized and successfully applied in the synthesis of ethyl oleate and the kinetic resolution of the (*R*,*S*)-1-phenyl-1-ethanol in organic medium.

4.2 MATERIALS AND METHODS

4.2.1 Bacterial strains, plasmids, enzymes and chemicals

The metagenomic library of fat-contaminated soil was built using *Escherichia coli* EPI300™-T1^{R} and pCC2FOS fosmid vector (CopyControl™ Fosmid Library Production Kit, Epicentre Biotechnologies, WI, USA). Sequencing was performed with the EZ-Tn5 < KAN-2 > Insertion Kit (Epicentre) and the DYEnamic ET Dye Terminator Kit (GE Healthcare, Uppsala, Sweden) [8].

In this present work, the system for expressing recombinant proteins was composed of *E. coli* strains TOP10 (Invitrogen, CA, USA), BL21(DE3), BL21(DE3)plysS, Rosetta (DE3)pLysS, Rosetta 2(DE3)plysS (Novagen, MI, USA), Shuffle Express (New England Biolabs, MA, USA) and BL21 Star (DE3) (Invitrogen, CA, USA), and the vectors pBluescript II KS(+) (Agilent Technologies, CA, USA), pET-28a(+) and pT7-7 (Addgene, MA, USA). Restriction enzymes (SmaI, NdeI and HindIII), T4 DNA ligase and the protein molecular mass markers were purchased from Thermo Fisher Scientific (MA, USA).

Phusion polymerase Taq polymerase (New England Biolabs, MA, USA) was used for DNA amplification. For DNA purification, the Axygen Gel Extraction Kit (Axygen Biosciences, CA, USA) was used. The HiTrap Chelating HP column was from GE Healthcare. The substrates triolein (65% purity), tridodecanoin (98%), tricaprylin (99%), tributyrin (97%), tripropionin (97%) and triacetin (99%) were from Sigma-Aldrich (MO, USA). All other chemicals were of analytical grade.

4.2.2 Identification, sequencing and cloning of the lipase and foldase genes

The clone with the lipase (*lipMF3*) and foldase (*lifMF3*) genes (pCC2FOS-*lipMF3*-*lifMF3*) was identified by functional screening performed by Glogauer et al. [8] and gave larger hydrolysis halos against tributyrin and tricaprylin than other clones in the library.

The clone pCC2FOS-*lipMF3-lifMF3* was sequenced by the transposon technique (EZ-Tn5™ <oriV/ KAN-2> Insertion Kit Epicentre® Biotechnologies). The plasmid was extracted from the clone [15] and sequenced with the ABI 377 DNA Sequencer (Applied Biosystems/HITACHI, CA, USA) and MegaBACE 1000 (GE Healthcare) sequencers, from both ends, using the DYEnamic ET Dye Terminator Kit (GE Life Sciences). Sequence assembly and editing were done with the CodonCode Aligner software (CodonCode Corporation, Centerville, MA, USA). The open reading frames (ORFs) were identified with the ORF Finder tool (NCBI) [16]: an ORF for a lipase and another for a foldase were identified.

The cloning strategy used the vector pBlueScript II KS (+) digested with SmaI restriction enzyme, giving rise to a linearized blunt-ended vector [17]. The genes were amplified from the pCC2FOS-*lipMF3-lifMF3* fosmid by PCR reactions, with an initial denaturation at 98 °C for 90 s, followed by 30 cycles (98 °C for 10 s, 60 °C for 20 s, 72 °C for 40 s) and a final extension at 72 °C for 5 min, using the mix Phusion high-fidelity DNA polymerase (New England Biolabs, MA, USA). PCR fragments were amplified with the primers described in Table S1 (obtained from Prodimol Biotechnologies, MG, Brazil) and then ligated to the linearized pBlueScript II KS (+) vector. After that, the lipase and foldase genes, both entire and the N-truncated, were digested at 37 °C for 4 h with NdeI and HindIII, purified with the Axygen Gel Extraction Kit (Biosciences) and subcloned into the pET28a(+) and pT7-7 vectors (Table S2).

The gene truncation regions were defined with the programs TMHMM v.2.0, SignalP 3.0 and ProtScale, which identified a signal peptide in the N-terminal region of the lipase and a transmembrane domain in the N-terminal region of the foldase. The entire and the N-truncated *lipMF3* genes contain 915 bp and 840 bp, respectively, and the entire and the N-truncated *lifMF3* genes contain 876 bp and 804 bp, respectively.

Nine clones were prepared (Table S2) and combined in nine different co-expression experiments (Table S3). The vector pET28a(+) was used to add a His-tag at the N-terminal region of the lipase or foldase.

4.2.3 Expression, analysis and protein purification

Co-expression of the lipase and foldase were carried out in different constructs and tested with different *E. coli* strains according to Table S4. The co-transformed cells were collected and transferred to 5 mL of Luria Bertani (LB) medium, with addition of

100 μg mL^{-1} of kanamycin (pET28a(+)) and 50 μg mL^{-1} of ampicillin (pT7-7). The culture was grown overnight and then inoculated into 100 mL of LB (1:100 v/v), with addition of the appropriate antibiotic (according to the resistance coded by the plasmid). This antibiotic-containing culture was grown at 37 ºC on an orbital shaker at 120 rpm until an optical density (OD_{600}) of 0.6 was reached. Isopropyl β-D-1-thiogalactopyranoside (IPTG) was then added (to give a concentration of 0.5 mmol L^{-1}) and the culture was incubated for another 18 h at 16 °C. The cell suspension was centrifuged at 4 000 × *g* for 10 min at 4 °C for cell recovery and the supernatant was discarded. The cell pellet was resuspended in 3 mL of a buffer containing 50 mmol L^{-1} Tris-HCl pH 8.0, 2 mmol L^{-1} $CaCl_2$, 0.25% (v/v) Igepal 630-CA and 500 mmol L^{-1} NaCl. The cells were sonicated in an ice bath for 12 cycles of 15 s, 90 W, with an interval of 30 s using a Sonicator® XL 2020 (Heat systems-Ultrasonics Inc., NY, USA). The sonicated crude extract was centrifuged for 30 min at 30 000 × *g* at 4 °C and samples were taken from the soluble fraction (supernatant) and the insoluble fraction (precipitate). Enzyme expression was confirmed by 12% SDS-PAGE [18] and by activity assays using the titrimetric method with olive oil as substrate in a pHStat.

The best construct for co-expression was selected for overexpression and purification. The soluble fraction of the co-expression obtained from 4 L of culture, after sonication of cells and centrifugation, was purified using a 5 mL HiTrap Chelating column (GE Healthcare) preequilibrated with buffer A (50 mmol L^{-1} Tris-HCl pH 8.0, 500 mmol L^{-1} NaCl, 2 mmol L^{-1} $CaCl_2$, 0.25% (v/v) Igepal CA-630, 10% (v/v) glycerol and 10 mmol L^{-1} imidazole). Elution was stepwise, with increasing concentrations (from 50 to 500 mmol L^{-1}) of imidazole in buffer A, with 2 column volumes of buffer being passed at each concentration. The fractions with the purified lipase were detected by SDS-PAGE gel and then were pooled. The purity was determined by densitometric analysis of the SDS-PAGE gel using the LabWorks Image Acquisition and Analysis software 4.0 (UVP BioImaging Systems, CA, USA). Imidazole was removed from purified fractions by dialysis using a solution containing 50 mmol L^{-1} Tris-HCl pH 8.0, 500 mmol L^{-1} NaCl, 2 mmol L^{-1} $CaCl_2$, 0.25% (v/v) Igepal CA-630 and 10% (v/v) glycerol.

The ProtParam tool of the Expasy server was used to determine the theoretical molecular weights and the pI values of the proteins. Protein electrophoresis was carried out by 12% SDS-PAGE [18] and gels were stained with Coomassie Blue.

Protein concentrations were determined by the Bradford assay using bovine serum albumin as the standard [19].

4.2.4 MALDI-TOF/MS analysis

The samples for analysis by matrix-assisted laser desorption/ionization (MALDI) time-of-flight (TOF) mass spectrometry (MS) were prepared by manually cutting protein spots from an SDS-PAGE gel corresponding to the N-truncated lipase and the entire foldase. The spots were in-gel digested with sequencing-grade modified trypsin (Promega, WI, USA) [20]. The digested samples were eluted with saturated matrix solution of α-cyano-4-hydroxycinnamic acid in 50% (v/v) acetonitrile and 0.1% trifluoroacetic acid. Then, an aliquot of each sample was placed on the MALDI plate. The mass spectra were obtained using a MALDI-TOF/TOF Autoflex II (Bruker Daltonics, HB, Germany) system, in the reflector positive ion mode with an acceleration voltage of 20 kV, delay time of 150 ns and acquisition mass range of 800–3200 Da. The mass spectra obtained were compared with the peptide masses predicted by *in silico* digestion of the N-truncated LipMF3 and entire LifMF3 sequences using the MS-Digest tool in Protein Prospector [21].

4.2.5 Sequence analysis and homology modeling of lipase and foldase

The amino acid sequences of LipMF3 and LifMF3 were compared to the sequences of 34 lipases of lipase family I [22] and the sequences of 21 foldases [23], respectively. Their classifications were based upon conserved motifs and biological properties. Multiple protein sequence alignment was performed with the ClustalW algorithm [24]. Phylogenetic analysis was carried out with the neighbor-joining method using the MEGA software, version 7. Bootstrapping (10 000 replicates) was used to estimate the confidence levels of the phylogenetic reconstructions [25].

To identify molecular templates for lipase and foldase modeling, the BLAST (NCBI) [26] alignment tool was used against the PDB [27]. The program DSSP [28] was used to estimate secondary structure elements and the program Aline [29] was used to show the protein alignments and the features of the amino acid sequence.

Homology modeling of the Lip-LifMF3 complex was performed by MODELLER software [30], with multiple templates for the lipase. The templates used as models

were chosen based on the results obtained in the MHOLline server according to the BATS (Blast Automatic Targeting for Structures) score [31] and then obtained from the PDB (Protein Data Bank). Superposition of the templates was performed with the Multiprot program [32], and they were structurally aligned with T-Coffee in the 3D mode [33].

Five hundred models that included the structural calcium ion were generated, further optimized by means of the variable target function method (VTFM), and then the one considered best had its loops optimized with the method available within MODELLER. The quality of the models was assessed by the programs PROCHECK [34], WHATCHECK [35] and MODELLER with the embedded normalized DOPE [36] and GA3415 scores [37].

4.2.6 Titrimetric determination of triacylglycerol-hydrolyzing activity

In the purification, lipase and foldase were co-eluted from the affinity column, therefore, this purified preparation containing LipMF3 complexed with its foldase (LipMF3), termed Lip-LifMF3, was used in activity and immobilization assays.

Hydrolytic activities were performed by the titrimetric method, using a Metrohm 718 STAT (pHStat) Titrino potentiometric automatic titrator (Metrohm, AR, Switzerland). The free fatty acids were titrated with 0.05 M NaOH during 5 min under previously described conditions [11,38,39]. The reaction emulsion consisted of 67 mmol L^{-1} of the substrate, 3% (w/v) gum arabic, 2 mmol L^{-1} $CaCl_2$, 2.5 mmol L^{-1} Tris and 150 mmol L^{-1} NaCl, dispersed in distilled water. The reactions were performed in a glass vessel thermostated at 37 °C containing 20 mL of the emulsion at pH 7.0 and were initiated by adding 0.025 mg of the enzyme to the reaction medium. Initial reaction velocities were determined by linear regression using Microsoft Excel. One unit of hydrolytic activity corresponds to the release of 1 µmol of fatty acid per min, under the assay conditions.

The effects of pH (4.5 to 11.0) and of temperature (10 to 80 °C) on the tributyrin-hydrolyzing activity of Lip-LifMF3 were evaluated at 30 °C and pH 6.5, respectively. The temperature stability was investigated by determining the residual tributyrin-hydrolyzing activity, measured at 40 °C and pH 6.5, after 1.5 h incubation at 30, 40, 50 and 60 °C. To determine the pH stability, LipMF3 was incubated for 24 h at 4 °C in various buffers at 50 mmol L^{-1} concentration: sodium acetate (pH 4.0 to 5.5),

succinate (pH 5.5 and 6.0), phosphate (pH 6.0 to 7.5), Tris-HCl (pH 7.5 and 9.0) and glycine-NaOH (pH 9.0 to 11.0). The residual tributyrin-hydrolyzing activities were measured at 40 °C and pH 6.5.

The stability in polar organic solvents was determined by incubating LipMF3 for 1.5 h at 30 °C in aqueous solutions containing dimethyl sulfoxide (DMSO, log *P* -1.3), isopropanol (log *P* 0.16), ethanol (log *P* -0.23), methanol (log *P* -0.77), propanol (log *P* 0.25) and butanol (log *P* 0.8) at the concentrations of 25% and 50% (v/v). A LipMF3 solution containing 2.5 mg mL^{-1} of protein in 40 µL of the buffer was added to 400 µL of solvent solution. After incubation, 100 µL of the mixture was transferred directly to the reaction vessel of the pHStat, where the residual tributyrin-hydrolyzing activities were determined at pH 6.5 and 40 °C. A hundred percent residual activity was taken as that obtained after incubation in an aqueous buffer (50 mmol L^{-1} Tris–HCl, pH 6.5) for 1.5 h.

To determine the effects of pH and temperature on the activity, and the effects of pH, temperature and organic solvents on the stability of LipMF3, the assays were performed with tributyrin as substrate. Corrections were made for the partial dissociation of butyric acid, assuming a pKa of 4.57.

The hydrolytic activity of LipMF3 was determined for triolein (C18), tridodecanoin (C12), tricaprylin (C8), tributyrin (C4), tripropionin (C3), triacetin (C2) and a commercial olive oil. The reactions were performed at pH 6.5 and 40 °C.

All measurements were performed in triplicate. Results are expressed as the average of these triplicate measurements ± the standard error of the mean.

4.2.7 Immobilization

Lip-LifMF3 was immobilized by physical adsorption onto Sepabeads FP-BU (which were kindly donated by Resindion SRL, MI, Italy) and by covalent binding onto Immobead 150P (Sigma-Aldrich, MO, USA). The two immobilized preparations are referred to hereafter as Lip-LifMF3-Immobead and Lip-LifMF3-Sepabeads. The support Sepabeads FP-BU was moistened with acetone solution (50%, v/v in water) for 30 min, then washed with distilled water and filtered. Immobead 150P had no previous treatment. For both supports, in the immobilization experiments, 0.6 g of the support was suspended in 30 mL of enzyme solution (protein loading of 20 mg per g of support) in a 125-mL flask. The flask was agitated on an orbital shaker at 180 rpm

and 4 °C. The experiments were done in triplicate. The time course of immobilization was evaluated by removing aliquots of the supernatant over time. The residual tributyrin-hydrolyzing activity in each aliquot was immediately determined by the titrimetric method. Finally, the immobilized enzyme was removed from the mixture by filtration with qualitative filter paper (Whatman No. 1), dried in a vacuum desiccator for 16 h and stored at 4 °C.

The immobilization efficiency (*IE* %) was calculated as:

$$IE = \frac{A_i - A_f}{A_i} \times 100\% \quad (1)$$

where A_i is the hydrolytic activity (U) of the enzyme solution before immobilization and A_f is the hydrolytic activity (U) remaining in the supernatant at the end of the immobilization procedure.

The recovered activity (*R* %) was calculated as:

$$R = \frac{A_o}{A_T} \times 100\% \quad (2)$$

where A_o is the observed tributyrin-hydrolyzing activity of the immobilized preparation (U g^{-1} of support) and A_T is the theoretical tributyrin-hydrolyzing activity of the immobilized preparation (U g^{-1} of support), calculated based on the amount of activity removed from the supernatant during the immobilization procedure.

4.2.8 Triacylglycerol-hydrolyzing activity in organic medium

For the immobilized preparations of Lip-LifMF3, the hydrolytic activity in organic medium was determined by adding 5 mL of the reaction medium containing 4.9 mL of *n*-hexane, 70 mmol L^{-1} triolein and 2% (v/v) distilled water to a 25-mL Erlenmeyer flask. The mixture was incubated in an orbital shaker at 200 rpm and 40 ºC and the reaction was started by the addition of either free or immobilized LipMF3 to the reaction medium. At intervals of 10 min, samples of 100 µL of the mixture were collected and analyzed for residual free fatty acids by the Lowry-Tinsley method [40]. One unit of lipase activity corresponds to the release of 1 µmol of fatty acid per minute, under the assay conditions.

4.2.9 Application of immobilized Lip-LifMF3 in ethyl oleate synthesis

The two immobilized preparations, Lip-LifMF3-Immobead and Lip-LifMF3-Sepabeads, were used for the synthesis of ethyl oleate in organic medium. Each 25-mL Erlenmeyer flask contained 4.9 mL of *n*-hexane, 70 mmol L^{-1} oleic acid and 210 mmol L^{-1} ethanol. The reaction was started with the addition of 150 mg of the immobilized preparation. The flasks were placed in an orbital shaker at 40 °C and 200 rpm and 100-µL samples of the mixture were collected at 30-min intervals and analyzed for residual free fatty acids by the Lowry-Tinsley method [40]. Calibration curves were constructed using oleic acid. The percentage conversion of free fatty acids and the esterification activity of Lip-LifMF3-Immobead and Lip-LifMF3-Sepabeads were calculated based on the consumption of free fatty acids. One unit of lipase esterification activity (U) corresponds to the consumption of 1 µmol of fatty acid per minute, under the assay conditions.

4.2.10 Evaluation of the enantioselectivity of immobilized Lip-LifMF3

Enantioselectivities of Lip-LifMF3-Immobead and Lip-LifMF3-Sepabeads were evaluated by transesterification of (*R,S*)-1-phenyl-1-ethanol with vinyl acetate. The reaction medium contained 2 mL of *n*-hexane, 0.1 mmol (*R*,*S*)-1-phenyl-1-ethanol and 0.4 mmol vinyl acetate. The reaction was started with the addition of 200 mg of the immobilized preparation and carried out at 35 ºC and 150 rpm. Samples were removed and analyzed by gas chromatography in a GC-2010 chromatograph (Shimadzu, Kyoto, Japan) equipped with a hydrogen flame ionization detector and a chiral column β-DEX 120 (30 m × 0.25 mm diameter, 0.25-µm film thickness). A sample of 1 µL of the medium was injected with a split ratio of 1:50, using H_2 as the carrier gas. The injector and detector were set at 220 °C. The oven program was as follows: initial value of 110 °C, heating at 1 °C min^{-1} up to 120 °C, 120 °C maintained for 10 min. Retention times are: (*S*)-1-phenylethyl acetate 13.5 min, (*R*)-1-phenylethyl acetate 14.3 min, (*R*)-1-phenyl-1-ethanol 14.8 min and (*S*)-1-phenyl-1-ethanol 15.6 min.

The enantiomeric excess (*ee* %) was calculated as:

$$ee = \left[\frac{R - S}{R + S}\right] \times 100\% \quad (3)$$

where *R* is the concentration of the *R*-enantiomer and *S* is the concentration of the *S*-enantiomer. For the substrate enantiomeric excess (ee_s), the concentrations of the *R*- and *S*-enantiomers of the substrate were used; for the product enantiomeric excess (ee_p), the concentrations of the *R*- and *S*-enantiomers of the product were used.

The conversion (*c* %) and enantiomeric ratio (*E,* i.e. (k_{catR}/K_{MR})/(k_{catS}/K_{MS})) were calculated from the values of ee_s and ee_p according to Chen et al. [41]:

$$c = \frac{ee_s}{\left(ee_s + ee_p\right)} \times 100\% \quad (4)$$

$$E = \frac{\ln\ [(1-c)(1-ee_s)]}{\ln\ [(1-c)(1+ee_s)]} \quad (5)$$

The absolute configurations of the enantiomers were attributed indirectly by comparing the retention times of the enantiomers produced in reactions catalyzed by immobilized Lip-LifMF3 with the retention times of the enantiomers produced in the same reactions catalyzed by the lipase B of *Candida antarctica* (CALB, Novozymes, Denmark), which has an (*R*)-enantiopreference for the substrate (*R*,*S*)-1-phenyl-1-ethanol [42,43].

4.3 RESULTS

4.3.1 Sequence analysis

Sequence analysis of the pCC2FOS-*lipMF3-lifMF3* clone identified a contig of 2357 bp. The sequence was compared to the National Center for Biological Information (NCBI) database using the BLAST program [26]. A lipase gene (*lipMF3*) with 918 bp was identified. It had 67% identity and 100% coverage with the triacylglycerol lipase of *Chromobacterium amazonense* (GenBank: WP_106076798.1) and 68% identity and 92% coverage with the triacylglycerol lipase of *Chromobacterium violaceum* (GenBank: KJH68104.1). The same contig also contained a 882-bp foldase gene (*lifMF3*) that had 47% identity and 86% coverage with the lipase secretion chaperone of *Chromobacterium violaceum* (GenBank: WP_081527615.1) and 46% identity and 86% coverage with the lipase chaperone of *Chromobacterium amazonense* (GenBank:

WP_106076797.1). Since both a lipase gene and a foldase gene were identified in the same operon in the clone pCC2FOS-*lipMF3*-*lifMF3*, the lipase probably needs the foldase to fold correctly. Therefore, the two genes were cloned. The lipase was referred to as LipMF3 and the foldase as LifMF3.

LipMF3 is probably secreted via the Sec mechanism (a type II pathway), since the SignalP 3.0 server identified a cleavage site of a signal peptide in the N-terminal region of the lipase. In the foldase, a transmembrane domain was identified by the TMHMM server v. 2.0. The program ProtScale confirmed the hydrophobicity of the N-terminal regions of the two proteins (Fig. S1). In the type II secretion mechanism, the signal peptide of the lipase is lost during the transport of the lipase to the periplasma [44] and the transmembrane region of the foldase is not required for the foldase activity [45]. Therefore, we chose to clone the entire and N-truncated genes of the lipase and the foldase with specific primers, since removal of the N-terminal region from these proteins may be advantageous for their expression in a heterologous host. The N-truncated genes corresponded to deletions of 72 bp for the lipase and 75 bp for the foldase.

The entire lipase LipMF3 has 305 amino acid residues, corresponding to a theoretical molecular mass of 32.4 kDa and a theoretical pI of 7.06. Phylogenetic analysis placed this lipase in family I, subfamily I.1 of the bacterial lipases, next to lipases of *Chromobacterium sp.* LipMF3 has 68% identity with the lipase of *C. violaceum*, 67% identity with the lipases of both *C. amazonense* and *C. piscinae* and 65% identity with the lipase of *C. subtsugae* (Fig. 1A). The main characteristics of lipases of the I.1 subfamily are the presence of a foldase cognate, a calcium binding site formed by two aspartate residues and a disulfide bond formed between two cysteine residues in conserved positions [22].

The entire foldase LifMF3 has 293 amino acid residues, corresponding to a theoretical molecular mass of 32.6 kDa and a theorical pI of 5.94. LifMF3 has 47% identity with the foldase of *C. violaceum* and 46% identity with the foldases of *C. subtsugae*, *C. haemolyticum* and *C. amazonense.* LifMF3 does not fit into any of the four families proposed in the classification of foldases by Rosenau and Jaeger [23], therefore it probably belongs to a new foldase family, along with the foldases of *Chromobacterium* sp. (Fig. 1B).

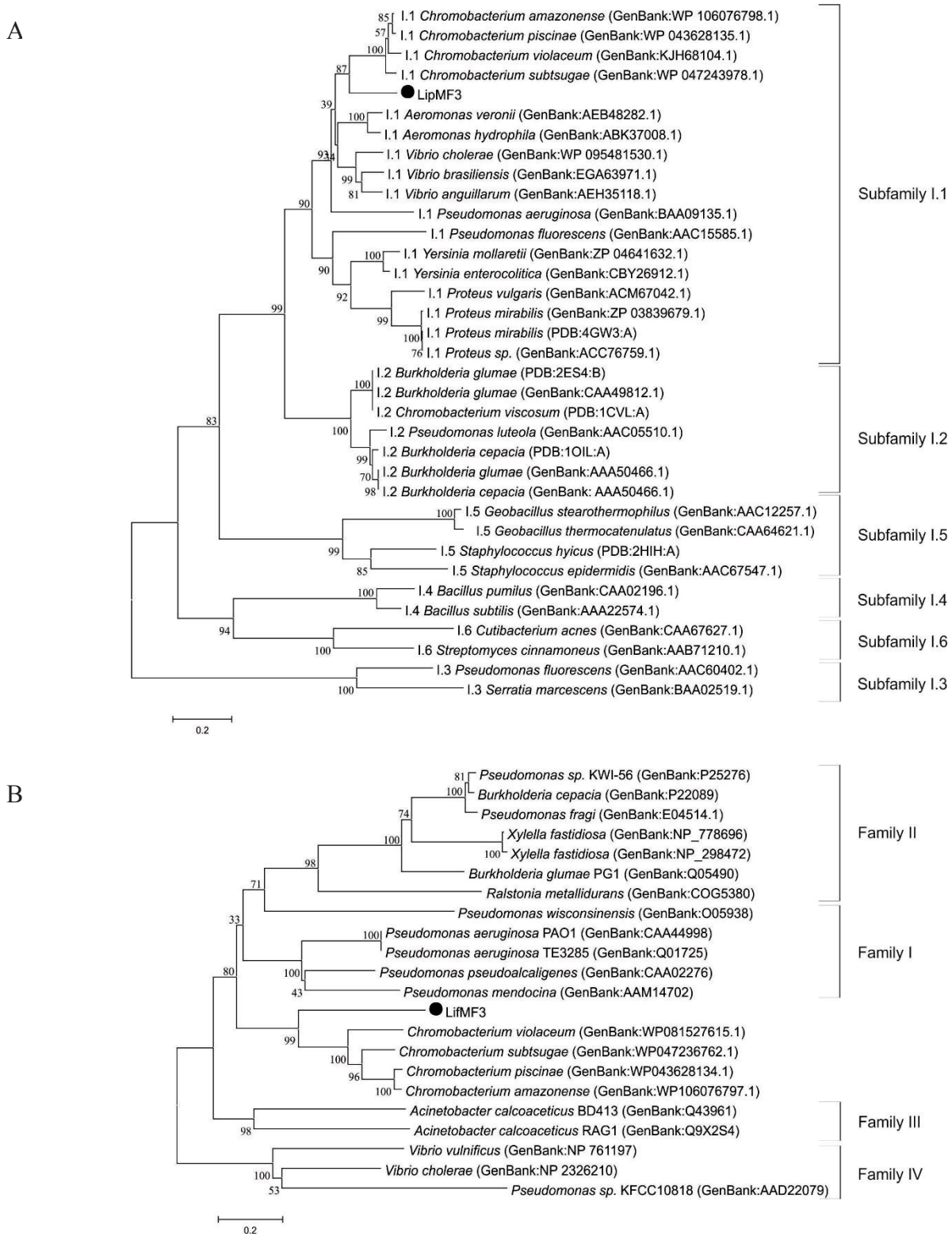

Fig. 1 Phylogenetic analysis of (A) LipMF3 and (B) LifMF3. The phylogenetic tree was generated with MEGA 7. LipMF3 is a member of subfamily I.1, with homology to *Chromobacterium* sp. lipases. LifMF3 probably belongs to a new family. The protein sequences were acquired from GenBank (NCBI). The scale represents the number of amino acid substitutions per site.

4.3.2 Homology modeling

The amino acid sequence of LipMF3 was structurally aligned with the sequences of other lipases with known 3D structure: the metagenomic lipase LipC12 (PDB code not available), *Proteus mirabilis* lipase (4HS9) and *B. glumae* lipase (2ES4), which have identities of 51%, 42% and 37%, respectively, to LipMF3. This alignment is shown in Fig. 2A, which indicates the secondary structure elements for the lipases with known 3D structure and the ones predicted for LipMF3, according to the obtained homology model. There are many conserved residues, including the conserved pentapeptide (Gly-X-Ser-X-Gly) (where X represents any amino acid). In LipMF3, this pentapeptide corresponds to residues 101 to 105 (Gly-His-Ser-Gln-Gly). The catalytic triad of LipMF3 is predicted to be formed by residues Ser103, Asp249 and His271. LipMF3 has two cysteine residues, Cys205-Cys255, which probably form a disulfide bond, conserved in many lipases of subfamilies I.1 and I.2 [22]. However, in the alignment shown in Fig. 2, only the lipase of *B. glumae* has this conserved disulfide bond. In addition, LipMF3 probably has a calcium binding site, formed by residues Asp231 and Asp273.

LifMF3 has 30% identity with the foldase of *B. glumae* (2ES4), the only lipase-specific foldase (Lif) for which the three-dimensional structure has been determined. The Lifs have a highly conserved motif, RXXFDY(F/C)L(S/T)A (where X represents any amino acid), located in the α1 helix in the N-terminal domain [23]. This motif is important for the interaction between the foldase and the lipase [47]. In LifMF3 (Fig. 2B), this motif is formed by the sequence RRLFDYYLA and is, therefore, not totally conserved. There are two differences. The first is that the 7th residue of this motif is a tyrosine residue (Y) in LifM3, rather than either a phenylalanine (F) or cysteine (C). The second is that the 8th and 10th residues of the conserved motif (L and A) are separated by either a serine (S) or a threonine (T) residue, in LifM3 there is no intervening residue, the alanine residue (A) directly follows the leucine residue (L).

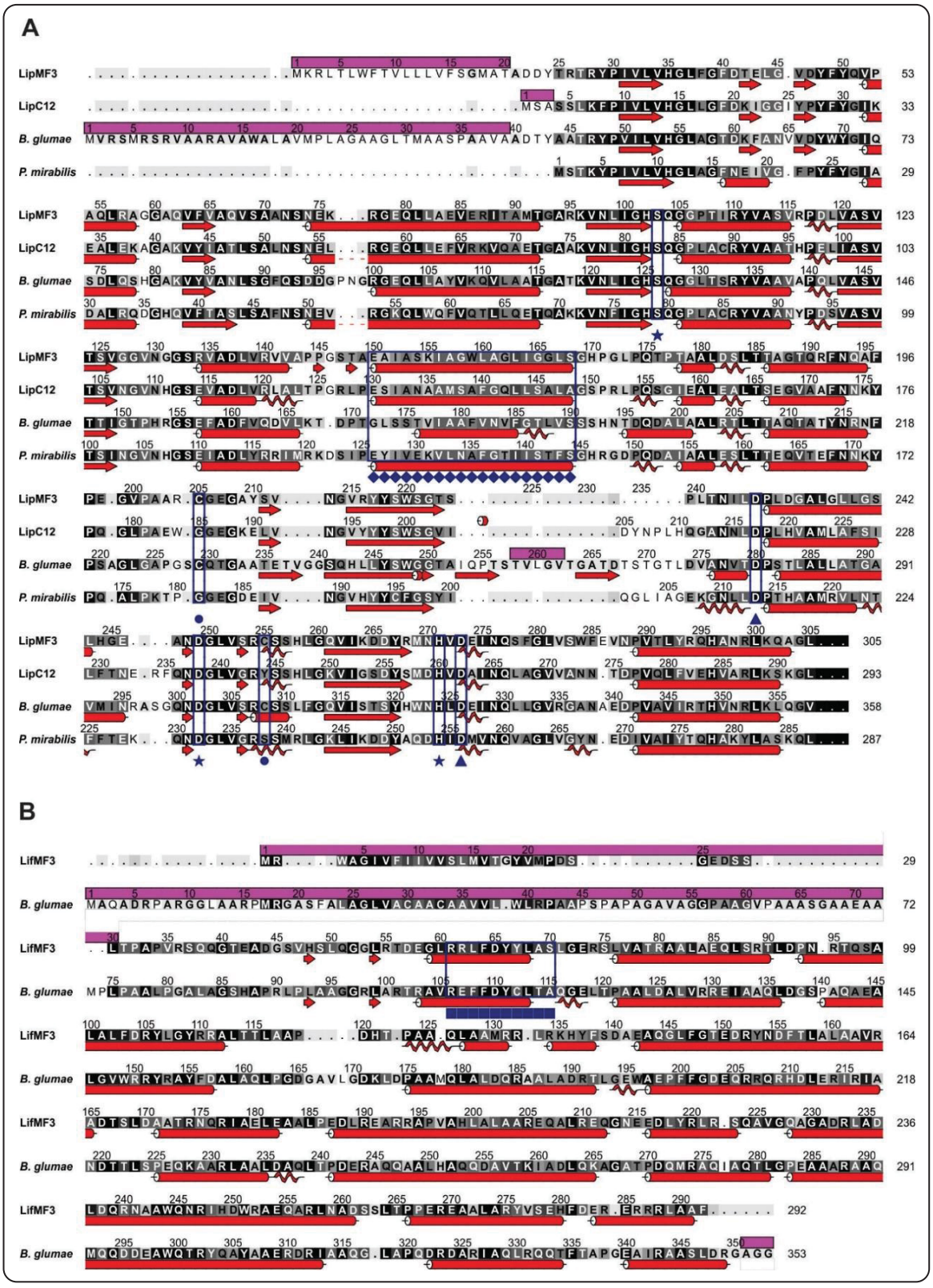

Fig. 2 Sequence alignment and secondary structure estimation of the (A) LipMF3 and (B) LifMF3. The background is colored according to the convention of ALSCRIPT Calcons [46]. Representations of secondary structures are given above the sequences: arrows represent β-strands and cylinders represent α-helices. Magenta bars indicate regions that were not modeled in the crystallographic structures. Stars indicate the catalytic triad, triangles indicate the residues of the binding site for Ca^{2+}, circles indicate disulfide bonds (where both residues are Cys), diamonds indicate the lid (α-helix 5) and squares indicate the conserved motif of foldases.

To predict the 3D structure of the complex formed by LipMF3 and LifMF3, a model was built by homology modeling with the MODELLER program, using 2ES4 as a template for the Lip-LifMF3 complex and LipC12 and 4HS9 as templates for LipMF3. The model was generated without the 20 amino acids in the N-terminal region of the lipase and the 30 amino acids in the N-terminal region of the foldase, since these regions are absent in the templates. The lipase was modeled in the closed conformation. The models were validated through the programs PROCHECK, WHATCHECK and VERIFY 3D.

According to the model, LipMF3 presents the typical α/β hydrolase fold, with a core formed by β-sheets surrounded by α-helices, and LifMF3 is composed of 11 α-helices (Fig. 3). The best model of the complex had normalized DOPE scores of -1.403 for LipMF3 and -0.114 for LifMF3 and a GA341 score of 1.000. The normalized DOPE scores of the LipMF3 and LifMF3 models were close to the scores of the templates (-1.864 for *B. glumae* lipase, -2.020 for *P. mirabilis* lipase, -1.717 for LipC12 and -0.424 for *B. glumae* foldase). The Ramachandran plot generated by the PROCHECK program showed that, for the LipMF3 model, 92.3% of the amino acid residues are in the most favorable regions, 7.3% of the residues are in additional allowed regions, while only the catalytic serine (S103) is in the disallowed region. In the templates, the catalytic serine is also in disallowed regions, this is expected for the nucleophile amino acid residue of enzymes with α/β hydrolase folds [48]. For LifMF3, 96.2% of the amino acid residues are in the most favored regions of the Ramachandran plot, while 3.3% of the residues are in additional allowed regions. Only Asp140, which is located at the beginning of α-helix 5, is in one of the generously allowed regions.

LipMF3 does not have an insertion of 21 amino acid residues between residues S224 and P225. This insertion is typical of the lipases of subfamily I.2, which have this insertion in an antiparallel β-sheet conformation [22,50]. In lipases belonging to the same subfamily as LipMF3, namely subfamily I.1, the missing this insert is only 15 amino acid residues, such as is the case for the lipase of *P. mirabilis* and LipC12.

LipMF3 is predicted to have a lid formed by α-helix 5 (Fig. 3). This lid has residues that are similar to those of the other lipases shown in the alignment of Fig. 2. The sequence of amino acid residues in the lids of the lipases of family I.1 are, in general, poorly conserved, which indicates that the lid opening mechanism and its interaction with different substrates may be specific for each lipase [50].

The molecular interaction between the lipase and the foldase in the model of the Lip-LifMF3 complex was analyzed with the PDBePISA program, which calculated a total buried interface area of 4883 Å². Eighteen non-redundant hydrogen bonds were estimated (TableS5). These bonds were mainly present in the N-terminal and C-terminal regions of the foldase. There were also 3 non-redundant salt bridges (Table S5). These interactions, together, make a thermodynamically stable complex, as confirmed by the free energy of dissociation (ΔG^{diss}) of 38.49 kJ mol^{-1} calculated by the PDBePISA program for the Lip-LifMF3 complex. This value of ΔG^{diss} is equivalent to a K_d at 25 °C of 1.79×10^{-7} M.

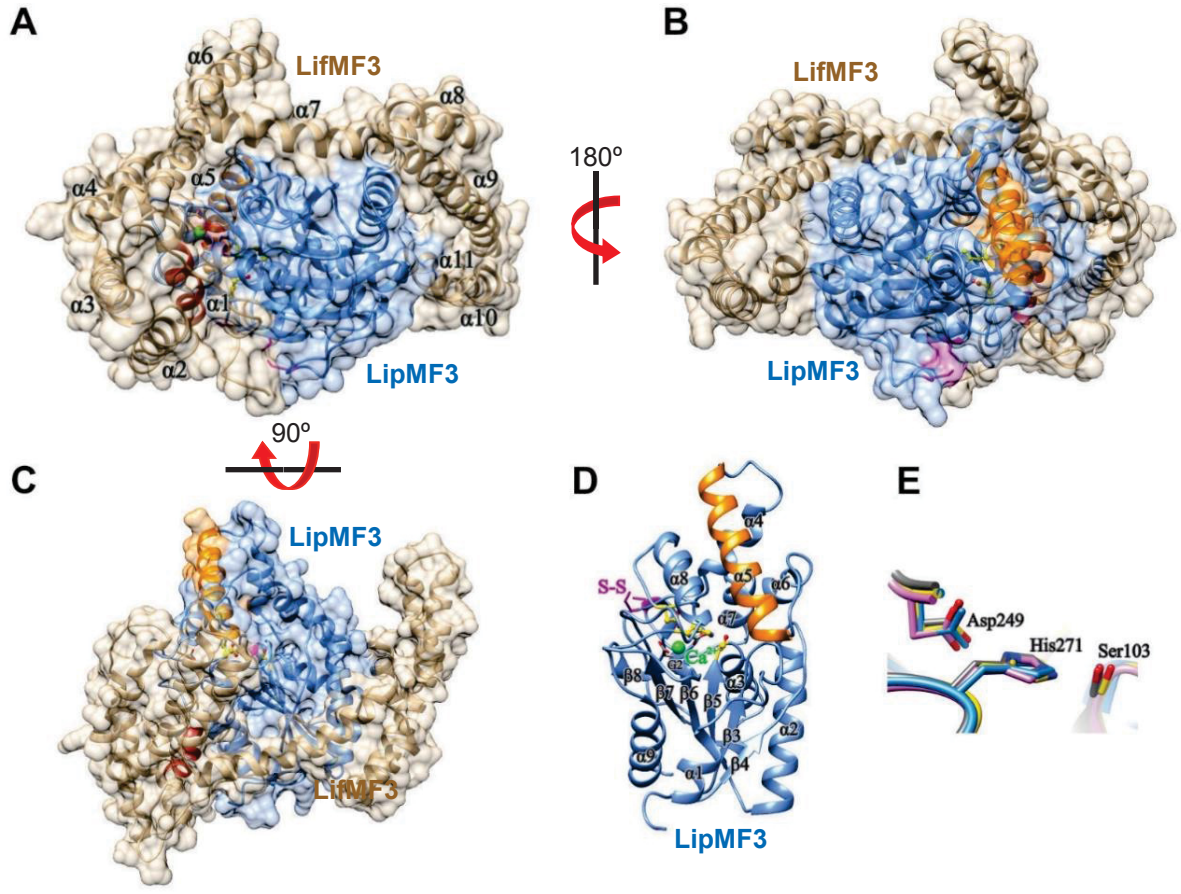

Fig. 3 (A) 3D model of the Lip-LifMF3 complex build with MODELLER. The secondary structure elements of LifMF3 are named as in the foldase of the *B. glumae* [49]. The conserved motif is in the red α-helix (α1). (B) At 180º rotation (vertical axis) from the orientation shown in (A). (C) At 90º rotation (horizontal axis) of the orientation shown in (A). (D) Lipase model, highlights are: the active site in yellow, the disulfide bridge in magenta, the calcium ion (Ca^{2+}) in green, and the α-helix lid in orange. α-helices and β-sheets are named as for *P. aeruginosa* lipase [50]. (E) Superposition of the catalytic triads of LipMF3 (yellow), *B. glumae* (blue), *P. mirabilis* (gray) and, LipC12 (lilac).

4.3.3 Cloning, co-expression and purification of LipMF3 and LifMF3

The genes were cloned into the pET28a(+) and pT7-7 vectors (Table S2) and co-transformed (Table S3). The co-transformations were evaluated according to the olive-oil hydrolyzing activity of the soluble fractions of the culture broth after co-expressions in different *E. coli* strains (Rosetta (DE3)pLysS, Rosetta 2 (DE3)plysS, BL21 (DE3), BL21 (DE3)plysS, Shuffle Express and BL21 Star (DE3)) (Table S4).

The highest specific olive-oil hydrolyzing activities (from 23 ± 2 to 39 ± 2 U mg^{-1}) were obtained with the co-expression of entire LipMF3-pET28a(+) and entire LifMF3-pT7-7. Lower specific hydrolytic activities were achieved for the co-expression of N-truncated LipMF3-pET28a(+) and entire LifMF3-pT7-7 (< 20 ± 0 U mg^{-1}), entire LipMF3-pET28a(+) and N-truncated LifMF3-pT7-7 (< 11 ± 0 U mg^{-1}) and entire LipMF3-LifMF3-pET28a(+) co-expressed in a single vector (< 9 ± 0 U mg^{-1}) (Table S4). Among the different *E. coli* strains, the highest specific activities were obtained with Rosetta (DE3)plysS and Rosetta 2(DE3)plysS. When the expression plasmids were changed (i.e. LipMF3 expressed using pT7-7 instead of pET28a(+), and LifMF3 expressed using pET28a(+) instead of pT7-7), tests were done only in Rosetta (DE3)pLysS and Rosetta 2(DE3)plysS. Lipase activities were low for all these constructions (Table S4).

No olive-oil hydrolyzing activity was detected in the crude extract when LipMF3 was expressed alone; this shows that LipMF3 needs the foldase LifMF3 to fold into an active conformation.

Based on the activity results, two constructs were initially chosen for characterization: the construct entire LipMF3-pET28a(+)/entire LifMF3-pT7-7 and the construct N-truncated LipMF3-pET28a(+)/entire LifMF3-pT7-7. In the first case, during purification, entire LipMF3-pET28a(+) did not bind to the nickel-charged affinity column, in spite of the presence of the His-tag at the amino terminal of LipMF3. It is possible that the His-tag of the LipMF3 was hindered by LifMF3, preventing it from binding to the nickel of the purification resin. In the second case, N-truncated-LipMF3 bound to the affinity column, therefore the construct N-truncated LipMF3-pET28a(+) and entire LifMF3-pT7-7 was selected for the overexpression and purification.

In the selected construct, most of the LipMF3 remained in the insoluble fraction in the form of inclusion bodies (Fig. 4A). As it was not possible to solubilize LipMF3 with activity, the soluble fraction obtained after co-expressed of this construct in

Rosetta (DE3)pLysS was used to purify the Lip-LifMF3 complex. The specific olive-oil hydrolyzing activity of the purified fraction was 860 U mg^{-1}, with a purification factor of 60-fold and a recovery of 40% of the activity measured in the soluble fraction after cell breakage (Table S6).

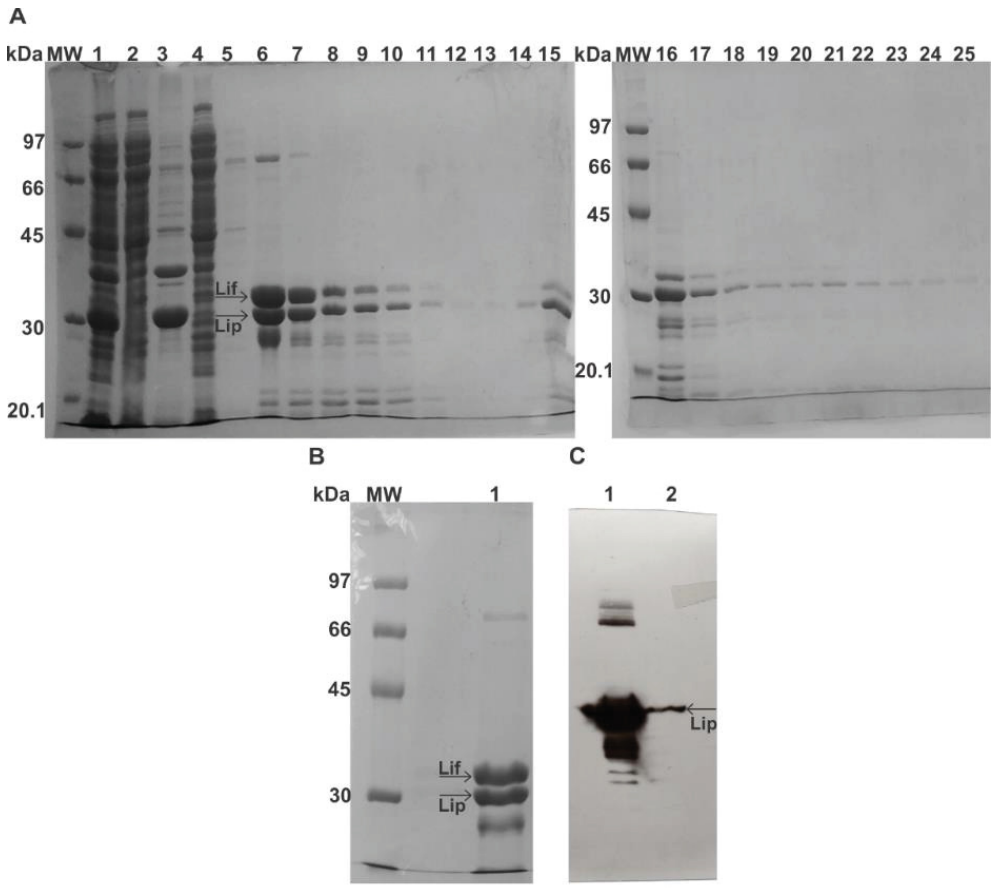

Fig. 4 Electrophoregrams (SDS-PAGE 12%) for purification steps of LipMF3. (A) Fractions of the chromatography. MW: molecular weight markers, 1: crude extract, 2: soluble fraction, 3: insoluble fraction, 4: flow through, 5: washing, 6-10: fractions eluted with 50 mM imidazole, 11-15: fractions eluted with 100 mM imidazole, 16-20: fractions eluted with 300 mM imidazole, 21-25: fractions eluted with 500 mM imidazole. (B) MW: molecular weight markers; 1: LipMF3 after dialysis, evaluated to be with 41% purity. (C) Western blot, 1: crude extract of the N-truncated LipMF3-pET28a(+), 2: soluble fraction of the N-truncated LipMF3-pET28a(+).

The SDS-PAGE gel of the eluate from the affinity column had protein bands corresponding to the molecular masses of both N-truncated LipMF3 (30.3 kDa) and entire LifMF3 (32.5 kDa) (Fig. 4A). This result indicates that the lipase and foldase are complexed in the soluble fraction after cell breakage and during the purification: Since only the lipase has a His-tag, the foldase cannot bind to the nickel-charged affinity column by itself.

The band on the SDS-PAGE gel corresponding to the molecular mass of the N-truncated LipMF3 was confirmed by Western blot analysis using anti-His antibody (Fig. 4C). Densitometry analysis showed that the purified fraction contains 41% lipase and 45% foldase (Fig. 4B), indicating that the complex is eluted from the affinity column in a 1:1 ratio of LipMF3 to LifMF3.

The bands corresponding to LipMF3 and LifMF3 were cut from the SDS-PAGE gel (Fig. 4B) and analyzed by mass spectrometry (MALDI-TOF). The mass spectra obtained were compared with the peptide masses predicted by *in silico* digestion of the N-truncated LipMF3 and entire LifMF3 sequences (Table S7). The sequence coverages obtained were 40% and 38% for lipase and foldase, respectively. Thus, the sequence coverages and the fragment masses of LipMF3 and LifMF3 confirmed the identity of the purified complex Lip-LifMF3.

The preparation containing Lip-LifMF3, purified as described above, was used in all subsequent experiments.

4.3.4 Hydrolytic activity of Lip-LifMF3 against triacylglycerols

Lip-LifMF3 hydrolyzed different substrates from triacetin to triolein (Fig. 5), with the highest activity being for tributyrin, 1650 U mg^{-1}. Despite this result, the good activity on olive oil and triolein shows that it is a true lipase. In the following experiments, tributyrin was used as substrate.

4.3.5 Effect of pH and temperature on Lip-LifMF3 activity and stability

The best temperature for Lip-LifMF3 activity was 40 °C (Fig. 6A). On the other hand, Lip-LifMF3 was most stable at 30 °C, the lowest temperature tested, with 72% residual hydrolytic activity after 24 h incubation. At 40 ºC, it reached half of the initial activity after 5.25 h (315 min). At 50 ºC and 60 ºC, the activity declined rapidly, reaching 50% of the initial activity in 60 min and in less than 10 min, respectively (Fig. 6B).

The highest hydrolytic activity was measured at pH 6.0-6.5 (the activities at these two pH values were not significantly different, p = 0.48) (Fig. 6C), with relative activities above 70% from pH 5.0 to pH 7.5. Lip-LifMF3 had residual activities above 80% over a wide pH range (5.5 to 11.0) when it was incubated for 24 h at 4 ºC (Fig. 6D).

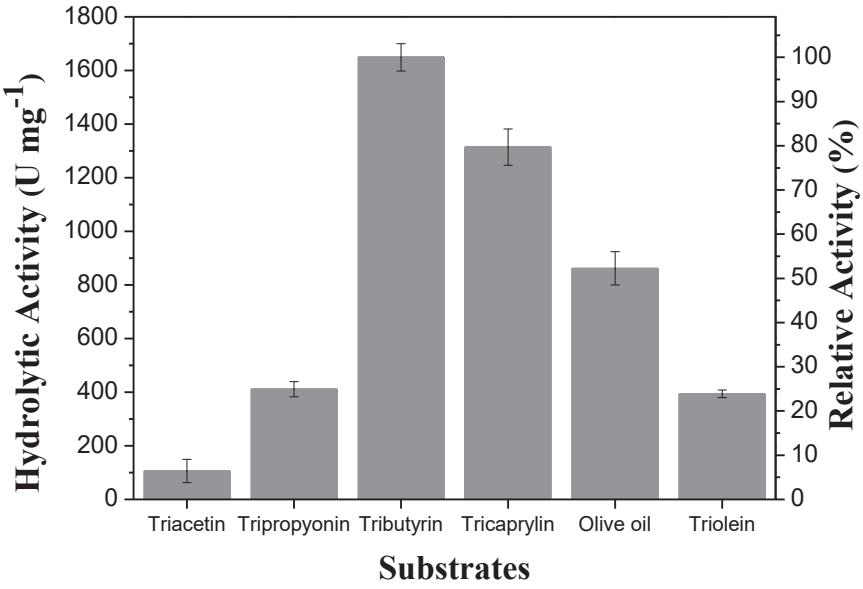

Fig. 5 Hydrolytic activity of Lip-LifMF3 towards different substrates, at 40 ºC, pH 6.5. The error bars represent the standard error of the mean (n = 3).

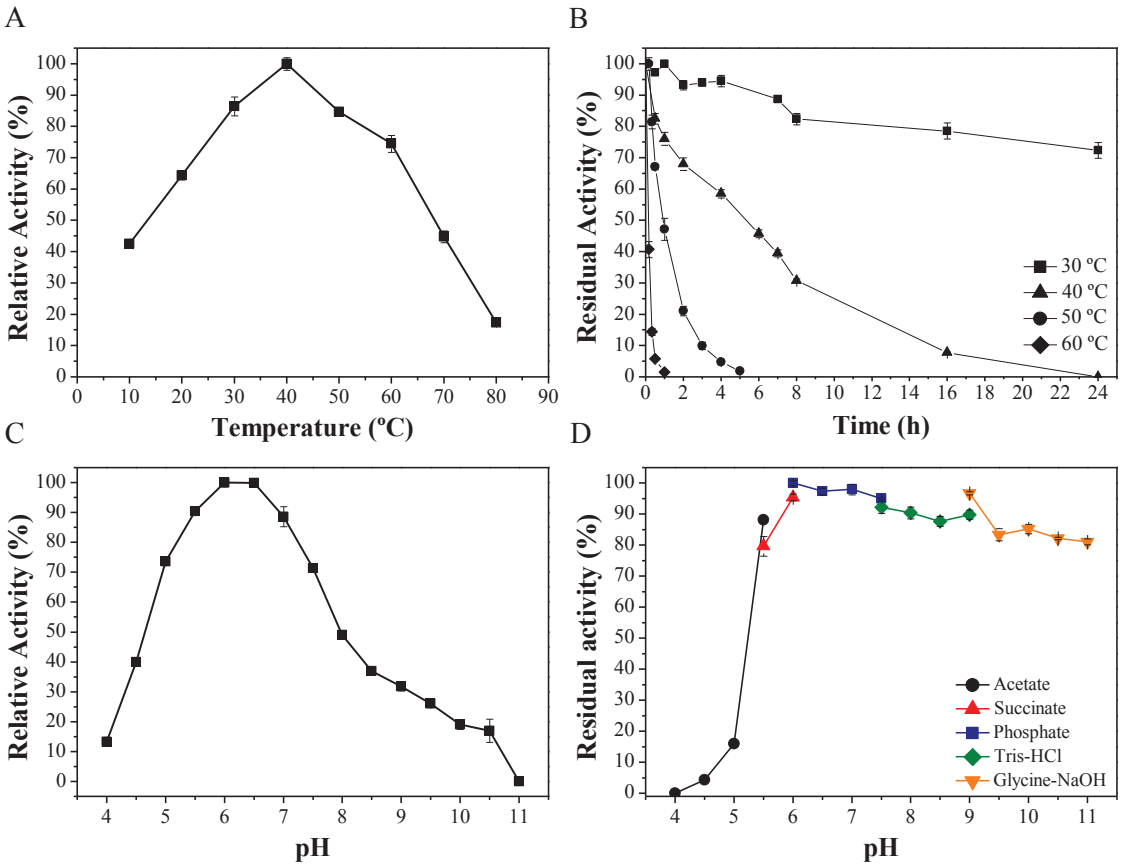

Fig. 6 Tributyrin-hydrolyzing activity of Lip-LifMF3. (A) Effect of temperature, determined at pH 6.5; (B) Stability at different temperatures, in all incubations the pH was 6.5; (C) Effect of pH determined at 37 ºC; (D) Stability at different pH values, Lip-LifMF3 was incubated for 24 h at 4 ºC. The error bars represent the standard error of the mean (n = 3).

4.3.6 Stability of Lip-LifMF3 in organic solvents

Free Lip-LifMF3 was incubated for 90 min in two concentrations (25% and 50%, v/v) of hydrophilic organic solvents. The residual activity of Lip-LifMF3 was measured using tributyrin as the substrate (Fig. 7). Lip-LifMF3 maintained around 100% of residual activity for all solvents at 25% (v/v), except for DMSO, in which there was an increase of 20% in the residual activity. For the solvents at 50% (v/v), the residual activities of Lip-LifMF3 were 70% or lower, except for DMSO (Fig. 7), in which the residual activity was 95%. Interestingly, even after incubation in 50% (v/v) methanol, ethanol and isopropanol, which commonly cause significant denaturation, Lip-LifMF3 still retained above 40% of its original activity. Significant denaturation did occur with 50% (v/v) propanol and 50% (v/v) butanol, for which the residual activities were only 3.25% and 0%, respectively.

The deleterious effect of hydrophilic solvents on lipase activity and stability has been reported for other lipases and has been attributed either to inhibition or to their ability of stripping the water molecules from the solvation layer that involves the enzyme, thereby causing the loss of the catalytically active structure of the enzyme [51]. The beneficial effect of DMSO on the activity and stability of lipases is also known. It has been suggested that DMSO replaces the water in the enzyme-substrate complex, stabilizing the transition state [52].

4.3.7 Immobilization and application of Lip-LifMF3

Lip-LifMF3 was immobilized onto two different supports, Immobead, by covalent bonding, and Sepabeads, by physical adsorption. Hereafter the two immobilized preparations will be called Lip-LifMF3-Sepabeads and Lip-LifMF3-Immobead.

The immobilization efficiency was 92% for Immobead and 96% for Sepabeads (Fig. 8). The rate of Lip-LifMF3 immobilization was much higher with Sepabeads than with Immobead: after 3 h, 91% of the enzymes had already been immobilized onto Sepabeads, while only 65% were immobilized onto Immobead.

Lip-LifMF3-Sepabeads had a higher triolein-hydrolyzing activity (216 ± 9 U g^{-1}) in organic medium than did Lip-LifMF3-Immobead (16 ± 0 U g^{-1}). These values correspond to retentions of hydrolytic activity of 101% and 8%, respectively.

Additionally, Lip-LifMF3-Sepabeads had an initial esterification activity of 20 ± 2 U g^{-1} for the synthesis of ethyl oleate, giving 94% conversion in 5 h, whereas Lip-LifMF3-Immobead had no esterification activity.

The enantioselectivities of Lip-LifMF3-Sepabeads and Lip-LifMF3-Immobead were evaluated for the transesterification of (*R*,*S*)-1-phenyl-1-ethanol. Lip-LifMF3-Sepabeads gave 40% conversion after 24 h, with a product enantiomeric excess (ee_p) of 90% to (*R*)-1-phenylethyl acetate and an enantiomeric ratio (*E*) of 33. For Lip-LifMF3-Immobead, the conversion was only 5% after 48 h. The retention time of the predominant enantiomer produced in reactions catalyzed by Lip-LifMF3-Sepabeads was the same as retention time of the predominant enantiomer observed in the reactions catalyzed by the lipase CALB, confirming the enantiopreference of Lip-LifMF3-Sepabeads for the *R*-isomer.

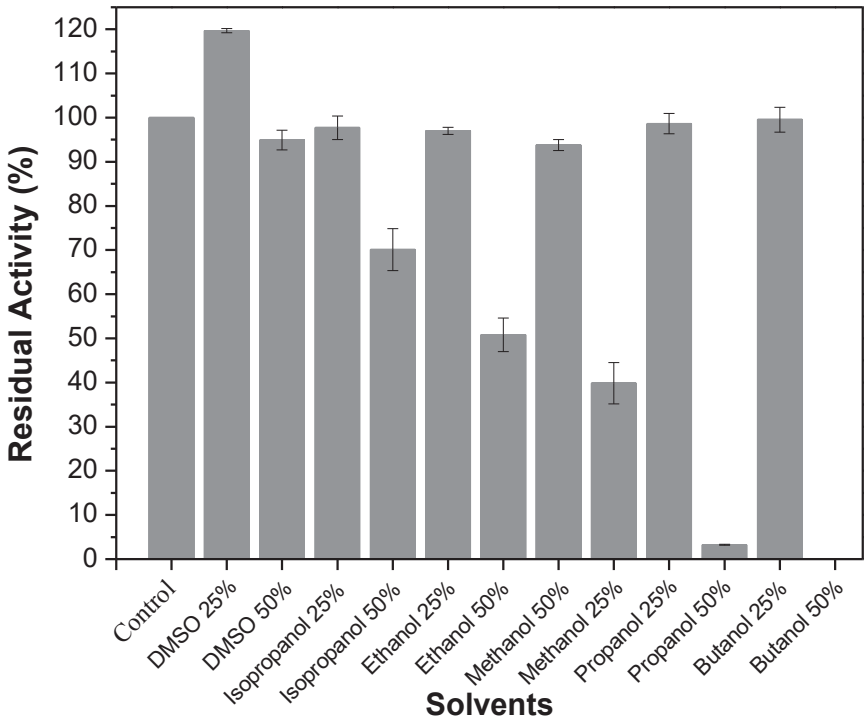

Fig. 7 Effect of hydrophilic organic solvents on the stability of Lip-LifMF3. Lip-LifMF3 was incubated for 1.5 h at 30 °C in aqueous solutions containing different organic solvents. The activity was measured using the titrimetric method with tributyrin as the substrate, at 40 ºC, pH 6.5. The error bars represent the standard error of the mean (n = 3).

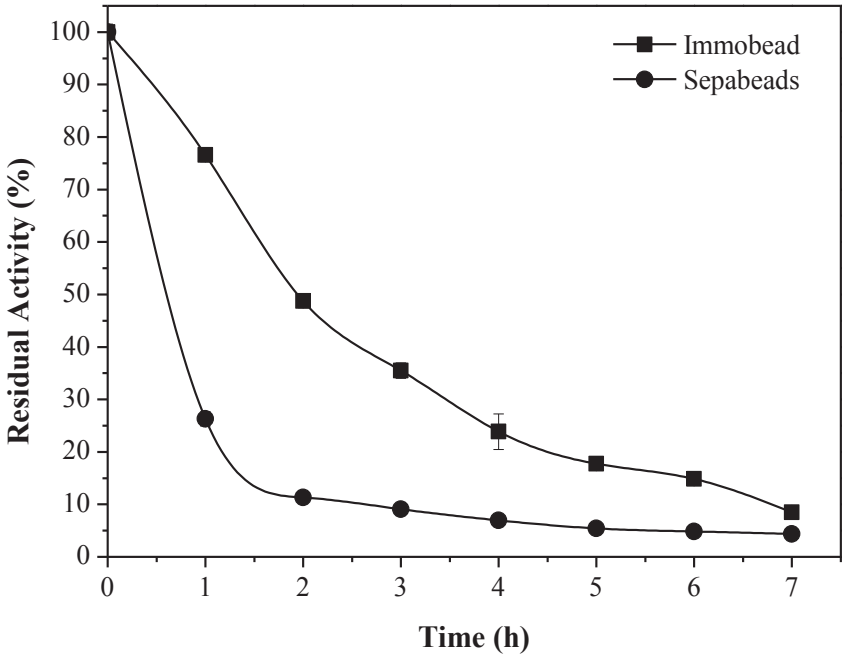

Fig. 8 Kinetics of immobilization of Lip-LifMF3 onto Immobead and Sepabeads. The residual activity in the supernatant was determined using the titrimetric method pHStat with tributyrin as substrate. Results are expressed as the average of triplicate assays ± the standard error of the mean (n = 3).

4.4 DISCUSSION

LipMF3 is a new metagenomic lipase belonging to subfamily I.1 of the bacterial lipases. It has several characteristics of this subfamily, such as the presence of a cognate foldase, a calcium binding site formed by two aspartate residues and a disulfide bond formed between two cysteine residues in conserved positions [22].

LipMF3 did not exhibit hydrolytic activity when expressed in the absence of its cognate foldase. Thus, co-expression was the strategy chosen to overexpress these two proteins, because it is a simple and efficient strategy for the expression of two genes simultaneously. However, much of the expressed LipMF3 was in the form of inclusion body. Many other foldase-dependent lipases have already been expressed in a heterologous host in the form of inclusion body [53–55].

An approach used to solubilize recombinant proteins is the use of different strains of *E. coli* for expression, however, inclusion bodies were formed in all six strains. The best *E. coli* strains for LipMF3 expression, in relation to the hydrolysis activity in the soluble fraction, were Rosetta (DE3)plysS and Rosetta 2 (DE3)plysS. This can be

explained by the particular feature of these strains: Rosetta (DE3)plysS has tRNAs for six rare codons (AGG, AGA, AUA, CUA, CCC, GGA) and Rosetta 2 (DE3)plysS has tRNAs for seven rare codons (AGA, AGG, AUA, CUA, GGA, CCC, CGG). LipMF3 has six (CCC, GGG, AGG, CGA, GGA, CGG) and LifMF3 has seven (GGG, AUA, CCC, GGA, CGG, CGA, AGG) rare codons in their nucleotide sequences.

The modeled Lip-LifMF3 complex presents a total buried interface area of 4883 Å², 18 hydrogen bonds and 3 salt bridges between the two proteins. Similar results were found by Pauwels et al. [49], who reported 20 hydrogen bonds, 1 salt bridge and a total buried interface area of 5400 Å² for Lip-Lif complex of *B. glumae*. The values of buried interface area of the Lip-LifMF3 complex and Lip-Lif complex of *B. glumae* are much larger than the values commonly found for protein complexes in crystallized structures (1600 ± 400 Å^2) [56]. Lip-LifMF3 complex has a K_d of 1.79 × 10^{-7} M, which classifies it as a complex of moderate affinity [57]. On the other hand, the K_d for Lip-Lif complex of *B. glumae* is 5 × 10^{-9} M, considerably smaller than the Lip-LifMF3 complex, which classifies the Lip-Lif complex of *B. glumae* as a complex of high affinity.

Lip-LifMF3 shows potential for application in biocatalysis reactions, since it showed high hydrolytic activity (862 ± 62 U mg^{-1} with olive oil and 1650 ± 62 U mg^{-1} with tributyrin), comparable to LipC12 (1722 U mg^{-1} with olive oil and 2187 U mg^{-1} with tributyrin) and LipG9 (1193 U mg^{-1} with olive oil and 1852 U mg^{-1} with tributyrin), other lipases from the same metagenomic library [8,9] and to commercial lipases (e.g. for *Rhizopus oryzae* 100 U mg^{-1} with olive oil and 900 U mg^{-1} with tributyrin) [58]. Lip-LifMF3 immobilized onto Sepabeads presented esterification activity for the synthesis of ethyl oleate (20 ± 2 U g^{-1}), higher than that presented by other lipases, such as the *Burkholderia contaminans* LTEB11 lipase (4 U g^{-1}) co-expressed with its cognate foldase in heterologous host *E. coli*, for the same reaction, this lipase also was immobilized onto Sepabeads [59].

In addition, Lip-LifMF3 immobilized on Sepabeads by adsorption also presented enantioselectivity for (*R*,*S*)-1-phenyl-1-ethanol, with preference for the (*R*)-enantiomer with E = 33, which is considered a good enantiomeric ratio [60]. The results show potential for application of Lip-LifMF3-Sepabeads in kinetic resolution, although enantiomeric ratio (E) was lower than that reported the metagenomic lipase LipG9 [13] and CALB, both with E >200, for the same reaction.

The reactions performed in organic medium, with immobilized Lip-LifMF3, showed a great difference depending on the support used in immobilization. The bond between the enzyme and Immobead is covalent, which may render the enzyme more rigid; in addition, the enzyme can bind in different conformations, with multi-point attachments, which can prevent access of the substrate to its active site. On the other hand, the immobilization in Sepabeads occurs by physical adsorption, with mainly hydrophobic interactions, since the support has the butyl functional group. These groups interact with the hydrophobic patches of the enzyme, mainly with the lid, which has a predominantly hydrophobic character, thus favoring the open conformation of the lipase [61].

Free Lip-LifMF3 is stable over a wide pH range (5.5 to 11.0) with residual activity above 80%, similar to that found for LipC12, which showed 90% residual activity after 24 h incubation at pH values from 6.0 to 11.0 [8], and more stable than LipG9 (activities above 80% in pH range 6.0 to 9.0) [9], which are enzymes identified from the same metagenomic library. LipMF3 can be classified as mesophilic, acting better in mild temperatures, up to 40 ºC, similar to LipC12 and LipG9, both with maximum activity at 30 °C. In addition, LipMF3 showed good stability in all polar organic solvents tested at 25% (v/v). LipMF3 was more stable in DMSO and isopropanol than LipG9 and showed stability similar to LipG9 in ethanol [9]. LipMF3 also showed higher stability than esterases DMWf18-543 and DMWf18-558, isolated from a deep-sea sediment metagenomic library, which did not present activity in 15% of ethanol, isopropanol and methanol [62].

4.5 CONCLUSION

In conclusion, LipMF3 is a new lipase isolated from a metagenomic library from fat-contaminated soil, with potential application in biotechnological reactions. It has good stability in a wide range of pH and organic solvents, high hydrolytic activity in aqueous medium against natural substrates, besides being capable to catalyze reactions of synthesis and resolution of racemic mixtures in organic medium. In view of these results, the continuity of studies on LipMF3 is promising. It is necessary to optimize reactions (different reaction media, temperatures and enzyme/substrate ratios) to achieve higher activities.

4.5.1 Acknowledgements

This research was supported by Universal grant (Projects 441015/2016-6) from CNPq (Conselho Nacional de Desenvolvimento Científico e Tecnológico), a Brazilian government agency for the advancement of science and technology. Research scholarships were granted to J.M.A, N.K, D.A.M., and E.M.S. by CNPq and to R.C.A. by CAPES (Coordenação de Aperfeiçoamento de Pessoal de Nível Superior), a Brazilian government agency for the development of personnel in higher education. This study was financed in part by the Coordenação de Aperfeiçoamento de Pessoal de Nível Superior - Brasil (CAPES) - Finance Code 001

4.5.2 Declaration of interest

The authors declare that they have no conflict of interest.

4.6 REFERENCES

[1] B.P. Dwivedee, S. Soni, M. Sharma, J. Bhaumik, J.K. Laha, U.C. Banerjee, Promiscuity of lipase-catalyzed reactions for organic synthesis: a recent update, ChemistrySelect. 3 (2018) 2441–2466. doi:10.1002/slct.201702954.

[2] K.-E. Jaeger, T. Eggert, Lipases for biotechnology, Curr. Opin. Biotechnol. 13 (2002) 390–397. doi:10.1016/S0958-1669(02)00341-5.

[3] N. Sarmah, D. Revathi, G. Sheelu, K. Yamuna Rani, S. Sridhar, V. Mehtab, C. Sumana, Recent advances on sources and industrial applications of lipases, Biotechnol. Prog. 34 (2018) 5–28. doi:10.1002/btpr.2581.

[4] K.K. Bhardwaj, R. Gupta, Synthesis of chirally pure enantiomers by lipase, J. Oleo Sci. 66 (2017) 1073–1084. doi:10.5650/jos.ess17114.

[5] A. Ray, Application of lipase in industry, Asian J. Pharm. Technol. 2 (2012) 33–37.

[6] J. Li, S. Chen, L. Li, Y. Yu, Z. Fei, D. Qiao, Y. Cao, Approach of directed evolution of microbial lipases and biodiesel catalysis, African J. Microbiol. Res. 6 (2012) 637–642. doi:10.5897/AJMR11.1458.

[7] F. Berini, C. Casciello, G.L. Marcone, F. Marinelli, Metagenomics: Novel enzymes from non-culturable microbes, FEMS Microbiol. Lett. 364 (2017) 1–19. doi:10.1093/femsle/fnx211.

[8] A. Glogauer, V.P. Martini, H. Faoro, G.H. Couto, M. Müller-Santos, R.A. Monteiro, D.A. Mitchell, E.M. de Souza, F.O. Pedrosa, N. Krieger, Identification and characterization of a new true lipase isolated through metagenomic approach, Microb. Cell Fact. 10 (2011) 54. doi:10.1186/1475-2859-10-54.

[9] V.P. Martini, A. Glogauer, M. Müller-Santos, J. Iulek, E.M. de Souza, D.A. Mitchell, F.O. Pedrosa, N. Krieger, First co-expression of a lipase and its specific foldase obtained by metagenomics, Microb. Cell Fact. 13 (2014) 35–41. doi:10.1186/s12934-014-0171-7.

[10] R.C. Alnoch, V.P. Martini, A. Glogauer, A.C.D.S. Costa, L. Piovan, M. Muller-Santos, E.M. de Souza, F. de Oliveira Pedrosa, D.A. Mitchell, N. Krieger, Immobilization and characterization of a new regioselective and enantioselective lipase obtained from a metagenomic library, PLoS One. 10 (2015) e0114945. doi:10.1371/journal.pone.0114945.

[11] A.D. Madalozzo, V.P. Martini, K.K. Kuniyoshi, E.M. De Souza, F.O. Pedrosa, A. Glogauer, G.M. Zanin, D.A. Mitchell, N. Krieger, Immobilization of LipC12, a new lipase obtained by metagenomics, and its application in the synthesis of biodiesel esters, J. Mol. Catal. B Enzym. 116 (2015) 45–51. doi:10.1016/j.molcatb.2015.03.002.

[12] A.D. Madalozzo, V.P. Martini, K.K. Kuniyoshi, E.M. de Souza, F. de O. Pedrosa, G.M. Zanin, D.A. Mitchell, N. Krieger, Synthesis of flavor esters and structured lipids by a new immobilized lipase, LipC12, obtained from metagenomics, Biocatal. Agric. Biotechnol. 8 (2016) 294–300. doi:10.1016/j.bcab.2016.10.006.

[13] P.T. Bandeira, R.C. Alnoch, A.R.M. de Oliveira, E.M. de Souza, F. de O. Pedrosa, N. Krieger, L. Piovan, Enzymatic kinetic resolution of aliphatic sec -alcohols by LipG9, a metagenomic lipase, J. Mol. Catal. B Enzym. 125 (2016) 58–63. doi:10.1016/j.molcatb.2015.12.010.

[14] R. Alnoch, R. Rodrigues de Melo, J. Palomo, E. Maltempi de Souza, N. Krieger, C. Mateo, New tailor-made alkyl-aldehyde bifunctional supports for lipase immobilization, Catalysts. 6 (2016) 191. doi:10.3390/catal6120191.

[15] J. Sambrook, Molecular cloning : a laboratory manual / J. Sambrook, E.F. Fritsch, T. Maniatis - Details - Trove, 3rd ed., 2001. https://trove.nla.gov.au/work/13615226 (accessed August 23, 2018).

[16] R. Agarwala, T. Barrett, J. Beck, D.A. Benson, C. Bollin, E. Bolton, D. Bourexis,

J.R. Brister, S.H. Bryant, K. Canese, C. Charowhas, K. Clark, M. DiCuccio, I. Dondoshansky, M. Feolo, K. Funk, L.Y. Geer, V. Gorelenkov, W. Hlavina, M. Hoeppner, B. Holmes, M. Johnson, V. Khotomlianski, A. Kimchi, M. Kimelman, P. Kitts, W. Klimke, S. Krasnov, A. Kuznetsov, M.J. Landrum, D. Landsman, J.M. Lee, D.J. Lipman, Z. Lu, T.L. Madden, T. Madej, A. Marchler-Bauer, I. Karsch-Mizrachi, T. Murphy, R. Orris, J. Ostell, C. O'Sullivan, V. Palanigobu, A.R. Panchenko, L. Phan, K.D. Pruitt, K. Rodarmer, W. Rubinstein, E.W. Sayers, V. Schneider, C.L. Schoch, G.D. Schuler, S.T. Sherry, K. Sirotkin, K. Siyan, D. Slotta, A. Soboleva, V. Soussov, G. Starchenko, T.A. Tatusova, K. Todorov, B.W. Trawick, D. Vakatov, Y. Wang, M. Ward, W.J. Wilbur, E. Yaschenko, K. Zbicz, Database resources of the national center for biotechnology information, Nucleic Acids Res. 45 (2017) D12–D17. doi:10.1093/nar/gkw1071.

[17] J. Ma, Y.-G. Wang, Y.-J. Wang, A simple, fast and efficient method for cloning blunt DNA fragments, African J. Biotechnol. 12 (2013) 4094–4097. doi:10.5897/AJB12.691.

[18] U.K. LAEMMLI, Cleavage of structural proteins during the assembly of the head of bacteriophage T4, Nature. 227 (1970) 680–685. doi:10.1038/227680a0.

[19] M.M. Bradford, A rapid and sensitive method for the quantitation of microgram quantities of protein utilizing the principle of protein-dye binding, Anal. Biochem. 72 (1976) 248–254.

[20] A. Shevchenko, M. Wilm, O. Vorm, M. Mann, Mass spectrometric sequencing of proteins from silver-stained polyacrylamide gels, Anal. Chem. 68 (1996) 850–858. doi:10.1021/ac950914h.

[21] R.J. Chalkley, P.R. Baker, L. Huang, K.C. Hansen, N.P. Allen, M. Rexach, A.L. Burlingame, Comprehensive analysis of a multidimensional liquid chromatography mass spectrometry dataset acquired on a quadrupole selecting, quadrupole collision cell, time-of-flight mass spectrometer: II. New developments in Protein Prospector allow for reliable and comprehensive automatic analysis of large datasets., Mol. Cell. Proteomics. 4 (2005) 1194–204. doi:10.1074/mcp.D500002-MCP200.

[22] J.L. ARPIGNY, K.-E. JAEGER, Bacterial lipolytic enzymes: classification and properties, Biochem. J. 343 (1999) 177. doi:10.1042/0264-6021:3430177.

[23] F. Rosenau, J. Tommassen, K.E. Jaeger, Lipase-specific foldases, ChemBioChem. 5 (2004) 152–161. doi:10.1002/cbic.200300761.

[24] J.D. Thompson, D.G. Higgins, T.J. Gibson, CLUSTAL W: improving the sensitivity of progressive multiple sequence alignment through sequence weighting, position-specific gap penalties and weight matrix choice., Nucleic Acids Res. 22 (1994) 4673–80. http://www.ncbi.nlm.nih.gov/pubmed/7984417 (accessed August 23, 2018).

[25] S. Kumar, G. Stecher, K. Tamura, MEGA7: Molecular evolutionary genetics analysis version 7.0 for bigger datasets, Mol. Biol. Evol. 33 (2016) 1870–1874. doi:10.1093/molbev/msw054.

[26] S.F. Altschul, T.L. Madden, A.A. Schäffer, J. Zhang, Z. Zhang, W. Miller, D.J. Lipman, Gapped BLAST and PSI-BLAST: a new generation of protein database search programs., Nucleic Acids Res. 25 (1997) 3389–402. http://www.ncbi.nlm.nih.gov/pubmed/9254694 (accessed August 24, 2018).

[27] H.M. Berman, J. Westbrook, Z. Feng, G. Gilliland, T.N. Bhat, H. Weissig, I.N. Shindyalov, P.E. Bourne, The protein data bank., Nucleic Acids Res. 28 (2000) 235–42. http://www.ncbi.nlm.nih.gov/pubmed/10592235 (accessed August 23, 2018).

[28] W. Kabsch, C. Sander, Dictionary of protein secondary structure: Pattern recognition of hydrogen-bonded and geometrical features, Biopolymers. 22 (1983) 2577–2637. doi:10.1002/bip.360221211.

[29] C.S. Bond, A.W. Schüttelkopf, IUCr, ALINE: a WYSIWYG protein-sequence alignment editor for publication-quality alignments, Acta Crystallogr. Sect. D Biol. Crystallogr. 65 (2009) 510–512. doi:10.1107/S0907444909007835.

[30] B. Webb, A. Sali, Comparative protein structure modeling using MODELLER, in: Curr. Protoc. Bioinforma., John Wiley & Sons, Inc., Hoboken, NJ, USA, 2016: p. 5.6.1-5.6.37. doi:10.1002/cpbi.3.

[31] P.V. Capriles, A.C. Guimarães, T.D. Otto, A.B. Miranda, L.E. Dardenne, W.M. Degrave, Structural modelling and comparative analysis of homologous, analogous and specific proteins from *Trypanosoma cruzi* versus *Homo sapiens*: putative drug targets for chagas' disease treatment, BMC Genomics. 11 (2010) 610. doi:10.1186/1471-2164-11-610.

[32] M. Shatsky, R. Nussinov, H.J. Wolfson, MultiProt — A multiple protein structural alignment algorithm, in: Springer, Berlin, Heidelberg, 2002: pp. 235–

250. doi:10.1007/3-540-45784-4_18.

[33] C. Notredame, D.G. Higgins, J. Heringa, T-coffee: a novel method for fast and accurate multiple sequence alignment, J. Mol. Biol. 302 (2000) 205–217. doi:10.1006/JMBI.2000.4042.

[34] R.A. Laskowski, M.W. MacArthur, D.S. Moss, J.M. Thornton, PROCHECK: a program to check the stereochemical quality of protein structures, J. Appl. Crystallogr. 26 (1993) 283–291. doi:10.1107/S0021889892009944.

[35] R.W.W. Hooft, G. Vriend, C. Sander, E.E. Abola, Errors in protein structures, Nature. 381 (1996) 272–272. doi:10.1038/381272a0.

[36] M.-Y. Shen, A. Sali, Statistical potential for assessment and prediction of protein structures., Protein Sci. 15 (2006) 2507–24. doi:10.1110/ps.062416606.

[37] F. Melo, R. Sánchez, A. Sali, Statistical potentials for fold assessment, Protein Sci. 11 (2009) 430–448. doi:10.1002/pro.110430.

[38] A. Tiss, F. Carrière, R. Verger, Effects of gum arabic on lipase interfacial binding and activity, Anal. Biochem. 294 (2001) 36–43. doi:10.1006/abio.2001.5095.

[39] W. Stuer, K.E. Jaeger, U.K. Winkler, Purification of extracellular lipase from *Pseudomonas aeruginosa*, J. Bacteriol. 168 (1986) 1070–1074. http://www.ncbi.nlm.nih.gov/pubmed/3096967 (accessed May 5, 2017).

[40] R.R. Lowry, I.J. Tinsley, Rapid colorimetric determination of free fatty acids, J. Am. Oil Chem. Soc. 53 (1976) 470–472. doi:10.1007/BF02636814.

[41] C.S. Chen, Y. Fujimoto, G. Girdaukas, C.J. Sih, Quantitative analyses of biochemical kinetic resolutions of enantiomers, J. Am. Chem. Soc. 104 (1982) 7294–7299. doi:10.1021/ja00389a064.

[42] M. Habulin, Ž. Knez, Optimization of (R,S)-1-phenylethanol kinetic resolution over *Candida antarctica* lipase B in ionic liquids, J. Mol. Catal. B Enzym. 58 (2009) 24–28. doi:10.1016/J.MOLCATB.2008.10.007.

[43] A. Overmeyer, S. Schrader-Lippelt, V. Kasche, G. Brunner, Lipase-catalysed kinetic resolution of racemates at temperatures from 40 °C to 160 °C in supercritical CO_2, Biotechnol. Lett. 21 (1999) 65–69. doi:10.1023/A:1005422524509.

[44] F. Rosenau, K.E. Jaeger, Bacterial lipases from *Pseudomonas*: regulation of gene expression and mechanisms of secretion, Biochimie. 82 (2000) 1023–1032. doi:10.1016/S0300-9084(00)01182-2.

[45] M. El Khattabi, C. Ockhuijsen, Specificity of the lipase-specific foldases of gram-negative bacteria and the role of the membrane anchor, Mol. Gen. Genet. 261 (1999) 770–776.

[46] G.J. Barton, ALSCRIPT: a tool to format multiple sequence alignments., Protein Eng. 6 (1993) 37–40. http://www.ncbi.nlm.nih.gov/pubmed/8433969 (accessed August 24, 2018).

[47] H. Shibata, H. Kato, J. Oda, Calcium ion-dependent reactivation of a *Pseudomonas* lipase by its specific modulating protein, LipB, J. Biochem. 123 (1998) 136–141. doi:10.1093/oxfordjournals.jbchem.a021900.

[48] M. Nardini, D.A. Lang, K. Liebeton, K.E. Jaeger, B.W. Dijkstra, Crystal structure of *Pseudomonas aeruginosa* lipase in the open conformation. The prototype for family I.1 of bacterial lipases, J. Biol. Chem. 275 (2000) 31219–31225. doi:10.1074/jbc.M003903200.

[49] K. Pauwels, A. Lustig, L. Wyns, J. Tommassen, S.N. Savvides, P. Van Gelder, Structure of a membrane-based steric chaperone in complex with its lipase substrate, Nat. Struct. Mol. Biol. 13 (2006) 374–375. doi:10.1038/nsmb1065.

[50] T.P. Korman, J.U. Bowie, Crystal structure of *Proteus mirabilis* lipase, a novel lipase from the Proteus/Psychrophilic subfamily of lipase family I.1, PLoS One. 7 (2012) 1–8. doi:10.1371/journal.pone.0052890.

[51] W. Tsuzuki, A. Ue, A. Nagao, Polar organic solvent added to an aqueous solution changes hydrolytic property of lipase., Biosci. Biotechnol. Biochem. 67 (2003) 1660–6. doi:10.1271/bbb.67.1660.

[52] D.H. Rammler, The effect of DMSO on several enzyme systems, Ann. N. Y. Acad. Sci. 141 (1967) 291–299. doi:10.1111/j.1749-6632.1967.tb34893.x.

[53] K. Novototskaya-Vlasova, L. Petrovskaya, E. Kryukova, E. Rivkina, D. Dolgikh, M. Kirpichnikov, Expression and chaperone-assisted refolding of a new cold-active lipase from *Psychrobacter cryohalolentis* K5T, Protein Expr. Purif. 91 (2013) 96–103. doi:10.1016/j.pep.2013.07.011.

[54] N. Akbari, K. Khajeh, N. Ghaemi, Z. Salemi, Efficient refolding of recombinant lipase from *Escherichia coli* inclusion bodies by response surface methodology, Protein Expr. Purif. 70 (2010) 254–259. doi:10.1016/j.pep.2009.10.009.

[55] K.R. Kim, D.Y. Kwon, S.H. Yoon, W.Y. Kim, K.H. Kim, Purification, refolding, and characterization of recombinant *Pseudomonas fluorescens* lipase, Protein Expr. Purif. 39 (2005) 124–129. doi:10.1016/j.pep.2004.09.014.

[56] S.J. Wodak, J. Janin, Structural basis of macromolecular recognition., Adv. Protein Chem. 61 (2002) 9–73. http://www.ncbi.nlm.nih.gov/pubmed/12461820 (accessed August 24, 2018).

[57] P.L. Kastritis, I.H. Moal, H. Hwang, Z. Weng, P.A. Bates, A.M.J.J. Bonvin, J. Janin, A structure-based benchmark for protein-protein binding affinity., Protein Sci. 20 (2011) 482–91. doi:10.1002/pro.580.

[58] L. Nini, L. Sarda, L.-C. Comeau, E. Boitard, J.-P. Dubès, H. Chahinian, Lipase-catalysed hydrolysis of short-chain substrates in solution and in emulsion: a kinetic study, Biochim. Biophys. Acta - Mol. Cell Biol. Lipids. 1534 (2001) 34–44. doi:10.1016/S1388-1981(01)00172-X.

[59] R.C. Alnoch, A.A. Stefanello, V. Paula Martini, J.L. Richter, C. Mateo, E.M. de Souza, D.A. Mitchell, M. Muller-Santos, N. Krieger, Co-expression, purification and characterization of the lipase and foldase of *Burkholderia contaminans* LTEB11, Int. J. Biol. Macromol. 116 (2018) 1222–1231. doi:10.1016/j.ijbiomac.2018.05.086.

[60] P. Gadler, K. Faber, New enzymes for biotransformations: microbial alkyl sulfatases displaying stereo- and enantioselectivity, Trends Biotechnol. 25 (2007) 83–88. doi:10.1016/j.tibtech.2006.11.006.

[61] J.M. Palomo, G. Muñoz, G. Fernández-Lorente, C. Mateo, R. Fernández-Lafuente, J.M. Guisán, Interfacial adsorption of lipases on very hydrophobic support (octadecyl–Sepabeads): immobilization, hyperactivation and stabilization of the open form of lipases, J. Mol. Catal. B Enzym. 19–20 (2002) 279–286. doi:10.1016/S1381-1177(02)00178-9.

[62] Y.-Y. Huo, S.-L. Jian, H. Cheng, Z. Rong, H.-L. Cui, X.-W. Xu, Two novel deep-sea sediment metagenome-derived esterases: residue 199 is the determinant of substrate specificity and preference, Microb. Cell Fact. 17 (2018) 16. doi:10.1186/s12934-018-0864-4.

4.7 SUPPLEMENTARY MATERIAL

Biochemical characterization and application of a new lipase and its cognate foldase from fat-contaminated soil metagenomic library

Janaina Marques de Almeida[a], Viviane Paula Martini[b], Jorge Iulek[c], Robson Carlos Alnoch[a], Vivian Rotuno Moure[a], Marcelo Muller dos Santos[a], Emanuel Maltempi de Souza[a], David Alexander Mitchell[a] and Nadia Krieger[d*].

[a] Departamento de Bioquímica e Biologia Molecular, Universidade Federal do Paraná, Cx. P. 19046, Centro Politécnico, Curitiba 81531-980, Paraná, Brazil.
[b] Instituto Federal do Paraná, Campus Irati, Irati 84500-000, Paraná, Brazil.
[c] Departamento de Química, Universidade Estadual de Ponta Grossa, Av. Carlos Cavalcanti, 4748, Ponta Grossa 84030-900, Paraná, Brazil.
[d] Departamento de Química, Universidade Federal do Paraná, Cx. P. 19032 Centro Politécnico, Curitiba 81531-980, Paraná, Brazil. * To whom correspondence should be addressed. E-mail: nkrieger@ufpr.br; Telephone: +55-41-33613470

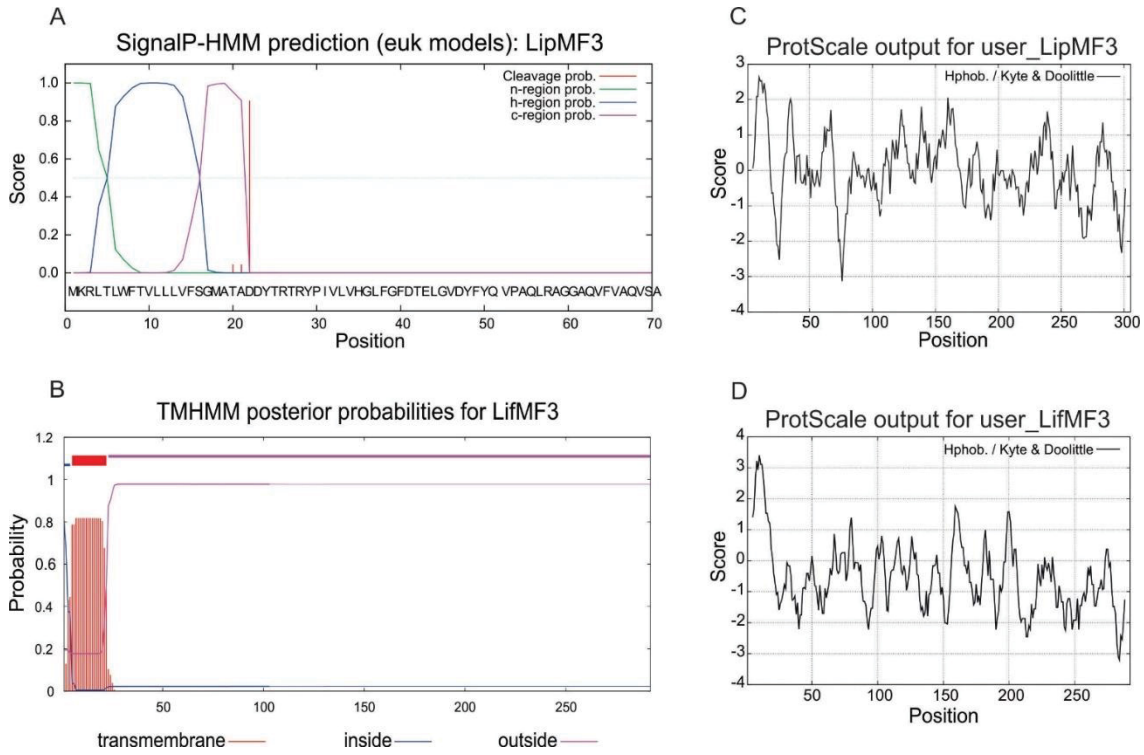

Fig. S1 Analysis of the N-terminal region of LipMF3 and LifMF3. (A) Prediction of a signal peptide in the gene sequence of *lipMF3* by the SignalP server. (B) Prediction of a transmembrane domain in the gene sequence of *lifMF3* by TMHMM server. (C) Estimation of hydrophobicity of the LipMF3 by Protscale (D) Estimation of hydrophobicity of the LifMF3 by Protscale.

Table S1 Primers for amplification of *lipMF3* and *lifMF3*.

Primer	Sequence	Restriction sites
Fw - Entire Lipase	AGCCATATGAAACGTTTAACGCTTTGG	Nde I
Rev - Entire Lipase	ATTAAGCTTGCATTACAGGCCCGCTT	Hind III
Fw - N-truncated Lipase	CGTCATATGGATTACACCCGCACC	Nde I
Rev - N-truncated Lipase	ATTAAGCTTGCATTACAGGCCCGCTT	Hind III
Fw - Entire Foldase	TGTCATATG CGTTGGGCAGGGATA	Nde I
Rev - Entire Foldase	ATCAAGCTT TTAGAATGCGGCCAG	Hind III
Fw - Entire Foldase	CGACATATG GGTGAGGATAGCTCCC	Nde I
Rev - Entire Foldase	ATCAAGCTT TTAGAATGCGGCCAG	Hind III
Fw - Entire Lipase-Foldase	AGCCATATGAAACGTTTAACGCTTTGG	Nde I
Rev - Entire Lipase-Foldase	ATCAAGCTT TTAGAATGCGGCCAG	Hind III

Table S2 Cloning of *lipMF3* and *lifMF3* into pET28a and pT7-7.

Clones	Vector	Gene (Protein)
1	pET28a(+)	entire *lipMF3* (entire lipase)
2	pET28a(+)	N-truncated *lipMF3* (N-truncated lipase)
3	pET28a(+)	entire *lifMF3* (entire foldase)
4	pET28a(+)	N-truncated *lifMF3* (N-truncated foldase)
5	pET28a(+)	entire *lipMF3*-*lifMF3* (entire lipase-foldase)
6	pT7-7	entire *lifMF3* (entire foldase)
7	pT7-7	N-truncated *lifMF3* (N-truncated foldase)
8	pT7-7	entire *lipMF3* (entire lipase)
9	pT7-7	N-truncated *lipMF3* (N-truncated lipase)

Table S3 Constructions of *lipMF3* and *lifMF3* in the expression vectors pET28a(+) and pT7-7.

Co-transformation	Lipase number	Lipase	Foldase number	Foldase
1.6	1	entire LipMF3 + pET28a	6	entire LifMF3 + pT7-7
1.7	1	entire LipMF3 + pET28a	7	N-truncated LifMF3 + pT7-7
2.6	2	N-truncated LipMF3 + pET28a	6	entire LifMF3 + pT7-7
2.7	2	N-truncated LipMF3 + pET28a	7	N-truncated LifMF3 + pT7-7
5.5	5	entire LipMF3-LifMF3 + pET28a	5	(*lip* e *lif* na mesma sequência)
8.3	8	entire LipMF3 + pT7-7	3	entire LifMF3 + pET28a
8.4	8	entire LipMF3 + pT7-7	4	N-truncated LifMF3 + pET28a
9.3	9	N-truncated LipMF3 + pT7-7	3	entire LifMF3 + pET28a
9.4	9	N-truncated LipMF3 + pT7-7	4	N-truncated LifMF3 + pET28a

Table S4 Olive-oil-hydrolyzing activity of the soluble fractions of the different co-expressions in different *E. coli* strains.

Co-expressions	***E. coli* strains**	**Volumetric activity (U mL^{-1})**	**Specific activity* (U mg^{-1})**
Control	Control BL21 (DE3) plysS	0 ± 0	0 ± 0
entire LipMF3-pET28a(+) entire LifMF3-pT7-7	Rosetta (DE3)pLysS	72 ± 0	32 ± 0
	Rosetta 2(DE3)plysS	72 ± 2	39 ± 2
	BL21 (DE3)	78 ± 3	24 ± 2
	BL21 (DE3)plysS	64 ± 3	24 ± 1
	Shuffle Express	44 ± 0	23 ± 3
	BL21 Star (DE3)	97 ± 4	32 ± 2
entire LipMF3-pET28a(+) N-truncated LifMF3-pT7-7	Rosetta (DE3)pLysS	0 ± 0	0 ± 0
	Rosetta 2(DE3)plysS	35 ± 0	11 ± 0
	BL21 (DE3)plysS	0 ± 0	0 ± 0
	BL21 (DE3)	5 ± 0	2 ± 0
	Shuffle Express	2 ± 0	1 ± 0
	BL21 Star (DE3)	4 ± 0	2 ± 0
N-truncated LipMF3-pET28a(+) entire LifMF3-pT7-7	Rosetta (DE3)pLysS	47 ± 4	20 ± 0
	Rosetta 2(DE3)plysS	19 ± 0	8 ± 0
	BL21 (DE3)	27 ± 1	9 ± 1
	BL21 (DE3)plysS	35 ± 1	12 ± 0
	Shuffle Express	31 ± 2	12 ± 1
	BL21 Star (DE3)	24 ± 3	7 ± 1
N-truncated LipMF3-pET28a(+) N-truncated LifMF3-pT7-7	Rosetta (DE3)pLysS	0 ± 0	0 ± 0
	Rosetta 2(DE3)plysS	2 ± 0	1 ± 0
	BL21 (DE3)	0 ± 0	0 ± 0
	BL21 (DE3)plysS	0 ± 0	0 ± 0
	Shuffle Express	0 ± 0	0 ± 0
	BL21 Star (DE3)	0 ± 0	0 ± 0
entire LipMF3-LifMF3-pET28a(+)	Rosetta (DE3)pLysS	13 ± 0	9 ± 0
	Rosetta 2(DE3)plysS	12 ± 0	8 ± 0
	BL21 (DE3)	0 ± 0	0 ± 0
	BL21 (DE3)plysS	0 ± 0	0 ± 0
	Shuffle Express	0 ± 0	0 ± 0
	BL21 Star (DE3)	0 ± 0	0 ± 0
N-truncated LipMF3-pT7-7 entire LifMF3-pET28a(+)	Rosetta (DE3)pLysS	1 ± 0	0 ± 0
	Rosetta 2(DE3)plysS	3 ± 1	1 ± 0
N-truncated LipMF3-pT7-7 N-truncated LifMF3-pET28a(+)	Rosetta (DE3)pLysS	2 ± 0	1 ± 0
	Rosetta 2(DE3)plysS	3 ± 0	1 ± 0
entire LipMF3-pT7-7 entire LifMF3-pET28a(+)	Rosetta (DE3)pLysS	1 ± 0	0 ± 0
	Rosetta 2(DE3)plysS	24 ± 0	9 ± 0
entire LipMF3-pT7-7 N-truncated LifMF3-pET28a(+)	Rosetta (DE3)pLysS	4 ± 1	2 ± 0
	Rosetta 2(DE3)plysS	2 ± 0	1 ± 0

*The activity was determined by the titrimetric method with olive oil as the substrate, using a pHStat at pH 7.0 and 37 °C. Results are expressed as the average of triplicates assays ± the standard error of the mean.

Table S5 List of interations between LipMF3 and LifMF3, as estimated by PDBePISA.

Hydrogen bonds	**Structure 1**	**Distance Å**	**Structure 2**
1	B:THR 41[OG1]	3.25	A:TYR 24[OH]
2	B:HIS 199[NE2]	3.19	A:GLN 62[OE1]
3	B:ARG 288[NE]	3.32	A:GLU 79[OE1]
4	B:ARG 288[NH2]	3.03	A:GLU 79[OE1]
5	B:ARG 288[NE]	3.01	A:GLU 79[OE2]
6	B:ARG 210[NE]	3.19	A:GLU 86[OE2]
7	B:ASN 241[ND2]	2.76	A:GLU 86[OE2]
8	B:SER 37[N]	3.67	A:ILE 263[O]
9	B:SER 37[OG]	2.78	A:TYR 267[OH]
10	B:ASN 154[ND2]	2.84	A:PHE 279[O]
11	B:THR 41[OG1]	3.29	A:GLN 295[O]
12	B:THR 41[OG1]	2.84	A:ASN 298[OD1]
13	B:GLU 42[N]	3.23	A:ASN 298[OD1]
14	B:ARG 36[O]	3.85	A:ARG 299[NH2]
15	B:SER 37[O]	2.83	A:ARG 299[NH2]
16	B:GLN 39[O]	2.82	A:ARG 299[NE]
17	B:GLN 39[O]	2.97	A:ARG 299[NH2]
18	B:GLU 42[O]	2.58	A:TYR 24[OH]
19	B:GLU 58[OE2]	3.44	A:GLN 55[NE2]
20	B:ASP 65[OD2]	3.85	A:ASN 288[ND2]
21	B:TYR 66[O]	3.25	A:GLN 295[NE2]
22	B:ALA 69[O]	2.84	A:LYS 264[NZ]
23	B:GLU 285[OE2]	2.76	A:ARG 116[NH1]
24	B:ARG 288[O]	3.58	A:TYR 111[OH]
Salt bridges	**Structure 1**	**Distance Å**	**Structure 2**
1	B:ARG 288[NE]	3.32	A:GLU 79[OE1]
2	B:ARG 288[NH2]	3.03	A:GLU 79[OE1]
3	B:ARG 288[NE]	3.01	A:GLU 79[OE2]
4	B:ARG 288[NH2]	3.98	A:GLU 79[OE2]
5	B:ARG 210[NE]	3.19	A:GLU 86[OE2]
6	B:ARG 210[NH2]	3.59	A:GLU 86[OE2]
7	B:GLU 285[OE2]	2.76	A:ARG 116[NH1]

Table S6 Purification of the Lip-LifMF3 complex.

Step	**Total protein (mg)**	**Total hydrolysis activity (U)**	**Specific hydrolysis activity (U mg^{-1})**	**Purification factor (fold)**	**Activity recovery (%)**
Crude soluble extract	1080	15444	14.3	1	100
Affinity chromatography	7.5	6450	860	60	42
Dialysis	7.2	6192	860	60	40

Hydrolysis activity by titrimetric method (pHStat) with olive oil as substrate.

Table S7 Predicted and measured (MALDI-TOF) masses of LipMF3 and LifMF3 proteolytic fragments.

Lipase			
Amino acid residues	**Predicted masses (m/z)**	**Measured masses (m/z)**	**Sequence**
60-70	1299.847	1299.701	(K)RGEQLLAEVER(I)
175-487	1403.880	1403.706	(R)FNQAFPEGVPAAR(C)
79-93	1577.057	1576.891	(R)KVNLIGHSQGGPTIR(Y)
41-59	1848.061	1847.924	(R)AGGAQVFVAQVSAANSNEK(R)
94-117	2348.322	2348.637	(R)YVASVRPDLVASVTSVGGVNGGSR(V)
252-277	3094.900	3094.509	(R)MNHVDEINQSFGLVSWFEVNPVTLYR(Q)
Foldase			
Amino acid residues	**Predicted masses (m/z)**	**Measured masses (m/z)**	**Sequence**
241-247	859.407	859.416	(R)NAAWQNR(I)
96-105	1121.618	1121.594	(R)TQSALALFDR(Y)
276-284	1181.541	1181.522	(R)YVSEHFDER(E)
153-164	1353.745	1353.716	(R)YNDFTLALAAVR(A)
178-190	1439.809	1439.774	(R)IAELEAALPEDLR(E)
63-74	1446.768	1446.726	(R)LFDYYLASLGER(S)
37-55	1926.972	1926.926	(R)SQQGTEADGSVHSLQGGLR(T)
136-152	1942.903	1942.856	(K)HYFSDAEAQGLFGTEDR(Y)

5 CONCLUSÕES

Neste trabalho, foram estudadas duas lipases isoladas da biblioteca metagenômica de solo contaminado com gordura animal (SCGA), resultando na avaliação do efeito da cauda de histidina (His-tag) nas propriedades catalíticas da lipase LipC12 e na caracterização bioquímica, molecular e estrutural da uma nova lipase denominada LipMF3.

A clonagem do gene *lipC12* em pET29a(+) e pTEV5 foi realizada e as variantes de LipC12 com e sem His-tag foram produzidas para determinação das propriedades catalíticas, determinação das mudanças estruturais e estudos de imobilização das duas variantes. Esse trabalho mostra pela primeira vez que a His-tag pode interferir significativamente na atividade de uma lipase e que esta interferência depende do tipo de reação catalisada pela enzima. As atividades de hidrólise de LipC12, de ambas as formas livre e imobilizada, contra substratos naturais e artificiais, foram significativamente aumentadas pela remoção da His-tag. Por outro lado, LipC12 com His-tag foi significativamente mais ativa e estável na presença de solventes orgânicos polares do que LipC12 sem His-tag. Assim sendo, para maior atividade de esterificação, em solventes orgânicos, sugere-se que a His-tag seja mantida; entretanto, para reações de hidrólise em meio aquoso, é recomendável a removoção da His-tag. Também foi possível determinar, por dicroísmo circular, que o efeito da His-tag na atividade de LipC12, não se deve a modificações na estrutura terciária da lipase. A imobilização das variantes de LipC12 (com e sem His-tag) foi realizada em Immobead 150 e estudos de dessorção de proteínas confirmaram que a His-tag não participa na ligação covalente da enzima ao suporte.

Em relação à nova lipase, LipMF3, este trabalho resultou na clonagem, expressão, purificação e caracterização de uma nova lipase complexada com a sua foldase LifMF3. A nova lipase pertence à família I.1 e apresenta 67% de identidade com a lipase de *Chromobacterium violaceum*. É uma lipase verdadeira, com maior atividade hidrolítica contra tributirina (1650 U mg $^{-1}$), pH 6,5 e temperatura de 40 ºC. Esta lipase apresenta-se estável em solventes orgânicos e em uma ampla faixa de pH. LipMF3 imobilizada apresentou atividade para a síntese de oleato de etila e enantiosseletividade para (*R*)-1-fenil-1-etanol, portanto, apresenta potencial para aplicação em reações biotecnológicas, como na síntese de ésteres de biodiesel e na resolução de compostos racêmicos.

5.1 RECOMENDAÇÕES PARA TRABALHOS FUTUROS

Os resultados obtidos com os estudos de remoção da His-tag de LipC2 e de caracterização de LipMF3 são promissores quando comparados com outras lipases de metagenômica, abrindo perspectivas para sua aplicação em diversos processos biocatalíticos. Portanto, sugerem-se como estudos futuros:

- Realizar estudos de dinâmica molecular de LipC12 com e sem His-tag, através de simulações destas variantes na presença de solventes orgânicos, a fim de compreender qual o efeito da His-tag nas propriedades catalíticas de LipC12;
- Realizar a clonagem e expressão de LipMF3 em outro sistema de expressão, como por exemplo, em *Pichia pastoris*, com o intuito de melhor a expressão e solubilidade da lipase;
- Realizar a clonagem dos genes *lipMF3* e *lifMF3* em vetor dual, como por exemplo pETDuet, a fim de melhorar o nível de expressão principalmente da foldase, para que as duas proteínas sejam expressas igualmente e assim melhorar a solubilidade da lipase;
- Realizar testes de redobramento *in vitro* de LipMF3, para recuperar as lipases presentes nos corpos de inclusão;
- Aplicar LipMF3 em outras reações de biocatálise, como por exemplo, na resolução cinética de álcoois primários, secundários e terciários;
- Cristalizar LipMF3 complexada à LifMF3 para determinação da estrutura tridimensional deste complexo, uma vez que a Lif de *Burkhoderia glumae* é a única Lif a ter a estrutura tridimensional determinada.

REFERÊNCIAS

ABDULLAH, N.; CHASE, H. A. Removal of poly-histidine fusion tags from recombinant proteins purified by expanded bed adsorption. **Biotechnology and Bioengineering**, v. 92, n. 4, p. 501–13, 20 nov. 2005. Disponível em: <http://doi.wiley.com/10.1002/bit.20633>.

ADLERCREUTZ, P. Immobilisation and application of lipases in organic media. **Chemical Society Reviews**, v. 42, n. 15, p. 6406, 7 ago. 2013. Disponível em: <http://www.ncbi.nlm.nih.gov/pubmed/23403895>. Acesso em: 3 maio. 2017.

AGARWALA, R.; BARRETT, T.; BECK, J.; BENSON, D. A.; BOLLIN, C.; BOLTON, E.; BOUREXIS, D.; BRISTER, J. R.; BRYANT, S. H.; CANESE, K.; CHAROWHAS, C.; CLARK, K.; DICUCCIO, M.; DONDOSHANSKY, I.; FEOLO, M.; FUNK, K.; GEER, L. Y.; GORELENKOV, V.; HLAVINA, W.; HOEPPNER, M.; HOLMES, B.; JOHNSON, M.; KHOTOMLIANSKI, V.; KIMCHI, A.; KIMELMAN, M.; KITTS, P.; KLIMKE, W.; KRASNOV, S.; KUZNETSOV, A.; LANDRUM, M. J.; LANDSMAN, D.; LEE, J. M.; LIPMAN, D. J.; LU, Z.; MADDEN, T. L.; MADEJ, T.; MARCHLER-BAUER, A.; KARSCH-MIZRACHI, I.; MURPHY, T.; ORRIS, R.; OSTELL, J.; O'SULLIVAN, C.; PALANIGOBU, V.; PANCHENKO, A. R.; PHAN, L.; PRUITT, K. D.; RODARMER, K.; RUBINSTEIN, W.; SAYERS, E. W.; SCHNEIDER, V.; SCHOCH, C. L.; SCHULER, G. D.; SHERRY, S. T.; SIROTKIN, K.; SIYAN, K.; SLOTTA, D.; SOBOLEVA, A.; SOUSSOV, V.; STARCHENKO, G.; TATUSOVA, T. A.; TODOROV, K.; TRAWICK, B. W.; VAKATOV, D.; WANG, Y.; WARD, M.; WILBUR, W. J.; YASCHENKO, E.; ZBICZ, K. Database resources of the national center for biotechnology information. **Nucleic Acids Research**, v. 45, n. D1, p. D12–D17, 4 jan. 2017. Disponível em: <http://www.ncbi.nlm.nih.gov/pubmed/27899561>. Acesso em: 23 ago. 2018.

AKATSUKA, H.; BINET, R.; KAWAI, E.; WANDERSMAN, C.; OMORI, K. Lipase secretion by bacterial hybrid ATP-binding cassette exporters: molecular recognition of the LipBCD, PrtDEF, and HasDEF exporters. **Journal of Bacteriology**, v. 179, n. 15, p. 4754–4760, ago. 1997. Disponível em: <http://jb.asm.org/lookup/doi/10.1128/jb.179.15.4754-4760.1997>.

AKATSUKA, H.; KAWAI, E.; OMORI, K.; SHIBATANI, T. The three genes lipB, lipC, and lipD involved in the extracellular secretion of the *Serratia marcescens* lipase which lacks an N-terminal signal peptide. **Journal of Bacteriology**, v. 177, n. 22, p. 6381–9, 1 nov. 1995. Disponível em: <http://www.ncbi.nlm.nih.gov/pubmed/7592412>. Acesso em: 30 ago. 2018.

AKBARI, N.; KHAJEH, K.; GHAEMI, N.; SALEMI, Z. Efficient refolding of recombinant lipase from *Escherichia coli* inclusion bodies by response surface methodology. **Protein Expression and Purification**, v. 70, n. 2, p. 254–259, 1 abr. 2010. Disponível em: <http://www.sciencedirect.com/science/article/pii/S1046592809002587>. Acesso em: 17 out. 2017.

ALBARRÁN-VELO, J.; GONZÁLEZ-MARTÍNEZ, D.; GOTOR-FERNÁNDEZ, V. Stereoselective biocatalysis: A mature technology for the asymmetric synthesis of pharmaceutical building blocks. **Biocatalysis and Biotransformation**, v. 36, n. 2, p.

102–130, 4 mar. 2018. Disponível em: <https://doi.org/10.1080/10242422.2017.1340457>.

ALBUQUERQUE, T. B.; DA SILVA, C. D. G.; DE OLIVEIRA, A. R.; DOS SANTOS, B. F.; DA SILVA, B. A. L.; KATLA, R.; ROCHA, M. P. D.; DOMINGUES, N. L. C. Lipase catalyzed 1,2-addition of thiols to imines under mild conditions. **New Journal of Chemistry**, v. 42, n. 3, p. 1642–1645, 2018. Disponível em: <http://xlink.rsc.org/?DOI=C7NJ03387G>.

ALMA'ABADI, A. D.; GOJOBORI, T.; MINETA, K. Marine Metagenome as a resource for novel enzymes. **Genomics, Proteomics and Bioinformatics**, v. 13, n. 5, p. 290–295, 2015.

ALNOCH, R. C.; MARTINI, V. P.; GLOGAUER, A.; COSTA, A. C. D. S.; PIOVAN, L.; MULLER-SANTOS, M.; DE SOUZA, E. M.; DE OLIVEIRA PEDROSA, F.; MITCHELL, D. A.; KRIEGER, N. Immobilization and characterization of a new regioselective and enantioselective lipase obtained from a metagenomic library. **PLoS ONE**, v. 10, n. 2, p. 1-18, 23 fev. 2015. Disponível em: <http://dx.plos.org/10.1371/journal.pone.0114945>.

ALNOCH, R. C.; STEFANELLO, A. A.; PAULA MARTINI, V.; RICHTER, J. L.; MATEO, C.; SOUZA, E. M. de; MITCHELL, D. A.; MULLER-SANTOS, M.; KRIEGER, N. Co-expression, purification and characterization of the lipase and foldase of *Burkholderia contaminans* LTEB11. **International Journal of Biological Macromolecules**, v. 116, p. 1222–1231, set. 2018. Disponível em: <https://doi.org/10.1016/j.ijbiomac.2018.05.086>.

ALNOCH, R.; RODRIGUES DE MELO, R.; PALOMO, J.; MALTEMPI DE SOUZA, E.; KRIEGER, N.; MATEO, C. New tailor-made alkyl-aldehyde bifunctional supports for lipase immobilization. **Catalysts**, v. 6, n. 12, p. 191, 2016. Disponível em: <http://www.mdpi.com/2073-4344/6/12/191>.

ALTSCHUL, S. F.; MADDEN, T. L.; SCHÄFFER, A. A.; ZHANG, J.; ZHANG, Z.; MILLER, W.; LIPMAN, D. J. Gapped BLAST and PSI-BLAST: a new generation of protein database search programs. **Nucleic Acids Research**, v. 25, n. 17, p. 3389–402, 1 set. 1997. Disponível em: <http://www.ncbi.nlm.nih.gov/pubmed/9254694>. Acesso em: 24 ago. 2018.

AMBARDAR, S.; GUPTA, R.; TRAKROO, D.; LAL, R.; VAKHLU, J. High Throughput sequencing: an overview of sequencing chemistry. **Indian Journal of Microbiology**, v. 56, n. 4, p. 394–404, dez. 2016. Disponível em: <http://www.ncbi.nlm.nih.gov/pubmed/27784934>. Acesso em: 2 out. 2018.

ANGKAWIDJAJA, C.; KANAYA, S. Family I.3 lipase: bacterial lipases secreted by the type I secretion system. **Cellular and Molecular Life Sciences**, v. 63, n. 23, p. 2804–2817, 13 dez. 2006. Disponível em: <http://link.springer.com/10.1007/s00018-006-6172-x>.

ARNAU, J.; LAURITZEN, C.; PETERSEN, G. E.; PEDERSEN, J. Current strategies for the use of affinity tags and tag removal for the purification of recombinant proteins. **Protein Expression and Purification**, v. 48, n. 1, p. 1–13, jul. 2006.

Disponível em: <http://linkinghub.elsevier.com/retrieve/pii/S1046592805004262>.

ARPIGNY, J. L.; JAEGER, K.-E. Bacterial lipolytic enzymes: classification and properties. **Biochemical Journal**, v. 343, n. 1, p. 177, 1 out. 1999. Disponível em: <http://www.biochemj.org/bj/343/bj3430177.htm>.

BAJPAI, P. Application of enzymes in the pulp and paper industry. **Biotechnology Progress**, v. 15, n. 2, p. 147–157, 5 abr. 1999. Disponível em: <http://doi.wiley.com/10.1021/bp990013k>. Acesso em: 27 ago. 2018.

BANDEIRA, P. T.; ALNOCH, R. C.; DE OLIVEIRA, A. R. M.; DE SOUZA, E. M.; DE O. PEDROSA, F.; KRIEGER, N.; PIOVAN, L. Enzymatic kinetic resolution of aliphatic sec-alcohols by LipG9, a metagenomic lipase. **Journal of Molecular Catalysis B: Enzymatic**, v. 125, n. March, p. 58–63, mar. 2016. Disponível em: <http://dx.doi.org/10.1016/j.molcatb.2015.12.010>.

BARTON, G. J. ALSCRIPT: a tool to format multiple sequence alignments. **Protein Engineering**, v. 6, n. 1, p. 37–40, jan. 1993. Disponível em: <http://www.ncbi.nlm.nih.gov/pubmed/8433969>. Acesso em: 24 ago. 2018.

BAUMANN, M.; STÜRMER, R.; BORNSCHEUER, U. T. A high-throughput-screening method for the identification of active and enantioselective hydrolases. **Angewandte Chemie International Edition**, v. 40, n. 22, p. 4201–4204, 19 nov. 2001. Disponível em: <http://doi.wiley.com/10.1002/1521-3773%2820011119%2940%3A22%3C4201%3A%3AAID-ANIE4201%3E3.0.CO%3B2-V>. Acesso em: 4 set. 2018.

BERINI, F.; CASCIELLO, C.; MARCONE, G. L.; MARINELLI, F. Metagenomics: Novel enzymes from non-culturable microbes. **FEMS Microbiology Letters**, v. 364, n. 21, p. 1–19, 2017.

BERMAN, H. M.; WESTBROOK, J.; FENG, Z.; GILLILAND, G.; BHAT, T. N.; WEISSIG, H.; SHINDYALOV, I. N.; BOURNE, P. E. The Protein Data Bank. **Nucleic Acids Research**, v. 28, n. 1, p. 235–42, 1 jan. 2000. Disponível em: <http://www.ncbi.nlm.nih.gov/pubmed/10592235>. Acesso em: 23 ago. 2018.

BERTOLDO, J. B.; RAZZERA, G.; VERNAL, J.; BROD, F. C. A.; ARISI, A. C. M.; TERENZI, H. Structural stability of *Staphylococcus xylosus* lipase is modulated by Zn^{2+} ions. **Biochimica et Biophysica Acta (BBA) - Proteins and Proteomics**, v. 1814, n. 9, p. 1120–1126, 1 set. 2011. Disponível em: <https://www.sciencedirect.com/science/article/pii/S1570963911001269>. Acesso em: 21 abr. 2018.

BERTRAM, M.; HILDEBRANDT, P.; WEINER, D. P.; PATEL, J. S.; BARTNEK, F.; HITCHMAN, T. S.; BORNSCHEUER, U. T. Characterization of lipases and esterases from metagenomes for lipid modification. **Journal of the American Oil Chemists' Society**, v. 85, n. 1, p. 47–53, 23 jan. 2008. Disponível em: <http://doi.wiley.com/10.1007/s11746-007-1161-2>. Acesso em: 29 set. 2018.

BETIKU, E. Molecular chaperones involved in heterologous protein folding in *Escherichia coli*. **Biotechnology and Molecular Biology Review**, v. 1, n. 2, p. 66–75, 2006.

BHARDWAJ, K. K.; GUPTA, R. Synthesis of chirally pure enantiomers by lipase. **Journal of Oleo Science**, v. 66, n. 10, p. 1073–1084, 2017. Disponível em: <https://www.jstage.jst.go.jp/article/jos/66/10/66_ess17114/_pdf/-char/en>.

BLANK, K.; MORFILL, J.; GUMPP, H.; GAUB, H. E. Functional expression of *Candida antarctica* lipase B in *Eschericha coli*. **Journal of Biotechnology**, v. 125, n. 4, p. 474–483, out. 2006. Disponível em: <http://linkinghub.elsevier.com/retrieve/pii/S0168165606003105>.

BOND, C. S.; SCHÜTTELKOPF, A. W.; IUCR. ALINE: a WYSIWYG protein-sequence alignment editor for publication-quality alignments. **Acta Crystallographica Section D Biological Crystallography**, v. 65, n. 5, p. 510–512, 1 maio 2009. Disponível em: <http://scripts.iucr.org/cgi-bin/paper?S0907444909007835>. Acesso em: 23 ago. 2018.

BORRELLI, G.; TRONO, D. Recombinant lipases and phospholipases and their use as biocatalysts for industrial applications. **International Journal of Molecular Sciences**, v. 16, n. 9, p. 20774–20840, 1 set. 2015. Disponível em: <http://www.mdpi.com/1422-0067/16/9/20774>.

BOSLEY, J. A.; PEILOW, A. D. Immobilization of lipases on porous polypropylene: Reduction in esterification efficiency at low loading. **Journal of the American Oil Chemists' Society**, v. 74, n. 2, p. 107–111, fev. 1997. Disponível em: <http://doi.wiley.com/10.1007/s11746-997-0153-6>. Acesso em: 7 maio. 2018.

BOU ALI, M.; BEN ALI, Y.; AISSA, I.; GARGOURI, Y. Eukaryotic expression system *Pichia pastoris* affects the lipase catalytic properties: A monolayer study. **PLoS ONE**, v. 9, n. 8, p. e104221, 18 ago. 2014. Disponível em: <http://dx.plos.org/10.1371/journal.pone.0104221>.

BOŽIČ, M.; VIVOD, V.; KAVČIČ, S.; LEITGEB, M.; KOKOL, V. New findings about the lipase acetylation of nanofibrillated cellulose using acetic anhydride as acyl donor. **Carbohydrate Polymers**, v. 125, n. 8, p. 340–351, 25 jul. 2015. Disponível em: <http://arxiv.org/abs/1011.1669>.

BRADFORD, M. M. A rapid and sensitive method for the quantitation of microgram quantities of protein utilizing the principle of protein-dye binding. **Analytical Biochemistry**, v. 72, p. 248–254, maio 1976.

BRAULT, G.; SHARECK, F.; HURTUBISE, Y.; LÉPINE, F.; DOUCET, N. Short-chain flavor ester synthesis in organic media by an *E. coli* whole-cell biocatalyst expressing a newly characterized heterologous lipase. **PLoS ONE**, v. 9, n. 3, p. e91872, 26 mar. 2014. Disponível em: <http://dx.plos.org/10.1371/journal.pone.0091872>. Acesso em: 29 set. 2018.

BUCHER, M. H.; EVDOKIMOV, A. G.; WAUGH, D. S. Differential effects of short affinity tags on the crystallization of *Pyrococcus furiosus* maltodextrin-binding protein. **Acta Crystallographica Section D: Biological Crystallography**, v. 58, n. 3, p. 392–397, 1 mar. 2002. Disponível em: <http://scripts.iucr.org/cgi-bin/paper?S0907444901021187>. Acesso em: 5 maio. 2017.

CADIRCI, B. H.; YASA, I. An organic solvents tolerant and thermotolerant lipase from

Pseudomonas fluorescens P21. **Journal of Molecular Catalysis B: Enzymatic**, v. 64, n. 3–4, p. 155–161, 1 jul. 2010. Disponível em: <https://www.sciencedirect.com/science/article/pii/S1381117709002434>. Acesso em: 21 abr. 2018.

CAO, Y.; ZHUANG, Y.; YAO, C.; WU, B.; HE, B. Purification and characterization of an organic solvent-stable lipase from *Pseudomonas stutzeri* LC2-8 and its application for efficient resolution of (R, S)-1-phenylethanol. **Biochemical Engineering Journal**, v. 64, p. 55–60, maio 2012. Disponível em: <http://linkinghub.elsevier.com/retrieve/pii/S1369703X12000733>. Acesso em: 27 ago. 2018.

CAPRILES, P. V.; GUIMARÃES, A. C.; OTTO, T. D.; MIRANDA, A. B.; DARDENNE, L. E.; DEGRAVE, W. M. Structural modelling and comparative analysis of homologous, analogous and specific proteins from *Trypanosoma cruzi* versus *Homo sapiens*: Putative drug targets for chagas' disease treatment. **BMC Genomics**, v. 11, n. 1, p. 610, 29 out. 2010. Disponível em: <http://bmcgenomics.biomedcentral.com/articles/10.1186/1471-2164-11-610>. Acesso em: 24 ago. 2018.

CARREA; RIVA. Properties and synthetic applications of enzymes in organic solvents. **Angewandte Chemie (International ed. in English)**, v. 39, n. 13, p. 2226–2254, 3 jul. 2000. Disponível em: <http://doi.wiley.com/10.1002/1521-3773%2820000703%2939%3A13%3C2226%3A%3AAID-ANIE2226%3E3.0.CO%3B2-L>.

CARSON, M.; JOHNSON, D. H.; MCDONALD, H.; BROUILLETTE, C.; DELUCAS, L. J. His-tag impact on structure. **Acta Crystallographica Section D Biological Crystallography**, v. 63, n. 3, p. 295–301, 1 mar. 2007. Disponível em: <http://www.ncbi.nlm.nih.gov/pubmed/17327666>.

CASTILLA, A.; PANIZZA, P.; RODRÍGUEZ, D.; BONINO, L.; DÍAZ, P.; IRAZOQUI, G.; RODRÍGUEZ GIORDANO, S. A novel thermophilic and halophilic esterase from *Janibacter* sp. R02, the first member of a new lipase family (Family XVII). **Enzyme and Microbial Technology**, v. 98, p. 86–95, mar. 2017. Disponível em: <http://www.ncbi.nlm.nih.gov/pubmed/28110668>. Acesso em: 30 ago. 2018.

CHALKLEY, R. J.; BAKER, P. R.; HUANG, L.; HANSEN, K. C.; ALLEN, N. P.; REXACH, M.; BURLINGAME, A. L. Comprehensive analysis of a multidimensional liquid chromatography mass spectrometry dataset acquired on a quadrupole selecting, quadrupole collision cell, time-of-flight mass spectrometer: II. New developments in Protein Prospector allow for reliable and comprehensive automatic analysis of large datasets. **Molecular & Cellular Proteomics : MCP**, v. 4, n. 8, p. 1194–204, 1 ago. 2005. Disponível em: <http://www.ncbi.nlm.nih.gov/pubmed/15937296>. Acesso em: 24 ago. 2018.

CHANG, S.-Y.; BONG, J.-H.; YOO, G.; LEE, M.; KANG, M.-J.; JOSE, J.; PYUN, J.-C. Activity control of autodisplayed proteins on the same outer membrane layer of *E. coli* by using Z-domain/streptavidin/and lipase/foldase systems. **Enzyme and Microbial Technology**, v. 96, p. 85–95, 1 jan. 2017. Disponível em: <http://www.sciencedirect.com/science/article/pii/S0141022916301983>. Acesso em:

17 out. 2017.

CHEN, C. S.; FUJIMOTO, Y.; GIRDAUKAS, G.; SIH, C. J. Quantitative analyses of biochemical kinetic resolutions of enantiomers. **Journal of the American Chemical Society**, v. 104, n. 25, p. 7294–7299, dez. 1982. Disponível em: <http://pubs.acs.org/doi/abs/10.1021/ja00389a064>. Acesso em: 24 ago. 2018.

CHOI, S.-L.; RHA, E.; LEE, S. J.; KIM, H.; KWON, K.; JEONG, Y.-S.; RHEE, Y. H.; SONG, J. J.; KIM, H.-S.; LEE, S.-G. Toward a generalized and high-throughput enzyme screening system based on artificial genetic circuits. **ACS Synthetic Biology**, v. 3, n. 3, p. 163–171, 21 mar. 2014. Disponível em: <http://www.ncbi.nlm.nih.gov/pubmed/24295047>. Acesso em: 7 set. 2018.

CHOW, J.; KOVACIC, F.; DALL ANTONIA, Y.; KRAUSS, U.; FERSINI, F.; SCHMEISSER, C.; LAUINGER, B.; BONGEN, P.; PIETRUSZKA, J.; SCHMIDT, M.; MENYES, I.; BORNSCHEUER, U. T.; ECKSTEIN, M.; THUM, O.; LIESE, A.; MUELLER-DIECKMANN, J.; JAEGER, K.-E.; STREIT, W. R. The metagenome-derived enzymes LipS and LipT increase the diversity of known lipases. **PLoS ONE**, v. 7, n. 10, p. e47665, 24 out. 2012. Disponível em: <http://dx.plos.org/10.1371/journal.pone.0047665>. Acesso em: 12 dez. 2014.

COSTA, S.; ALMEIDA, A.; CASTRO, A.; DOMINGUES, L. Fusion tags for protein solubility, purification and immunogenicity in *Escherichia coli*: the novel Fh8 system. **Frontiers in Microbiology**, v. 5, n. FEB, p. 63, 2014. Disponível em: <http://www.ncbi.nlm.nih.gov/pubmed/24600443>. Acesso em: 20 out. 2017.

DE CASTRO, M. S.; SINISTERRA GAGO, J. Lipase-catalyzed synthesis of chiral amides: A systematic study of the variables that control the synthesis. **Tetrahedron**, v. 54, n. 12, p. 2877–2892, mar. 1998. Disponível em: <http://linkinghub.elsevier.com/retrieve/pii/S004040209883024X>.

DE MONPEZAT, T. de L.; DE JESO, B.; BUTOUR, J.-L.; CHAVANT, L.; SANCHOLLE, M. A fluorimetric method for measuring lipase activity based on umbelliferyl esters. **Lipids**, v. 25, n. 10, p. 661–664, out. 1990. Disponível em: <http://doi.wiley.com/10.1007/BF02536018>. Acesso em: 4 set. 2018.

DUONG, F.; SOSCIA, C.; LAZDUNSKI, A.; MURGIER, M. The *Pseudomonas fluorescens* lipase has a C-terminal secretion signal and is secreted by a three-component bacterial ABC-exporter system. **Molecular Microbiology**, v. 11, n. 6, p. 1117–1126, 1 mar. 1994. Disponível em: <http://doi.wiley.com/10.1111/j.1365-2958.1994.tb00388.x>. Acesso em: 30 ago. 2018.

DWIVEDEE, B. P.; SONI, S.; SHARMA, M.; BHAUMIK, J.; LAHA, J. K.; BANERJEE, U. C. Promiscuity of lipase-catalyzed reactions for organic synthesis: A recent update. **ChemistrySelect**, v. 3, n. 9, p. 2441–2466, 2018.

EL KHATTABI, M.; GELDER, P. Van; BITTER, W.; TOMMASSEN, J. Role of the lipase-specific foldase of *Burkholderia glumae* as a steric chaperone. **Journal of Biological Chemistry**, v. 275, n. 35, p. 26885–26891, 19 jun. 2000. Disponível em: <http://www.jbc.org/cgi/doi/10.1074/jbc.M003258200>.

EL KHATTABI, M.; OCKHUIJSEN, C. Specificity of the lipase-specific foldases of

gram-negative bacteria and the role of the membrane anchor. **Molecular And General Genetics**, v. 261, p. 770–776, 1999.

ELEND, C.; SCHMEISSER, C.; LEGGEWIE, C.; BABIAK, P.; CARBALLEIRA, J. D.; STEELE, H. L.; REYMOND, J.-L.; JAEGER, K.-E.; STREIT, W. R. Isolation and biochemical characterization of two novel metagenome-derived esterases. **Applied and Environmental Microbiology**, v. 72, n. 5, p. 3637–45, maio 2006. Disponível em: <http://www.ncbi.nlm.nih.gov/pubmed/16672512>. Acesso em: 28 ago. 2018.

ELLIS, J. Proteins as molecular chaperones. **Nature**, v. 328, n. 6129, p. 378–379, 30 jul. 1987. Disponível em: <http://www.nature.com/doifinder/10.1038/328378a0>. Acesso em: 1 out. 2018.

ELLIS, R. J. The general concept of molecular chaperones. **Philosophical Transactions of the Royal Society B: Biological Sciences**, v. 339, n. 1289, p. 257–261, 29 mar. 1993. Disponível em: <http://rstb.royalsocietypublishing.org/cgi/doi/10.1098/rstb.1993.0023>.

EWIS, H. E.; ABDELAL, A. T.; LU, C.-D. Molecular cloning and characterization of two thermostable carboxyl esterases from *Geobacillus stearothermophilus*. **Gene**, v. 329, p. 187–195, 31 mar. 2004. Disponível em: <https://www.sciencedirect.com/science/article/pii/S037811904000083?via%3Dihub>. Acesso em: 28 ago. 2018.

FERNÁNDEZ-ÁLVARO, E.; SNAJDROVA, R.; JOCHENS, H.; DAVIDS, T.; BÖTTCHER, D.; BORNSCHEUER, U. T. A Combination of *in vivo* selection and cell sorting for the identification of enantioselective biocatalysts. **Angewandte Chemie International Edition**, v. 50, n. 37, p. 8584–8587, 5 set. 2011. Disponível em: <http://doi.wiley.com/10.1002/anie.201102360>. Acesso em: 4 set. 2018.

FERNÁNDEZ-ARROJO, L.; GUAZZARONI, M. E.; LÓPEZ-CORTÉS, N.; BELOQUI, A.; FERRER, M. Metagenomic era for biocatalyst identification. **Current Opinion in Biotechnology**, v. 21, n. 6, p. 725–733, 2010.

FERREIRA-DIAS, S.; SANDOVAL, G.; PLOU, F.; VALERO, F. The potential use of lipases in the production of fatty acid derivatives for the food and nutraceutical industries. **Electronic Journal of Biotechnology**, v. 16, n. 3, 15 maio 2013. Disponível em: <http://www.ejbiotechnology.info/index.php/ejbiotechnology/article/view/1417>.

FERRER, M.; BARGIELA, R.; MARTÍNEZ-MARTÍNEZ, M.; MIR, J.; KOCH, R.; GOLYSHINA, O. V.; GOLYSHIN, P. N. Biodiversity for biocatalysis: A review of the α/β-hydrolase fold superfamily of esterases-lipases discovered in metagenomes. **Biocatalysis and Biotransformation**, v. 33, n. 5–6, p. 235–249, 2016.

FERRER, M.; MARTÍNEZ-MARTÍNEZ, M.; BARGIELA, R.; STREIT, W. R.; GOLYSHINA, O. V.; GOLYSHIN, P. N. Estimating the success of enzyme bioprospecting through metagenomics: Current status and future trends. **Microbial Biotechnology**, v. 9, n. 1, p. 22–34, 1 jan. 2015. Disponível em: <http://doi.wiley.com/10.1111/1751-7915.12309>. Acesso em: 1 out. 2018.

FRENKEN, L. G. J.; BOS, J. W.; VISSER, C.; MÜLLER, W.; TOMMASSEN, J.; VERRIPS, C. T. An accessory gene, lipB, required for the production of active *Pseudomonas glumae* lipase. **Molecular Microbiology**, v. 9, n. 3, p. 579–589, 1 ago. 1993. Disponível em: <http://doi.wiley.com/10.1111/j.1365-2958.1993.tb01718.x>. Acesso em: 1 out. 2018.

GADLER, P.; FABER, K. New enzymes for biotransformations: Microbial alkyl sulfatases displaying stereo- and enantioselectivity. **Trends in Biotechnology**, v. 25, n. 2, p. 83–88, fev. 2007. Disponível em: <http://linkinghub.elsevier.com/retrieve/pii/S0167779906002927>. Acesso em: 26 ago. 2018.

GAO, W.; FAN, H.; CHEN, L.; WANG, H.; WEI, D. Efficient kinetic resolution of secondary alcohols using an organic solvent-tolerant esterase in non-aqueous medium. **Biotechnology Letters**, v. 38, n. 7, p. 1165–1171, 30 jul. 2016a. Disponível em: <http://link.springer.com/10.1007/s10529-016-2091-6>. Acesso em: 20 out. 2018.

GAO, W.; WU, K.; CHEN, L.; FAN, H.; ZHAO, Z.; GAO, B.; WANG, H.; WEI, D. A novel esterase from a marine mud metagenomic library for biocatalytic synthesis of short-chain flavor esters. **Microbial Cell Factories**, v. 15, n. 1, p. 1–12, 2016b.

GARCÍA-URDIALES, E.; ALFONSO, I.; GOTOR, V. Enantioselective enzymatic desymmetrizations in organic synthesis. **Chemical Reviews**, v. 105, n. 1, p. 313–354, jan. 2005. Disponível em: <http://pubs.acs.org/doi/abs/10.1021/cr040640a>. Acesso em: 27 ago. 2018.

GLOGAUER, A.; MARTINI, V. P.; FAORO, H.; COUTO, G. H.; MÜLLER-SANTOS, M.; MONTEIRO, R. A.; MITCHELL, D. A.; DE SOUZA, E. M.; PEDROSA, F. O.; KRIEGER, N. Identification and characterization of a new true lipase isolated through metagenomic approach. **Microbial Cell Factories**, v. 10, n. 1, p. 54, 15 jul. 2011. Disponível em: <http://www.microbialcellfactories.com/content/10/1/54>. Acesso em: 3 dez. 2014.

GOTOR-FERNÁNDEZ, V.; BRIEVA, R.; GOTOR, V. Lipases: Useful biocatalysts for the preparation of pharmaceuticals. **Journal of Molecular Catalysis B: Enzymatic**, v. 40, n. 3–4, p. 111–120, jun. 2006. Disponível em: <http://linkinghub.elsevier.com/retrieve/pii/S1381117706000750>.

GRÄSLUND, S.; NORDLUND, P.; WEIGELT, J.; BRAY, J.; GILEADI, O.; KNAPP, S.; OPPERMANN, U.; ARROWSMITH, C.; HUI, R.; MING, J.; DHE-PAGANON, S.; PARK, H.; SAVCHENKO, A.; YEE, A.; EDWARDS, A.; VINCENTELLI, R.; CAMBILLAU, C.; KIM, R.; KIM, S.-H.; RAO, Z.; SHI, Y.; TERWILLIGER, T. C.; KIM, C.-Y.; HUNG, L.-W.; WALDO, G. S.; PELEG, Y.; ALBECK, S.; UNGER, T.; DYM, O.; PRILUSKY, J.; SUSSMAN, J. L.; STEVENS, R. C.; LESLEY, S. A.; WILSON, I. A.; JOACHIMIAK, A.; COLLART, F.; DEMENTIEVA, I.; DONNELLY, M. I.; ESCHENFELDT, W. H.; KIM, Y.; STOLS, L.; WU, R.; ZHOU, M.; BURLEY, S. K.; EMTAGE, J. S.; SAUDER, J. M.; THOMPSON, D.; BAIN, K.; LUZ, J.; GHEYI, T.; ZHANG, F.; ATWELL, S.; ALMO, S. C.; BONANNO, J. B.; FISER, A.; SWAMINATHAN, S.; STUDIER, F. W.; CHANCE, M. R.; SALI, A.; ACTON, T. B.; XIAO, R.; ZHAO, L.; MA, L. C.; HUNT, J. F.; TONG, L.; CUNNINGHAM, K.; INOUYE,

M.; ANDERSON, S.; JANJUA, H.; SHASTRY, R.; HO, C. K.; WANG, D.; WANG, H.; JIANG, M.; MONTELIONE, G. T.; STUART, D. I.; OWENS, R. J.; DAENKE, S.; SCHÜTZ, A.; HEINEMANN, U.; YOKOYAMA, S.; BÜSSOW, K.; GUNSALUS, K. C. Protein production and purification. **Nature Methods**, v. 5, n. 2, p. 135–146, fev. 2008. Disponível em: <https://www.nature.com/nmeth/journal/v5/n2/full/nmeth.f.202.html>. Acesso em: 22 out. 2017.

GREEN, E. R.; MECSAS, J. Bacterial Secretion Systems – An overview. **American Society for Microbiology**, v. 4, n. 1, p. 1–32, 2015.

GREENFIELD, N. J. Using circular dichroism spectra to estimate protein secondary structure. **Nature Protocols**, v. 1, n. 6, p. 2876–90, jan. 2006. Disponível em: <http://www.nature.com/doifinder/10.1038/nprot.2006.202>.

GUAZZARONI, M.-E.; SILVA-ROCHA, R.; WARD, R. J. Synthetic biology approaches to improve biocatalyst identification in metagenomic library screening. **Microbial Biotechnology**, v. 8, n. 1, p. 52–64, 1 jan. 2015. Disponível em: <http://doi.wiley.com/10.1111/1751-7915.12146>. Acesso em: 3 set. 2018.

GUPTA, D.; TUTEJA, N. Chaperones and foldases in endoplasmic reticulum stress signaling in plants. **Plant Signaling & Behavior**, v. 6, n. 2, p. 232–236, 2011. Disponível em: <http://www.tandfonline.com/doi/abs/10.4161/psb.6.2.15490>.

GUPTA, R.; GUPTA, N.; RATHI, P. Bacterial lipases: An overview of production, purification and biochemical properties. **Applied Microbiology and Biotechnology**, v. 64, n. 6, p. 763–781, 1 jun. 2004. Disponível em: <http://link.springer.com/10.1007/s00253-004-1568-8>.

HABULIN, M.; KNEZ, Ž. Optimization of (R,S)-1-phenylethanol kinetic resolution over *Candida antarctica* lipase B in ionic liquids. **Journal of Molecular Catalysis B: Enzymatic**, v. 58, n. 1–4, p. 24–28, 1 jun. 2009. Disponível em: <https://www.sciencedirect.com/science/article/pii/S138111770800221X>. Acesso em: 26 out. 2018.

HANDELSMAN, J. Metagenomics: Application of genomics to uncultured microorganisms. **Microbiology and Molecular Biology Reviews**, v. 69, n. 1, p. 195–195, 2004. Disponível em: <http://mmbr.asm.org/cgi/doi/10.1128/MMBR.69.1.195.2005>.

HANDELSMAN, J.; RONDON, M. R.; BRADY, S. F.; CLARDY, J.; GOODMAN, R. M. Molecular biological access to the chemistry of unknown soil microbes: A new frontier for natural products. **Chemistry & Biology**, v. 5, n. 10, p. R245-9, out. 1998. Disponível em: <http://www.ncbi.nlm.nih.gov/pubmed/9818143>. Acesso em: 24 ago. 2018.

HANDRICK, R.; REINHARDT, S.; FOCARETE, M. L.; SCANDOLA, M.; ADAMUS, G.; KOWALCZUK, M.; JENDROSSEK, D. A new type of thermoalkalophilic hydrolase of *Paucimonas lemoignei* with high specificity for amorphous polyesters of short chain-length hydroxyalkanoic acids. **The Journal of Biological Chemistry**, v. 276, n. 39, p. 36215–24, 28 set. 2001. Disponível em:

<http://www.ncbi.nlm.nih.gov/pubmed/11457823>. Acesso em: 28 ago. 2018.

HASAN, F.; SHAH, A. A.; HAMEED, A. Industrial applications of microbial lipases. **Enzyme and Microbial Technology**, v. 39, n. 2, p. 235–251, jun. 2006. Disponível em: <http://www.sciencedirect.com/science/article/pii/S0141022905004606>. Acesso em: 21 jul. 2014.

HOBSON, A. H.; BUCKLEY, C. M.; AAMAND, J. L.; JØRGENSEN, S. T.; DIDERICHSEN, B.; MCCONNELL, D. J. Activation of a bacterial lipase by its chaperone. **Proceedings of the National Academy of Sciences of the United States of America**, v. 90, n. 12, p. 5682–6, 15 jun. 1993. Disponível em: <http://www.ncbi.nlm.nih.gov/pubmed/7685908>. Acesso em: 1 set. 2018.

HOBSON, A. H.; BUCKLEY, C. M.; JORGENSEN, S. T.; DIDERICHSEN, B.; MCCONNELL, D. J. Interaction of the *Pseudomonas cepacia* DSM3959 lipase with its chaperone, limA. **Journal of Biochemistry**, v. 118, n. 3, p. 575–581, 1995.

HOOFT, R. W. W.; VRIEND, G.; SANDER, C.; ABOLA, E. E. Errors in protein structures. **Nature**, v. 381, n. 6580, p. 272–272, 23 maio 1996. Disponível em: <http://www.ncbi.nlm.nih.gov/pubmed/8692262>. Acesso em: 24 ago. 2018.

HORCHANI, H.; OUERTANI, S.; GARGOURI, Y.; SAYARI, A. The N-terminal His-tag and the recombination process affect the biochemical properties of *Staphylococcus aureus* lipase produced in *Escherichia coli*. **Journal of Molecular Catalysis B: Enzymatic**, v. 61, n. 3, p. 194–201, 2009a. Disponível em: <http://www.sciencedirect.com/science/article/pii/S1381117709001714>. Acesso em: 5 maio. 2017.

HORCHANI, H.; SABRINA, L.; RÉGINE, L.; SAYARI, A.; GARGOURI, Y.; VERGER, R. Heterologous expression and N-terminal His-tagging processes affect the catalytic properties of staphylococcal lipases: A monolayer study. **Journal of Colloid and Interface Science**, v. 350, n. 2, p. 586–594, 2010. Disponível em: <http://dx.doi.org/10.1016/j.jcis.2010.07.021>.

HOSOKAWA, M.; HOSHINO, Y.; NISHIKAWA, Y.; HIROSE, T.; YOON, D. H.; MORI, T.; SEKIGUCHI, T.; SHOJI, S.; TAKEYAMA, H. Droplet-based microfluidics for high-throughput screening of a metagenomic library for isolation of microbial enzymes. **Biosensors and Bioelectronics**, v. 67, p. 379–385, 2015. Disponível em: <http://dx.doi.org/10.1016/j.bios.2014.08.059>.

HUO, Y.-Y.; JIAN, S.-L.; CHENG, H.; RONG, Z.; CUI, H.-L.; XU, X.-W. Two novel deep-sea sediment metagenome-derived esterases: Residue 199 is the determinant of substrate specificity and preference. **Microbial Cell Factories**, v. 17, n. 1, p. 16, 30 dez. 2018. Disponível em: <https://doi.org/10.1186/s12934-018-0864-4>.

IHARA, F.; OKAMOTO, I.; AKAO, K.; NIHIRA, T.; YAMADA, Y. Lipase modulator protein (LimL) of *Pseudomonas* sp. strain 109. **Journal of Bacteriology**, v. 177, n. 5, p. 1254–1258, 1995.

INAGAMI, T.; STURTEVANT, J. M. The trypsin-catalyzed hydrolysis of benzoyl-l-arginine ethyl ester. **Biochimica et Biophysica Acta**, v. 38, p. 64–79, jan. 1960. Disponível em: <http://linkinghub.elsevier.com/retrieve/pii/0006300260911963>.

Acesso em: 5 maio. 2017.

JAEGER, K.-E.; EGGERT, T. Lipases for biotechnology. **Current Opinion in Biotechnology**, v. 13, n. 4, p. 390–397, ago. 2002. Disponível em: <http://linkinghub.elsevier.com/retrieve/pii/S0958166902003415>.

JAEGER, K.-E.; RANSAC, S.; DIJKSTRA, B. W.; COLSON, C.; HEUVEL, M. van; MISSET, O. Bacterial lipases. **Journal of Physics A: Mathematical and Theoretical**, v. 15, p. 29–63, 1994.

JAEGER, K. E.; REETZ, M. T. Microbial lipases form versatile tools for biotechnology. **Trends in Biotechnology**, v. 16, n. 9, p. 396–403, 1998.

JALLOULI, R.; ALI, M. B.; CHARFEDDINE, M.; GARGOURI-BOUZID, R.; GARGOURI, Y.; BEZZINE, S. Heterologous overexpression and biochemical characterization of the (galactophospho)lipase from *Fusarium solani* in *Pichia pastoris* that is expressed in planta. **International Journal of Biological Macromolecules**, v. 84, p. 94–100, 2016. Disponível em: <http://dx.doi.org/10.1016/j.ijbiomac.2015.12.005>.

JANES, L. E.; KAZLAUSKAS, R. J. Quick E. A fast spectrophotometric method to measure the enantioselectivity of hydrolases. **The Journal of Organic Chemistry**, v. 62, p. 4560–4561, 1997.

JASWAL, S. S.; TRUHLAR, S. M. E.; DILL, K. A.; AGARD, D. A. Comprehensive analysis of protein folding activation thermodynamics reveals a universal behavior violated by kinetically stable proteases. **Journal of Molecular Biology**, v. 347, n. 2, p. 355–366, 2005.

JAVED, S.; AZEEM, F.; HUSSAIN, S.; RASUL, I.; SIDDIQUE, M. H.; RIAZ, M.; AFZAL, M.; KOUSER, A.; NADEEM, H. Bacterial lipases: A review on purification and characterization. **Progress in Biophysics and Molecular Biology**, v. 132, p. 23–34, 2018. Disponível em: <https://doi.org/10.1016/j.pbiomolbio.2017.07.014>.

JEON, J. H.; KIM, J.-T.; KANG, S. G.; LEE, J.-H.; KIM, S.-J. Characterization and its potential application of two esterases derived from the arctic sediment metagenome. **Marine Biotechnology**, v. 11, n. 3, p. 307–316, 24 jun. 2009. Disponível em: <http://link.springer.com/10.1007/s10126-008-9145-2>. Acesso em: 24 out. 2018.

JØRGENSEN, S.; SKOV, K. W.; DIDERICHSEN, B. Cloning, sequence, and expression of a lipase gene from *Pseudomonas cepacia*: Lipase production in heterologous hosts requires two *Pseudomonas* genes. **Journal of Bacteriology**, v. 173, n. 2, p. 559–567, 1991.

JOSE, J.; MEYER, T. F. The autodisplay story, from discovery to biotechnical and biomedical applications. **Microbiology and Molecular Biology Reviews**, v. 71, n. 4, p. 600–619, 2007. Disponível em: <http://mmbr.asm.org/cgi/doi/10.1128/MMBR.00011-07>.

KABSCH, W.; SANDER, C. Dictionary of protein secondary structure: Pattern recognition of hydrogen-bonded and geometrical features. **Biopolymers**, v. 22, n. 12, p. 2577–2637, 1 dez. 1983. Disponível em:

<https://onlinelibrary.wiley.com/doi/abs/10.1002/bip.360221211>. Acesso em: 23 ago. 2018.

KAGEYAMA, Y.; NIHIRA, T.; YAMADA, Y. Lipase-catalyzed synthesis of macrocyclic lactones in organic solvents. **Annals of the New York Academy of Sciences**, v. 613, n. 1, p. 681–685, 1 dez. 1990. Disponível em: <http://doi.wiley.com/10.1111/j.1749-6632.1990.tb18245.x>. Acesso em: 23 out. 2018.

KAMAL, Z.; YEDAVALLI, P.; DESHMUKH, M. V.; RAO, N. M. Lipase in aqueous-polar organic solvents: Activity, structure, and stability. **Protein Science**, v. 22, n. 7, p. 904–915, 2013.

KANAMORI, Y.; WATANABE, M.; KAWAUCHI, K.; CHEN, Y.-G.; YANAGISHITA, H.; HIRATA, H. Kinetic resolution of enantiomers in racemic and enantiomerically enriched 2-alkanols by *Pseudomonas cepacia* lipase catalyzed transesterification with isopropenyl acetate in organic solvent. **Journal of Oleo Science**, v. 54, n. 1, p. 21–31, 2005.

KANG, C.-H.; OH, K.-H.; LEE, M.-H.; OH, T.-K.; KIM, B. H.; YOON, J.-H. A novel family VII esterase with industrial potential from compost metagenomic library. **Microbial Cell Factories**, v. 10, p. 41, 29 maio 2011. Disponível em: <http://www.ncbi.nlm.nih.gov/pubmed/21619698>. Acesso em: 24 out. 2018.

KAPOOR, M.; MAJUMDER, A. B.; GUPTA, M. N. Promiscuous lipase-catalyzed C–C bond formation reactions between 4 nitrobenzaldehyde and 2-cyclohexen-1-one in biphasic medium: aldol and morita–baylis–hillman adduct formations. **Catalysis Letters**, v. 145, n. 2, p. 527–532, 23 fev. 2014. Disponível em: <http://link.springer.com/10.1007/s10562-014-1429-8>. Acesso em: 3 set. 2018.

KASTRITIS, P. L.; MOAL, I. H.; HWANG, H.; WENG, Z.; BATES, P. A.; BONVIN, A. M. J. J.; JANIN, J. A structure-based benchmark for protein-protein binding affinity. **Protein Science**, v. 20, n. 3, p. 482–91, mar. 2011. Disponível em: <http://www.ncbi.nlm.nih.gov/pubmed/21213247>. Acesso em: 5 nov. 2018.

KENNEDY, J.; O'LEARY, N. D.; KIRAN, G. S.; MORRISSEY, J. P.; O'GARA, F.; SELVIN, J.; DOBSON, A. D. W. Functional metagenomic strategies for the discovery of novel enzymes and biosurfactants with biotechnological applications from marine ecosystems. **Journal of Applied Microbiology**, v. 111, n. 4, p. 787–799, 2011.

KHAN, F. I.; LAN, D.; DURRANI, R.; HUAN, W.; ZHAO, Z.; WANG, Y. The Lid domain in lipases: structural and functional determinant of enzymatic properties. **Frontiers in Bioengineering and Biotechnology**, v. 5, n. March, p. 1–13, 2017. Disponível em: <http://journal.frontiersin.org/article/10.3389/fbioe.2017.00016/full>.

KIM, E.-Y.; OH, K.-H.; LEE, M.-H.; KANG, C.-H.; OH, T.-K.; YOON, J.-H. Novel cold-adapted alkaline lipase from an intertidal flat metagenome and proposal for a new family of bacterial lipases. **Applied and Environmental Microbiology**, v. 75, n. 1, p. 257–60, jan. 2009. Disponível em: <http://www.ncbi.nlm.nih.gov/pubmed/18931297>. Acesso em: 28 ago. 2018.

KIM, H.; KWON, K. K.; RHA, E.; LEE, S.-G. Genetic Enzyme Screening System: A

method for high-throughput functional screening of novel enzymes from metagenomic libraries. **Hydrocarbon and Lipid Microbiology Protocols**, p. 3–12, 2015.

KIM, J.; SEOK, S.; HONG, E.; YOO, T. H.; SEO, M.; RYU, Y. Crystal structure and characterization of esterase Est25 mutants reveal improved enantioselectivity toward (S)-ketoprofen ethyl ester. **Applied Microbiology and Biotechnology**, v. 101, n. 6, p. 2333–2342, 3 mar. 2017. Disponível em: <http://link.springer.com/10.1007/s00253-016-7989-3>. Acesso em: 20 out. 2018.

KIM, K. R.; KWON, D. Y.; YOON, S. H.; KIM, W. Y.; KIM, K. H. Purification, refolding, and characterization of recombinant *Pseudomonas fluorescens* lipase. **Protein Expression and Purification**, v. 39, n. 1, p. 124–129, 2005.

KIM, Y. J.; CHOI, G. S.; KIM, S. B.; YOON, G. S.; KIM, Y. S.; RYU, Y. W. Screening and characterization of a novel esterase from a metagenomic library. **Protein Expression and Purification**, v. 45, n. 2, p. 315–323, 2006.

KIMPLE, M. E.; BRILL, A. L.; PASKER, R. L. Overview of affinity tags for protein purification. In: **Current Protocols in Protein Science**. Hoboken, NJ, USA: John Wiley & Sons, Inc., 2013. 73p. 9.9.1-9.9.23.

KONARZYCKA-BESSLER, M.; BORNSCHEUER, U. T. A high-throughput-screening method for determining the synthetic activity of hydrolases. **Angewandte Chemie International Edition**, v. 42, n. 12, p. 1418–1420, 28 mar. 2003. Disponível em: <http://doi.wiley.com/10.1002/anie.200390365>. Acesso em: 26 set. 2018.

KORMAN, T. P.; BOWIE, J. U. Crystal structure of *Proteus mirabilis* Lipase, a novel lipase from the *Proteus/Psychrophilic* subfamily of lipase family I.1. **PLoS ONE**, v. 7, n. 12, p. 1–8, 2012.

KORMAN, T. P.; SAHACHARTSIRI, B.; CHARBONNEAU, D. M.; HUANG, G. L.; BEAUREGARD, M.; BOWIE, J. U. Dieselzymes: development of a stable and methanol tolerant lipase for biodiesel production by directed evolution. **Biotechnology for Biofuels**, v. 6, n. 1, p. 70, jan. 2013. Disponível em: <http://www.biotechnologyforbiofuels.com/content/6/1/70>. Acesso em: 14 jul. 2015.

KOUKER, G.; JAEGER, K. E. Specific and sensitive plate assay for bacterial lipases. **Applied and Environmental Microbiology**, v. 53, n. 1, p. 211–3, jan. 1987. Disponível em: <http://www.ncbi.nlm.nih.gov/pubmed/3103532>. Acesso em: 4 set. 2018.

KRANEN, E.; DETZEL, C.; WEBER, T.; JOSE, J. Autodisplay for the co-expression of lipase and foldase on the surface of *E. coli*: washing with designer bugs. **Microbial Cell Factories**, v. 13, n. 1, p. 1–12, 2014. Disponível em: <Microbial Cell Factories>.

KUMAR, A.; DHAR, K.; KANWAR, S. S.; ARORA, P. K. Lipase catalysis in organic solvents: advantages and applications. **Biological Procedures Online**, v. 18, p. 2, 2016. Disponível em: <http://www.ncbi.nlm.nih.gov/pubmed/26766927>. Acesso em: 3 maio. 2017.

KUMAR, R.; BANOTH, L.; BANERJEE, U. C.; KAUR, J. Enantiomeric separation of

pharmaceutically important drug intermediates using a metagenomic lipase and optimization of its large scale production. **International Journal of Biological Macromolecules**, v. 95, p. 995–1003, 2017. Disponível em: <http://dx.doi.org/10.1016/j.ijbiomac.2016.10.088>.

KUMAR, S.; STECHER, G.; TAMURA, K. MEGA7: Molecular evolutionary genetics analysis version 7.0 for bigger datasets. **Molecular Biology and Evolution**, v. 33, n. 7, p. 1870–1874, 1 jul. 2016. Disponível em: <https://academic.oup.com/mbe/article-lookup/doi/10.1093/molbev/msw054>. Acesso em: 23 ago. 2018.

KUMAR, V.; YEDAVALLI, P.; GUPTA, V.; RAO, N. M. Engineering lipase A from mesophilic *Bacillus subtilis* for activity at low temperatures. **Protein Engineering, Design and Selection**, v. 27, n. 3, p. 73–82, mar. 2014.

KUMARI, A.; BARONIAN, K.; KUNZE, G.; GUPTA, R. Extracellular expression of YlLip11 with a native signal peptide from *Yarrowia lipolytica* MSR80 in three different yeast hosts. **Protein Expression and Purification**, v. 110, p. 138–144, 2015. Disponível em: <http://dx.doi.org/10.1016/j.pep.2015.02.016>.

KUSNEZOWA, A.; LEICHERT, L. I. In silico approach to designing rational metagenomic libraries for functional studies. **BMC Bioinformatics**, v. 18, n. 1, p. 1–11, 2017.

LAEMMLI, U. K. Cleavage of structural proteins during the assembly of the head of bacteriophage T4. **Nature**, v. 227, n. 5259, p. 680–685, 15 ago. 1970. Disponível em: <http://www.nature.com/doifinder/10.1038/227680a0>. Acesso em: 5 maio. 2017.

LASKOWSKI, R. A.; MACARTHUR, M. W.; MOSS, D. S.; THORNTON, J. M. PROCHECK: A program to check the stereochemical quality of protein structures. **Journal of Applied Crystallography**, v. 26, n. 2, p. 283–291, 1 abr. 1993. Disponível em: <http://scripts.iucr.org/cgi-bin/paper?S0021889892009944>. Acesso em: 24 ago. 2018.

LEE, H. S.; KWON, K. K.; KANG, S. G.; CHA, S. S.; KIM, S. J.; LEE, J. H. Approaches for novel enzyme discovery from marine environments. **Current Opinion in Biotechnology**, v. 21, n. 3, p. 353–357, 2010. Disponível em: <http://dx.doi.org/10.1016/j.copbio.2010.01.015>.

LEE, H. W.; BYUN, S. M. The pore size of the autotransporter domain is critical for the active translocation of the passenger domain. **Biochemical and Biophysical Research Communications**, v. 307, n. 4, p. 820–825, ago. 2003. Disponível em: <http://linkinghub.elsevier.com/retrieve/pii/S0006291X03012695>. Acesso em: 30 ago. 2018.

LEE, M.-H.; LEE, C.-H.; OH, T.-K.; SONG, J. K.; YOON, J.-H. Isolation and characterization of a novel lipase from a metagenomic library of tidal flat sediments: evidence for a new family of bacterial lipases. **Applied and Environmental Microbiology**, v. 72, n. 11, p. 7406–9, nov. 2006. Disponível em: <http://www.ncbi.nlm.nih.gov/pubmed/16950897>. Acesso em: 28 ago. 2018.

LEVISSON, M.; VAN DER OOST, J.; KENGEN, S. W. M. Characterization and

structural modeling of a new type of thermostable esterase from *Thermotoga maritima*. **FEBS Journal**, v. 274, n. 11, p. 2832–2842, jun. 2007. Disponível em: <http://www.ncbi.nlm.nih.gov/pubmed/17466017>. Acesso em: 28 ago. 2018.

LI, J.; CHEN, S.; LI, L.; YU, Y.; FEI, Z.; QIAO, D.; CAO, Y. Approach of directed evolution of microbial lipases and biodiesel catalysis. **African Journal of Microbiology Research**, v. 6, n. 3, p. 637–642, 2012a. Disponível em: <http://www.academicjournals.org/AJMR>.

LI, K.; HE, T.; LI, C.; FENG, X.-W.; WANG, N.; YU, X.-Q. Lipase-catalysed direct Mannich reaction in water: utilization of biocatalytic promiscuity for C–C bond formation in a “one-pot” synthesis. **Green Chemistry**, v. 11, n. 6, p. 777, 8 jun. 2009. Disponível em: <http://xlink.rsc.org/?DOI=b817524a>. Acesso em: 2 out. 2018.

LI, M.; YANG, L.-R.; XU, G.; WU, J.-P. Cloning and characterization of a novel lipase from *Stenotrophomonas maltophilia* GS11: The first member of a new bacterial lipase family XVI. **Journal of Biotechnology**, v. 228, p. 30–36, 20 jun. 2016. Disponível em: <http://www.ncbi.nlm.nih.gov/pubmed/27117245>. Acesso em: 30 ago. 2018.

LI, S.; YANG, X.; YANG, S.; ZHU, M.; WANG, X. Technology prospecting on enzymes: application, marketing and engineering. **Computational and Structural Biotechnology Journal**, v. 2, n. 3, p. e201209017, 2012b. Disponível em: <http://linkinghub.elsevier.com/retrieve/pii/S2001037014600957>.

LIU, J. K.; NAG, A.; SHAW, J. F. Lipase-catalyzed synthesis of fatty acid diethanolamides. **Journal of Agricultural and Food Chemistry**, v. 49, n. 12, p. 5761–5764, 2001.

LIU, P.; WANG, Y.-F.; EWIS, H. E.; ABDELAL, A. T.; LU, C.-D.; HARRISON, R. W.; WEBER, I. T. Covalent reaction intermediate revealed in crystal structure of the *Geobacillus stearothermophilus* carboxylesterase Est30. **Journal of Molecular Biology**, v. 342, n. 2, p. 551–561, 10 set. 2004. Disponível em: <https://www.sciencedirect.com/science/article/pii/S0022283604007740?via%3Dihub>. Acesso em: 28 ago. 2018.

LOUIS-JEUNE, C.; ANDRADE-NAVARRO, M. A.; PEREZ-IRATXETA, C. Prediction of protein secondary structure from circular dichroism using theoretically derived spectra. **Proteins: Structure, Function, and Bioinformatics**, v. 80, n. 2, p. 374–381, fev. 2012.

LOWRY, R. R.; TINSLEY, I. J. Rapid colorimetric determination of free fatty acids. **Journal of the American Oil Chemists Society**, v. 53, n. 7, p. 470–472, jul. 1976b. Disponível em: <http://link.springer.com/10.1007/BF02636814>. Acesso em: 5 maio. 2017.

LU, P.; GAO, X.; DONG, H.; LIU, Z.; SECUNDO, F.; XUE, C.; MAO, X. Identification of a novel esterase from marine environmental genomic dna libraries and its application in production of free all- *trans* -astaxanthin. **Journal of Agricultural and Food Chemistry**, v. 66, n. 11, p. 2812–2821, 21 mar. 2018. Disponível em: <http://pubs.acs.org/doi/10.1021/acs.jafc.7b06062>. Acesso em: 29 set. 2018.

LUO, Y.; ZHENG, Y.; JIANG, Z.; MA, Y.; WEI, D. A novel psychrophilic lipase from

Pseudomonas fluorescens with unique property in chiral resolution and biodiesel production via transesterification. **Applied Microbiology and Biotechnology**, v. 73, n. 2, p. 349–355, 6 nov. 2006. Disponível em: <http://www.ncbi.nlm.nih.gov/pubmed/16724189>. Acesso em: 3 set. 2018.

MA, F.; CHUNG, M. T.; YAO, Y.; NIDETZ, R.; LEE, L. M.; LIU, A. P.; FENG, Y.; KURABAYASHI, K.; YANG, G. Y. Efficient molecular evolution to generate enantioselective enzymes using a dual-channel microfluidic droplet screening platform. **Nature Communications**, v. 9, n. 1, p. 1–8, 2018.

MA, J.; WANG, Y.-G.; WANG, Y.-J. A simple, fast and efficient method for cloning blunt DNA fragments. **African Journal of Biotechnology**, v. 12, n. 26, p. 4094–4097, 2013. Disponível em: <http://www.academicjournals.org/AJB>. Acesso em: 23 ago. 2018.

MADALOZZO, A. D.; MARTINI, V. P.; KUNIYOSHI, K. K.; DE SOUZA, E. M.; PEDROSA, F. O.; GLOGAUER, A.; ZANIN, G. M.; MITCHELL, D. A.; KRIEGER, N. Immobilization of LipC12, a new lipase obtained by metagenomics, and its application in the synthesis of biodiesel esters. **Journal of Molecular Catalysis B: Enzymatic**, v. 116, p. 45–51, 2015. Disponível em: <http://dx.doi.org/10.1016/j.molcatb.2015.03.002>.

MADALOZZO, A. D.; MARTINI, V. P.; KUNIYOSHI, K. K.; SOUZA, E. M. de; PEDROSA, F. de O.; ZANIN, G. M.; MITCHELL, D. A.; KRIEGER, N. Synthesis of flavor esters and structured lipids by a new immobilized lipase, LipC12, obtained from metagenomics. **Biocatalysis and Agricultural Biotechnology**, v. 8, p. 294–300, 2016. Disponível em: <http://www.sciencedirect.com/science/article/pii/S1878818116302444>. Acesso em: 5 maio. 2017.

MADAN, B.; MISHRA, P. Co-expression of the lipase and foldase of *Pseudomonas aeruginosa* to a functional lipase in *Escherichia coli*. **Applied Microbiology and Biotechnology**, v. 85, n. 3, p. 597–604, 2010.

MADHAVAN, A.; SINDHU, R.; PARAMESWARAN, B.; SUKUMARAN, R. K.; PANDEY, A. Metagenome Analysis: a Powerful Tool for Enzyme Bioprospecting. **Applied Biochemistry and Biotechnology**, v. 183, n. 2, p. 636–651, 2017.

MAJOREK, K. A.; KUHN, M. L.; CHRUSZCZ, M.; ANDERSON, W. F.; MINOR, W. Double Trouble—buffer selection and his-tag presence may be responsible for nonreproducibility of biomedical experiments. **Protein Science**, v. 23, n. 10, p. 1359–1368, out. 2014.

MARTÍNEZ-MARTÍNEZ, M.; ALCAIDE, M.; TCHIGVINTSEV, A.; REVA, O.; POLAINA, J.; BARGIELA, R.; GUAZZARONI, M. E.; CHICOTE, Á.; CANET, A.; VALERO, F.; EGUIZABAL, E. R.; GUERRERO, M. del C.; YAKUNIN, A. F.; FERRER, M. Biochemical diversity of carboxyl esterases and lipases from lake arreo (Spain): A metagenomic approach. **Applied and Environmental Microbiology**, v. 79, n. 12, p. 3553–3562, 2013.

MARTINI, V. P.; GLOGAUER, A.; IULEK, J.; SOUZA, E. M.; PEDROSA, F. O.;

KRIEGER, N. Crystallization and preliminary crystallographic analysis of LipC12, a true lipase isolated through a metagenomics approach. **Acta Crystallographica Section F: Structural Biology and Crystallization Communications**, v. 68, n. 2, p. 175–177, 2012.

MARTINI, V. P.; GLOGAUER, A.; MÜLLER-SANTOS, M.; IULEK, J.; DE SOUZA, E. M.; MITCHELL, D. A.; PEDROSA, F. O.; KRIEGER, N. First co-expression of a lipase and its specific foldase obtained by metagenomics. **Microbial Cell Factories**, v. 13, n. 1, p. 35–41, 2014.

MELO, F.; SÁNCHEZ, R.; SALI, A. Statistical potentials for fold assessment. **Protein Science**, v. 11, n. 2, p. 430–448, 13 abr. 2009. Disponível em: <http://doi.wiley.com/10.1002/pro.110430>. Acesso em: 24 ago. 2018.

Microbial Lipases Market worth 590.2 Million USD by 2023. Disponível em: <https://www.marketsandmarkets.com/PressReleases/microbial-lipase.asp>. Acesso em: 29 out. 2018.

MIRETE, S.; MORGANTE, V.; GONZÁLEZ-PASTOR, J. E. Functional metagenomics of extreme environments. **Current Opinion in Biotechnology**, v. 38, p. 143–149, 2016.

MOKOENA, N.; MATHIBA, K.; TSEKOA, T.; STEENKAMP, P.; RASHAMUSE, K. Functional characterisation of a metagenome derived family VIII esterase with a deacetylation activity on β-lactam antibiotics. **Biochemical and Biophysical Research Communications**, v. 437, n. 3, p. 342–348, 2013.

MONTERO, S.; BLANCO, A.; VIRTO, M. D.; LANDETA, L. C.; AGUD, I.; SOLOZABAL, R.; LASCARAY, J. M.; DE RENOBALES, M.; LLAMA, M. J.; SERRA, J. L. Immobilization of *Candida rugosa* lipase and some properties of the immobilized enzyme. **Enzyme and Microbial Technology**, v. 15, n. 3, p. 239–47, 1 mar. 1993. Disponível em: <https://www.sciencedirect.com/science/article/pii/014102299390144Q>. Acesso em: 7 maio. 2018.

MOSBAH, H.; SAYARI, A.; BEZZINE, S.; GARGOURI, Y. Expression, purification, and characterization of His-tagged *Staphylococcus xylosus* lipase wild-type and its mutant Asp 290 Ala. **Protein Expression and Purification**, v. 47, n. 2, p. 516–523, 2006.

MÜLLER, C. A.; PERZ, V.; PROVASNEK, C.; QUARTINELLO, F.; GUEBITZ, G. M.; BERG, G. Discovery of polyesterases from moss-associated microorganisms. **Applied and Environmental Microbiology**, v. 83, n. 4, p. e02641-16, 15 fev. 2017. Disponível em: <http://www.ncbi.nlm.nih.gov/pubmed/27940546>. Acesso em: 28 out. 2018.

NARDINI, M.; LANG, D. A.; LIEBETON, K.; JAEGER, K. E.; DIJKSTRA, B. W. Crystal structure of *Pseudomonas aeruginosa* lipase in the open conformation. The prototype for family I.1 of bacterial lipases. **Journal of Biological Chemistry**, v. 275, n. 40, p. 31219–31225, 2000.

NINI, L.; SARDA, L.; COMEAU, L.-C.; BOITARD, E.; DUBÈS, J.-P.; CHAHINIAN, H.

Lipase-catalysed hydrolysis of short-chain substrates in solution and in emulsion: a kinetic study. **Biochimica et Biophysica Acta (BBA) - Molecular and Cell Biology of Lipids**, v. 1534, n. 1, p. 34–44, 30 nov. 2001. Disponível em: <https://www.sciencedirect.com/science/article/pii/S138819810100172X?via%3Dihub>. Acesso em: 26 ago. 2018.

NOTREDAME, C.; HIGGINS, D. G.; HERINGA, J. T-coffee: a novel method for fast and accurate multiple sequence alignment. **Journal of Molecular Biology**, v. 302, n. 1, p. 205–217, 8 set. 2000. Disponível em: <https://www.sciencedirect.com/science/article/pii/S0022283600940427?via%3Dihub>. Acesso em: 24 ago. 2018.

NOVOTOTSKAYA-VLASOVA, K.; PETROVSKAYA, L.; KRYUKOVA, E.; RIVKINA, E.; DOLGIKH, D.; KIRPICHNIKOV, M. Expression and chaperone-assisted refolding of a new cold-active lipase from *Psychrobacter cryohalolentis* K5T. **Protein Expression and Purification**, v. 91, n. 1, p. 96–103, set. 2013. Disponível em: <http://dx.doi.org/10.1016/j.pep.2013.07.011>.

OGINO, H.; INOUE, S.; AKAGI, R.; YASUDA, M.; DOUKYU, N.; ISHIMI, K. Refolding of a recombinant organic solvent-stable lipase, which is overexpressed and forms an inclusion body, and activation with lipase-specific foldase. **Biochemical Engineering Journal**, v. 40, n. 3, p. 507–511, 1 jul. 2008. Disponível em: <http://www.sciencedirect.com/science/article/pii/S1369703X08000478>. Acesso em: 17 out. 2017.

OH, K.-H.; NGUYEN, G.-S.; KIM, E.-Y.; KOURIST, R.; BORNSCHEUER, U.; OH, T.-K.; YOON, J.-H. Characterization of a novel esterase isolated from intertidal flat metagenome and its tertiary alcohols synthesis. **Journal of Molecular Catalysis B: Enzymatic**, v. 80, p. 67–73, 1 ago. 2012. Disponível em: <https://www.sciencedirect.com/science/article/pii/S1381117712000951>. Acesso em: 23 out. 2018.

OMORI, K.; ISOYAMA-TANAKA, J.; IHARA, F.; YAMADA, Y.; NIHIRA, T. Active lactonizing lipase (LipL) efficiently overproduced by *Pseudomonas* strains as heterologous expression hosts. **Journal of Bioscience and Bioengineering**, v. 100, n. 3, p. 323–330, 2005. Disponível em: <http://www.sciencedirect.com/science?_ob=ArticleURL&_udi=B6VSD-4HCDTM5-H&_user=494590&_rdoc=1&_fmt=&_orig=search&_sort=d&view=c&_acct=C000024058&_version=1&_urlVersion=0&_userid=494590&md5=e52706c9de13f7e039d7d1727d5b9099%5Cnpapers:>.

OUYANG, L.-M.; LIU, J.-Y.; QIAO, M.; XU, J.-H. Isolation and biochemical characterization of two novel metagenome-derived esterases. **Applied Biochemistry and Biotechnology**, v. 169, n. 1, p. 15–28, 2 jan. 2013. Disponível em: <http://link.springer.com/10.1007/s12010-012-9949-4>. Acesso em: 24 out. 2018.

OVERMEYER, A.; SCHRADER-LIPPELT, S.; KASCHE, V.; BRUNNER, G. Lipase-catalysed kinetic resolution of racemates at temperatures from 40 °C to 160 °C in supercritical CO2. **Biotechnology Letters**, v. 21, n. 1, p. 65–69, 1999. Disponível em: <http://link.springer.com/10.1023/A:1005422524509>. Acesso em: 26 out. 2018.

PALMER, I.; WINGFIELD, P. T. Preparation and extraction of insoluble (Inclusion body) proteins from *Escherichia coli*. **Current Protocols in Protein Science**, n. 8 M, p. 1–25, 2004.

PALOMO, J.M.; MUNOZ, G.; FERNANDEZ-LORENTE, G.; MATEO, C.; FERNANDEZ-LAFUENTE, R.; GUISAN, J.M. Interfacial adsorption of lipases on very hydrophobic support (octadecyl-Sepabeads): immobilization, hyperactivation and stabilization of the open form of lipases. **Journal of Molecular Catalysis. B Enzymatic**, v. 19, p. 279–286, 2002.

PARAPOULI, M.; FOUKIS, A.; STERGIOU, P.-Y.; KOUKOURITAKI, M.; MAGKLARAS, P.; GKINI, O. A.; PAPAMICHAEL, E. M.; AFENDRA, A.-S.; HATZILOUKAS, E. Molecular, biochemical and kinetic analysis of a novel, thermostable lipase (LipSm) from *Stenotrophomonas maltophilia* Psi-1, the first member of a new bacterial lipase family (XVIII). **Journal of Biological Research-Thessaloniki**, v. 25, n. 1, p. 4, 8 dez. 2018. Disponível em: <http://www.ncbi.nlm.nih.gov/pubmed/29456971>. Acesso em: 30 ago. 2018.

PAUWELS, K.; LUSTIG, A.; WYNS, L.; TOMMASSEN, J.; SAVVIDES, S. N.; VAN GELDER, P. Structure of a membrane-based steric chaperone in complex with its lipase substrate. **Nature Structural & Molecular Biology**, v. 13, n. 4, p. 374–375, 5 abr. 2006. Disponível em: <http://www.nature.com/articles/nsmb1065>.

PAUWELS, K.; SANCHEZ DEL PINO, M. M.; FELLER, G.; VAN GELDER, P. Decoding the folding of *Burkholderia glumae* lipase: folding intermediates en route to kinetic stability. **PLoS ONE**, v. 7, n. 5, p. 1–9, 15 maio 2012. Disponível em: <http://dx.plos.org/10.1371/journal.pone.0036999>.

PEÑA-GARCÍA, C.; MARTÍNEZ-MARTÍNEZ, M.; REYES-DUARTE, D.; FERRER, M. High throughput screening of esterases, lipases and phospholipases in mutant and metagenomic libraries: A Review. **Combinatorial Chemistry & High Throughput Screening**, p. 605–615, 2016. Disponível em: <http://www.ncbi.nlm.nih.gov/pubmed/26552433>.

PENG, Q.; WANG, X.; SHANG, M.; HUANG, J.; GUAN, G.; LI, Y.; SHI, B. Isolation of a novel alkaline-stable lipase from a metagenomic library and its specific application for milkfat flavor production. **Microbial Cell Factories**, v. 13, n. 1, p. 1, jan. 2014. Disponível em: <http://www.pubmedcentral.nih.gov/articlerender.fcgi?artid=3880967&tool=pmcentrez&rendertype=abstract>. Acesso em: 16 dez. 2014.

QIAGEN. **The QIAexpressionist. A handbook for high-level expression and purification of 6xHis-tagged proteins**. 5. ed. [s.l: s.n.]

QUYEN, T. D.; VU, C. H.; THU LE, G. T. Enhancing functional production of a chaperone-dependent lipase in *Escherichia coli* using the dual expression cassette plasmid. **Microbial Cell Factories**, v. 11, n. 1, p. 29, 2012. Disponível em: <http://www.microbialcellfactories.com/content/11/1/29>.

RARAVINDAN, P. A. and T. V. Lipase applications in food industry. **Indian Journal of Biotechnology**, v. 6, n. April, p. 141–158, 2007.

RAMMLER, D. H. The effect of dmso on several enzyme systems. **Annals of the New York Academy of Sciences**, v. 141, n. 1 Biological Ac, p. 291–299, mar. 1967. Disponível em: <http://doi.wiley.com/10.1111/j.1749-6632.1967.tb34893.x>. Acesso em: 5 maio. 2017.

RAO, L.; XUE, Y.; ZHENG, Y.; LU, J. R.; MA, Y. A novel alkaliphilic *Bacillus* esterase belongs to the 13th bacterial lipolytic enzyme family. **PLoS ONE**, v. 8, n. 4, 2013.

RAO, L.; XUE, Y.; ZHOU, C.; TAO, J.; LI, G.; LU, J. R.; MA, Y. A thermostable esterase from *Thermoanaerobacter tengcongensis* opening up a new family of bacterial lipolytic enzymes. **Biochimica et Biophysica acta**, v. 1814, n. 12, p. 1695–702, dez. 2011. Disponível em: <http://www.ncbi.nlm.nih.gov/pubmed/21907313>. Acesso em: 28 ago. 2018.

RAY, A. Application of Lipase in Industry. **Asian Journal of Pharmaceutical Technology**, v. 2, n. 2, p. 33–37, 2012.

REETZ, M. T.; BECKER, M. H.; KLEIN, H.-W.; STÖCKIGT, D. A method for high-throughput screening of enantioselective catalysts. **Angewandte Chemie International Edition**, v. 38, n. 12, p. 1758–1761, 14 jun. 1999. Disponível em: <http://doi.wiley.com/10.1002/%28SICI%291521-3773%2819990614%2938%3A12%3C1758%3A%3AAID-ANIE1758%3E3.0.CO%3B2-8>. Acesso em: 3 out. 2018.

REYES-DUARTE, D.; FERRER, M.; GARCÍA-ARELLANO, H. Functional-based screening methods for lipases, esterases, and phospholipases in metagenomic libraries. **Lipases and Phospholipases**,.p. 101–113, 2012.

ROSENAU, F.; JAEGER, K. E. Bacterial lipases from *Pseudomonas*: regulation of gene expression and mechanisms of secretion. **Biochimie**, v. 82, n. 11, p. 1023–1032, 2000.

ROSENAU, F.; TOMMASSEN, J.; JAEGER, K. E. Lipase-specific foldases. **ChemBioChem**, v. 5, n. 2, p. 152–161, 2004.

SAHOO, R. K.; KUMAR, M.; SUKLA, L. B.; SUBUDHI, E. Bioprospecting hot spring metagenome: lipase for the production of biodiesel. **Environmental Science and Pollution Research**, v. 24, n. 4, p. 3802–3809, 28 fev. 2017. Disponível em: <http://link.springer.com/10.1007/s11356-016-8118-7>. Acesso em: 25 out. 2018.

SAMBROOK, J. **Molecular cloning : a laboratory manual / J. Sambrook, E.F. Fritsch, T. Maniatis - Details - Trove**. 3. ed. 2001.

SANDKVIST, M. Type II secretion and pathogenesis. **Infection and Immunity**, v. 69, n. 6, p. 3523–35, jun. 2001. Disponível em: <http://www.ncbi.nlm.nih.gov/pubmed/11349009>. Acesso em: 30 ago. 2018.

SARMAH, N.; REVATHI, D.; SHEELU, G.; YAMUNA RANI, K.; SRIDHAR, S.; MEHTAB, V.; SUMANA, C. Recent advances on sources and industrial applications of lipases. **Biotechnology Progress**, v. 34, n. 1, p. 5–28, 2018.

SARROUH, B. Up-to-date insight on industrial enzymes applications and global

market. **Journal of Bioprocessing & Biotechniques**, v. s1, n. 01, 2012. Disponível em: <https://www.omicsonline.org/up-to-date-insight-on-industrial-enzymes-applications-and-global-market-2155-9821.S4-002.php?aid=3921>.

SAYARI, A.; MOSBAH, H.; VERGER, R.; GARGOURI, Y. The N-terminal His-tag affects the enantioselectivity of staphylococcal lipases: A monolayer study. **Journal of Colloid and Interface Science**, v. 313, n. 1, p. 261–267, 2007.

SCHLOSS, P. D.; HANDELSMAN, J. Biotechnological prospects from metagenomics. **Current Opinion in Biotechnology**, v. 14, n. 3, p. 303–310, 2003.

SCHMID, R. D.; VERGER, R. Lipases: interfacial enzymes with attractive applications. **Angewandte Chemie International Edition**, v. 37, n. 12, p. 1608–1633, 3 jul. 1998. Disponível em: <http://doi.wiley.com/10.1002/%28SICI%291521-3773%2819980703%2937%3A12%3C1608%3A%3AAID-ANIE1608%3E3.0.CO%3B2-V>. Acesso em: 5 maio. 2017.

SCHMIDT, M.; BORNSCHEUER, U. T. High-throughput assays for lipases and esterases. **Biomolecular Engineering**, v. 22, n. 1–3, p. 51–56, 2005.

SEO, H. S.; KIM, S. E.; HAN, K. Y.; PARK, J. S.; KIM, Y. H.; SIM, S. J.; LEE, J. Functional fusion mutant of *Candida antarctica* lipase B (CalB) expressed in Escherichia coli. **Biochimica et Biophysica Acta - Proteins and Proteomics**, v. 1794, n. 3, p. 519–525, 2009.

SHARIFF, F. M.; RAHMAN, R. N. Z. R. A.; BASRI, M.; SALLEH, A. B. A newly isolated thermostable lipase from *Bacillus* sp. **International Journal of Molecular sciences**, v. 12, n. 5, p. 2917–34, 2011. Disponível em: <http://www.ncbi.nlm.nih.gov/pubmed/21686158>. Acesso em: 21 abr. 2018.

SHATSKY, M.; NUSSINOV, R.; WOLFSON, H. J. MultiProt — A multiple protein structural alignment algorithm. In **Algorithms in Bioinformatics**, v. 2452, Edited by Guigó R, Gusfield D. Berlin Heidelberg: Springer; 2002: 235–250. Lecture

SHEN, M.-Y.; SALI, A. Statistical potential for assessment and prediction of protein structures. **Protein Science**, v. 15, n. 11, p. 2507–24, nov. 2006. Disponível em: <http://www.ncbi.nlm.nih.gov/pubmed/17075131>. Acesso em: 24 ago. 2018.

SHEVCHENKO, A.; WILM, M.; VORM, O.; MANN, M. Mass spectrometric sequencing of proteins from silver-stained polyacrylamide gels. **Analytical Chemistry**, v. 68, n. 5, p. 850–858, jan. 1996. Disponível em: <http://pubs.acs.org/doi/abs/10.1021/ac950914h>. Acesso em: 23 ago. 2018.

SHIBATA, H.; KATO, H.; ODA, J. Calcium ion-dependent reactivation of a *Pseudomonas* lipase by its specific modulating protein, LipB. **Journal of Biochemistry**, v. 123, n. 1, p. 136–141, 1998.

SHIMURA, S.; TSUZUKI, W.; SUZUKI, T. Determination of lipase activity in organic fluorescent substrate and its application to of lipase inhibitor solvent using the screening. **Analytical Sciences February**, v. 7, 1991. Disponível em: <https://www.jstage.jst.go.jp/article/analsci1985/7/1/7_1_15/_pdf>. Acesso em: 4 set. 2018.

SIMON, C.; DANIEL, R. Metagenomic analyses: Past and future trends. **Applied and Environmental Microbiology**, v. 77, n. 4, p. 1153–1161, 2011.

SOLIMAN, N. A.; KNOLL, M.; ABDEL-FATTAH, Y. R.; SCHMID, R. D.; LANGE, S. Molecular cloning and characterization of thermostable esterase and lipase from *Geobacillus thermoleovorans* YN isolated from desert soil in Egypt. **Process Biochemistry**, v. 42, n. 7, p. 1090–1100, 1 jul. 2007. Disponível em: <https://www.sciencedirect.com/science/article/pii/S1359511307001316>. Acesso em: 24 ago. 2018.

STUDIER, F. W.; MOFFATT, B. A. Use of bacteriophage T7 RNA polymerase to direct selective high-level expression of cloned genes. **Journal of Molecular Biology**, v. 189, n. 1, p. 113–130, maio 1986.

STUER, W.; JAEGER, K. E.; WINKLER, U. K. Purification of extracellular lipase from *Pseudomonas aeruginosa*. **Journal of Bacteriology**, v. 168, n. 3, p. 1070–1074, dez. 1986. Disponível em: <http://www.ncbi.nlm.nih.gov/pubmed/3096967>. Acesso em: 5 maio. 2017.

TANG, L.; XIA, Y.; WU, X.; CHEN, X.; ZHANG, X.; LI, H. Screening and characterization of a novel thermostable lipase with detergent-additive potential from the metagenomic library of a mangrove soil. **Gene**, v. 625, p. 64–71, 2017.

TEIXEIRA, A. R. S.; FLOURAT, A. L.; PERU, A. A. M.; BRUNISSEN, F.; ALLAIS, F. Lipase-catalyzed baeyer-villiger oxidation of cellulose-derived levoglucosenone into (S)-γ-Hydroxymethyl-α,β-Butenolide: Optimization by Response Surface Methodology. **Frontiers in Chemistry**, v. 4, p. 16, 19 abr. 2016. Disponível em: <http://journal.frontiersin.org/Article/10.3389/fchem.2016.00016/abstract>. Acesso em: 2 out. 2018.

TERPE, K. Overview of tag protein fusions: from molecular and biochemical fundamentals to commercial systems. **Applied Microbiology and Biotechnology**, v. 60, n. 5, p. 523–533, 2003a. Disponível em: <http://link.springer.com/10.1007/s00253-002-1158-6>.

THIELGES, M. C.; CHUNG, J. K.; AXUP, J. Y.; FAYER, M. D. Influence of histidine tag attachment on picosecond protein dynamics. **Biochemistry**, v. 50, n. 25, p. 5799–5805, 2011.

THOMPSON, J. D.; HIGGINS, D. G.; GIBSON, T. J. CLUSTAL W: improving the sensitivity of progressive multiple sequence alignment through sequence weighting, position-specific gap penalties and weight matrix choice. **Nucleic Acids Research**, v. 22, n. 22, p. 4673–80, 11 nov. 1994. Disponível em: <http://www.ncbi.nlm.nih.gov/pubmed/7984417>. Acesso em: 23 ago. 2018.

TISS, A.; CARRIÈRE, F.; VERGER, R. Effects of Gum Arabic on Lipase interfacial binding and activity. **Analytical Biochemistry**, v. 294, n. 1, p. 36–43, jul. 2001a.

TORSVIK, V.; SØRHEIM, R.; GOKSØYR, J. Total bacterial diversity in soil and sediment communities—A review. **Journal of Industrial Microbiology & Biotechnology**, v. 17, n. 3–4, p. 170–178, 1996. Disponível em: <http://link.springer.com/10.1007/BF01574690>.

TRAUB, P. C.; SCHMIDT-DANNERT, C.; SCHMITT, J.; SCHMID, R. D. Gene synthesis, expression in *E . coli* , and in vitro refolding of *Pseudomonas* sp. KWI 56 and *Chromobacterium viscosum* lipases and their chaperones. **Applied Microbiology and Biotechnology**, v. 55, n. 2, p. 198–204, 1 mar. 2001. Disponível em: <http://link.springer.com/10.1007/s002530000492>. Acesso em: 2 set. 2018.

TSUZUKI, W.; UE, A.; KITAMURA, Y. Effect of dimethylsulfoxide on hydrolysis of lipase. **Bioscience, Biotechnology, and Biochemistry**, v. 65, n. 9, p. 2078–2082, 22 jan. 2001. Disponível em: <http://www.tandfonline.com/doi/full/10.1271/bbb.65.2078>. Acesso em: 23 out. 2017.

TSUZUKI, W.; UE, A.; NAGAO, A. Polar organic solvent added to an aqueous solution changes hydrolytic property of lipase. **Bioscience, Biotechnology, and Biochemistry**, v. 67, n. 8, p. 1660–6, 22 jan. 2003. Disponível em: <http://www.tandfonline.com/doi/full/10.1271/bbb.67.1660>. Acesso em: 5 maio. 2017.

TUFFIN, M.; ANDERSON, D.; HEATH, C.; COWAN, D. A. Metagenomic gene discovery: How far have we moved into novel sequence space? **Biotechnology Journal**, v. 4, n. 12, p. 1671–1683, 2009.

UCHIYAMA, T.; ABE, T.; IKEMURA, T.; WATANABE, K. Substrate-induced gene-expression screening of environmental metagenome libraries for isolation of catabolic genes. **Nature Biotechnology**, v. 23, n. 1, p. 88–93, 2005.

UCHIYAMA, T.; MIYAZAKI, K. Functional metagenomics for enzyme discovery: challenges to efficient screening. **Current Opinion in Biotechnology**, v. 20, n. 6, p. 616–622, dez. 2009. Disponível em: <http://linkinghub.elsevier.com/retrieve/pii/S0958166909001244>. Acesso em: 28 ago. 2018.

VALLEJO, L. F.; RINAS, U. Strategies for the recovery of active proteins through refolding of bacterial inclusion body proteins. **Microbial Cell Factories**, v. 3, p. 1–12, 2004.

VAN DEN BERG, S.; LÖFDAHL, P. Å.; HÄRD, T.; BERGLUND, H. Improved solubility of TEV protease by directed evolution. **Journal of Biotechnology**, v. 121, n. 3, p. 291–298, 2006. Disponível em: <http://www.sciencedirect.com/science/article/pii/S0168165605004840>. Acesso em: 5 maio. 2017.

VILLENEUVE, P.; MUDERHWA, J. M.; GRAILLE, J.; HAAS, M. J. Customizing lipases for biocatalysis: a survey of chemical, physical and molecular biological approaches. **Journal of Molecular Catalysis B: Enzymatic**, v. 9, n. 4–6, p. 113–148, 21 abr. 2000. Disponível em: <https://www.sciencedirect.com/science/article/pii/S1381117799001071>. Acesso em: 23 out. 2018.

WAHLER, D.; BOUJARD, O.; LEFÈVRE, F.; REYMOND, J.-L. Adrenaline profiling of lipases and esterases with 1,2-diol and carbohydrate acetates. **Tetrahedron**, v. 60,

n. 3, p. 703–710, 12 jan. 2004. Disponível em: <https://www.sciencedirect.com/science/article/pii/S004040200301915X>. Acesso em: 4 set. 2018.

WANG, C.-C.; TSOU, C.-L. Enzymes as chaperones and chaperones as enzymes. **FEBS Letters**, v. 425, n. 3, p. 382–384, 3 abr. 1998. Disponível em: <http://www.sciencedirect.com/science/article/pii/S0014579398002725>. Acesso em: 17 out. 2017.

WANG, S.; MENG, X.; ZHOU, H.; LIU, Y.; SECUNDO, F.; LIU, Y. Enzyme stability and activity in non-aqueous reaction systems: a mini review. **Catalysts**, v. 6, n. 2, p. 32, 22 fev. 2016. Disponível em: <http://www.mdpi.com/2073-4344/6/2/32>. Acesso em: 5 maio. 2017.

WAUGH, D. S. Making the most of affinity tags. **Trends in Biotechnology**, v. 23, n. 6, p. 316–320, 2005a.

WAUGH, D. S. An overview of enzymatic reagents for the removal of affinity tags. **Protein Expression and Purification**, v. 80, n. 2, p. 283–293, dez. 2011. Disponível em: <http://linkinghub.elsevier.com/retrieve/pii/S1046592811002038>.

WEBB, B.; SALI, A. Comparative protein structure modeling using MODELLER. In: **Current Protocols in Bioinformatics**. Hoboken, NJ, USA: John Wiley & Sons, Inc., 2016. 54p. 5.6.1-5.6.37.

WILHELM, S.; ROSENAU, F.; BECKER, S.; BUEST, S.; HAUSMANN, S.; KOLMAR, H.; JAEGER, K.-E. Functional cell-surface display of a lipase-specific chaperone. **ChemBioChem**, v. 8, n. 1, p. 55–60, 2 jan. 2007. Disponível em: <http://www.ncbi.nlm.nih.gov/pubmed/17173269>. Acesso em: 2 set. 2018.

WODAK, S. J.; JANIN, J. Structural basis of macromolecular recognition. **Advances in Protein Chemistry**, v. 61, p. 9–73, 2002. Disponível em: <http://www.ncbi.nlm.nih.gov/pubmed/12461820>. Acesso em: 24 ago. 2018.

WU, X.; YOU, P.; SU, E.; XU, J.; GAO, B.; WEI, D. In vivo functional expression of a screened *P. aeruginosa* chaperone-dependent lipase in *E. coli*. **BMC Biotechnology**, v. 12, n. 1, p. 1, 2012. Disponível em: <BMC Biotechnology>.

XIAO, H.; BAO, Z.; ZHAO, H. High Throughput screening and selection methods for directed enzyme evolution. **Industrial & Engineering Chemistry Research**, v. 54, n. 16, p. 4011–4020, 29 abr. 2015. Disponível em: <http://www.ncbi.nlm.nih.gov/pubmed/26074668>. Acesso em: 7 nov. 2018.

XING, M. N.; ZHANG, X. Z.; HUANG, H. Application of metagenomic techniques in mining enzymes from microbial communities for biofuel synthesis. **Biotechnology Advances**, v. 30, n. 4, p. 920–929, 2012. Disponível em: <http://dx.doi.org/10.1016/j.biotechadv.2012.01.021>.

YAN, W.; LI, F.; WANG, L.; ZHU, Y.; DONG, Z.; BAI, L. Discovery and characterizaton of a novel lipase with transesterification activity from hot spring metagenomic library. **Biotechnology Reports**, v. 14, p. 27–33, 2017.

YARZA, P.; YILMAZ, P.; PRUESSE, E.; GLÖCKNER, F. O.; LUDWIG, W.; SCHLEIFER, K. H.; WHITMAN, W. B.; EUZÉBY, J.; AMANN, R.; ROSSELLÓ-MÓRA, R. Uniting the classification of cultured and uncultured bacteria and archaea using 16S rRNA gene sequences. **Nature Reviews Microbiology**, v. 12, n. 9, p. 635–645, 2014. Disponível em: <http://dx.doi.org/10.1038/nrmicro3330>.

YUN, J.; RYU, S. Screening for novel enzymes from metagenome and SIGEX, as a way to improve it. **Microbial Cell Factories**, v. 4, n. 1, p. 8, 25 mar. 2005. Disponível em: <http://www.ncbi.nlm.nih.gov/pubmed/15790425>. Acesso em: 3 set. 2018.

ZARAFETA, D.; MOSCHIDI, D.; LADOUKAKIS, E.; GAVRILOV, S.; CHRYSINA, E. D.; CHATZIIOANNOU, A.; KUBLANOV, I.; SKRETAS, G.; KOLISIS, F. N. Metagenomic mining for thermostable esterolytic enzymes uncovers a new family of bacterial esterases. **Scientific Reports**, v. 6, n. 1, p. 38886, 19 dez. 2016. Disponível em: <http://www.nature.com/articles/srep38886>. Acesso em: 27 ago. 2018.

ZHAO, D.; HUANG, Z. Effect of His-Tag on expression, purification, and structure of zinc finger protein, ZNF191(243-368). **Bioinorganic Chemistry and Applications**, v. 2016, 2016.

ZHAO, Z.; ZHANG, L.; LI, F.; TANG, X.; MA, Y.; WANG, C.; WANG, Z.; ZHAO, R.; WANG, L. A novel oxidation of salicyl alcohols catalyzed by lipase. **Catalysts**, v. 7, n. 12, p. 354, 2017. Disponível em: <www.mdpi.com/journal/catalysts>. Acesso em: 2 out. 2018.

ZHENG, J.; LIU, L.; LIU, C.; JIN, Q. Molecular cloning and heterologous expression of a true lipase in *Pichia pastoris* isolated via a metagenomic approach. **Journal of Molecular Microbiology and Biotechnology**, v. 22, n. 5, p. 300–311, 2012.

ANEXO 1 – PERMISSÕES PARA REPRODUÇÃO

O Capítulo I traz a reprodução integral do seguinte artigo:

ALMEIDA, J. M.; MOURE, V. R.; MÜLLER-SANTOS, M.; SOUZA, E. M.; PEDROSA, F. O.; MITCHELL, D. A.; KRIEGER, N. Tailoring recombinant lipases: keeping the His-tag favors esterification reactions, removing it favors hydrolysis reactions. **Scientific Reports**, v.8, p. 1-11, 2018.

Permissão para reprodução da FIGURA 1.

NARDINI, M.; LANG, D. A.; LIEBETON, K.; JAEGER, K. E.; DIJKSTRA, B. W. Crystal structure of Pseudomonas aeruginosa lipase in the open conformation. The prototype for family I.1 of bacterial lipases. **Journal of Biological Chemistry**, v. 275, n. 40, p. 31219–31225, 2000.

ISSN: 1083-351X
Publication year(s): 1905 - present
Author/Editor: AMERICAN SOCIETY FOR BIOCHEMISTRY & MOLECULAR BIOL
Publisher: AMERICAN SOCIETY FOR BIOCHEMISTRY AND MOLECULAR BI
Language: English
Country of publication: United States of America

Permissão para reprodução da FIGURA 3.

ROSENAU, F.; TOMMASSEN, J.; JAEGER, K. E. Lipase-specific foldases. ChemBioChem, v. 5, n. 2, p. 152–161, 2004.

License Number	4466160027089
License date	Nov 11, 2018
Licensed Content Publisher	John Wiley and Sons
Licensed Content Publication	ChemBioChem
Licensed Content Title	Lipase-Specific Foldases
Licensed Content Author	Frank Rosenau, Jan Tommassen, Karl-Erich Jaeger
Licensed Content Date	Jan 29, 2004
Licensed Content Volume	5
Licensed Content Issue	2
Licensed Content Pages	10
Type of use	Dissertation/Thesis
Requestor type	University/Academic
Format	Print and electronic
Portion	Figure/table
Number of figures/tables	1
Original Wiley figure/table number(s)	Graphical Abstract
Will you be translating?	No
Title of your thesis / dissertation	Lipases de metagenômica: caracterização de uma nova lipase LipMF3 e modificação estrutural de LipC12
Expected completion date	Dec 2018
Expected size (number of pages)	152
Requestor Location	Mrs. Janaina de Almeida Rua Carlos Pradi, 213 Curitiba, Paraná 81530-180 Brazil Attn: Mrs. Janaina de Almeida
Publisher Tax ID	EU826007151
Total	0.00 USD

Permissão para reprodução da FIGURA 5.

MIRETE, S.; MORGANTE, V.; GONZÁLEZ-PASTOR, J. E. Functional metagenomics of extreme environments. Current Opinion in Biotechnology, v. 38, p. 143–149, 2016.

Licensed Content Publisher	Elsevier
Licensed Content Publication	Current Opinion in Biotechnology
Licensed Content Title	Functional metagenomics of extreme environments
Licensed Content Author	Salvador Mirete,Verónica Morgante,José Eduardo González-Pastor
Licensed Content Date	April 2016
Licensed Content Volume	38
Licensed Content Issue	n/a
Licensed Content Pages	7
Type of Use	reuse in a thesis/dissertation
Portion	figures/tables/illustrations
Number of figures/tables/illustrations	1
Format	electronic
Are you the author of this Elsevier article?	No
Will you be translating?	Yes, without English rights
Number of languages	1
Languages	Português
Original figure numbers	Graphical abstract
Title of your thesis/dissertation	Lipases de metagenômica: caracterização de uma nova lipase LipMF3 e modificação estrutural de LipC12
Expected completion date	Dec 2018
Estimated size (number of pages)	152
Requestor Location	Mrs. Janaina de Almeida Rua Carlos Pradi, 213 Curitiba, Paraná 81530-180 Brazil Attn: Mrs. Janaina de Almeida
Publisher Tax ID	GB 494 6272 12
Total	0.00 USD